

MRC

Centre for Developmental
and Biomedical Genetics

 **CVBRU**
NIHR Cardiovascular Biomedical Research Unit
SHEFFIELD



The
University
Of
Sheffield.

**KIAA1109 is differentially expressed in
whole blood early after myocardial
infarction in humans and is required for
vascular integrity in zebrafish**

Sara Solaymani-Kohal

A thesis submitted for the degree of
Doctor of Philosophy
At the University of Sheffield
Department of Cardiovascular Science

September 2012

Acknowledgments

First and foremost I would like to extend my heartfelt gratitude to my supervisor, Dr Tim Chico, who has always been incredibly supportive and guided me with care and patience in my growth as a scientist.

To the wonderful members of the lab Caroline, Emily, Karen, Olly, Becks and Simon, I will be forever indebted for all the support and laughter you have all provided.

Many thanks go to my advisor Dr Alireza Fazeli for all his advice and guidance.

I would also like to take this opportunity to thank the staff in the CDBG aquarium for all their hard work and effort to keep the fish healthy.

My most sincere thanks to the patients, nurses and staff at the Sheffield Cardiovascular Biomedical Research Unit for all their efforts and generosity. In particular I would like to thank Dr Marta Milo, Dr Paul Heath, Dr Sinnakarupan Mathavan and Dr Serene Lee Gek Ping, for all their help and support.

Finally I would like to thank my wonderful parents and husband for their never-ending love and support throughout these years.

Statement of contribution

The Sheffield NIHR Cardiovascular Biomedical Research Unit (CVBRU) recruited the patients and collected the samples used in Chapter 3. RNA extraction from these samples was carried out by Dr Marta Milo, Ms Sarah Craig and myself. RNA preparation and microarray hybridisation of these samples was carried out by Dr Paul Heath in the University of Sheffield Microarray Core Facility. Normalization and analysis of these data was carried out by Dr Marta Milo. All subsequent data interpretation, annotation was carried out by myself.

For the studies in Chapter 5, RNA extraction of KIAA1109 morphants was carried out by myself and shipped to our collaborators at the Genome Institute of Singapore (Dr Sinnakarupan Mathavan) where these samples were hybridised to their custom made microarrays. Microarray data normalization and analysis was carried out by Dr Serene Lee Gek Ping at the Genome Institute of Singapore. Data interpretation and annotation was carried out by myself.

I performed all the other experimental work and analysis detailed in this thesis.

Table of Contents

Acknowledgments.....	2
Statement of contribution	3
Index of figures	10
Index of tables	14
Abstract	16
Outcomes from the following work	18
Publications:	18
Presentations:	18
Oral presentations:	18
Abbreviations.....	20
Chapter 1. Introduction.....	22
1.1. Cardiovascular disease	23
1.1.1. Atherosclerosis	23
1.1.2. Plaque Neovascularization.....	24
1.1.3. Acute coronary syndromes	24
1.1.3.1. Myocardial infarction	26
1.2. Role of peripheral blood components in Acute Coronary Syndromes	29
1.2.1. Platelets	29
1.2.2. Leukocytes	30
1.2.3. Erythrocytes	30
1.2.4. Plasma Factors	31

1.3. Use of microarrays for gene expression profiling	32
1.3.1. Whole blood gene expression profiling in cardiovascular disease	33
1.4. Zebrafish are a useful tool for gene function assessment	36
1.4.1. Vascular formation in the zebrafish.....	36
1.4.2. Vascular Endothelial Growth Factor (VEGF)	37
1.4.3. Vascular integrity	40
1.5. Genetic manipulation in zebrafish	41
1.5.1. Transgenesis	41
1.5.2. Use of antisense oligonucleotides for gene knockdown	41
1.6. Hypotheses	44
1.7. Aims	44
Chapter 2: Materials and Methods	45
2.1. Patients and Blood Collection.....	46
2.1.1. Recruitment criteria.....	46
2.1.2. Patient demographics	46
2.1.3. Blood collection	47
2.2. RNA extraction from human blood	47
2.2.1. Tempus™ Blood RNA Tube	47
2.3. RNA treatment	49
2.3.1. Using GLOBINclear™ to deplete haemoglobin RNA.....	49
2.3.2. Agilent Bioanalyzer™ Assessment	52
2.3.3 Linear Amplification and labelling.....	54
2.3.4 Linear IVT.....	55

2.3.4.1. Assembling the first-strand master mix (to synthesize the first-strand cDNA)	55
2.3.4.2 Assembling the Second-Strand Master Mix (to synthesize the second-strand cDNA).....	55
2.3.4.3 Assembling the IVT Master Mix (to label the RNA with Biotin).....	55
2.3.4.4 Purification of amplified RNA	55
2.3.5 Evaluation and Fragmentation of RNA	57
2.4. Hybridization	57
2.5. Microarray	58
2.5.1. Affymetrix microarray	58
2.5.2. Validation by quantitative Real Time-PCR	60
2.5.3. Zebrafish morphant microarray	60
2.5.3.1. Whole embryo RNA extraction.....	60
2.6. Zebrafish Husbandry	62
2.6.1. Home Office Regulations.....	62
2.6.2. Embryo Collection	62
2.6.3. Zebrafish Strains and Lines Utilised	63
2.6.4. Zebrafish anaesthesia and mounting	63
2.7 Morpholino injections	63
2.8. RNA probe synthesis	65
2.9. Whole Mount <i>In-Situ</i> Hybridization	67
2.10. Phenotypic analysis of KIAA1109 knockdown.....	69
2.10.1. Heart rate measurements	69
2.10.2. Velocity calculation measurements.....	69

2.10.3. Vessel diameter measurements.....	69
2.10.4. Haemorrhage volume quantification.....	69
2.10.5. Endothelial cell nuclei quantification.....	71
2.10.6. Dextran injection.....	71
2.10.7. Response to laser injury.....	72
2.11. The effect of small molecule VEGF induction.....	72
2.12. Statistical Analysis.....	74
2.12.1 Microarray normalization.....	74
Chapter 3: Identifying Differentially Expressed Genes in Peripheral Blood of Patients Presenting with Acute Coronary Syndrome (ACS).....	78
3.1. Introduction.....	79
3.1.1. Expression analysis of patient peripheral blood.....	79
3.2. Results.....	79
3.2.1. Defining differential expression.....	79
3.2.2 Identifying gene expression differences in peripheral blood from patients with MI compared with unstable angina.....	82
3.3. Discussion.....	93
Chapter 4: An examination of the role of KIAA1109 in vascular development in zebrafish.....	97
4.1. Introduction.....	98
4.1.1. Role of KIAA1109 in humans.....	98
4.2. Results:.....	103
4.2.1. qRT-PCR validation of KIAA1109 down regulation.....	103

4.2.2. Expression of KIAA1109 in zebrafish	103
4.2.3. Survival of KIAA1109 morphant embryos	106
4.2.4. Effect of KIAA1109 morpholino knockdown on cardiovascular performance	108
4.2.4.1. Heart rate.....	108
4.2.4.2. Arterial velocity	110
4.2.5. Effect of KIAA1109 morpholino knockdown on embryonic vascular development.....	112
4.2.5.1. ISV formation	112
4.2.5.2. Axial vessel formation.....	112
4.2.5.3. The effect of KIAA1109 morpholino knockdown on the cerebral vasculature.....	116
4.2.5.4. The effect of KIAA1109 morpholino knockdown on endothelial cell number	121
4.2.5.5. Vascular integrity	125
4.2.6. VEGF rescue of cerebral haemorrhaging.....	129
4.3. Thrombocyte adhesion and thrombosis	137
4.4. Discussion.....	140
Chapter 5: Transcriptional profiling of KIAA1109 morphants	146
5.1. Introduction.....	147
5.1.1. Bioinformatic analysis of microarray datasets	147
5.1.1.1. PANTHER.....	147
5.1.1.2. STRING	147
5.2. Results	148
5.2.1. RNA extraction.....	148

5.2.2. PANTHER analysis of differentially expressed genes	149
5.3. Differentially expressed genes	157
5.3.1. Ligand of numb protein X-1 (<i>LNX1</i>).....	157
5.3.2 Renin (<i>ren</i>).....	160
5.3.3. Calcium/calmodulin-dependent protein kinase (<i>camk2g2</i>)	162
5.3.4 Glutamate receptor, ionotropic, N-methyl D-aspartate 1a (<i>grin1a</i>)	162
5.3.5. Protocadherin 1 gamma 2 (<i>PCDH1γ2</i>).....	165
5.3.6. Nodal related 2 (<i>ndr2</i>)	165
5.4. Discussion.....	169
Chapter 6: General discussion	172
6.1. General discussion.....	173
References	181
Appendix 1.....	187

Index of figures

Chapter 1.

Figure 1.1. Simplified summary of mechanisms and processes in plaque formation.....	25
Figure 1.2. Electrocardiographic changes seen in ACS.....	27
Figure 1.3. A summary of the microarray process.....	34
Figure 1.4. An illustration of brain vascular formation in 1-3dpf zebrafish.....	39

Chapter 2.

Figure 2.1. Sites of measurements of vessel size and haemodynamics.	70
Figure 2.2. Site of lasery injury	73

Chapter 3.

Figure 3.1. Summary of sample collection.....	81
Figure 3.2: Heat maps of genes differentially expressed in MI compared to UA	87
Figure 3.3. Heat map illustrating expression patterns at different time points..	92

Chapter 4.

Figure 4.1. STRING output of KIAA1109 interaction with genes.	102
Figure 4.2. qRT-PCR validation of KIAA1109.....	104
Figure 4.3. Expression of KIAA1109 in 1-5dpf cDNA.....	104
Figure 4.5. Survival of mismatch control and KIAA1109 morphant nacre embryos	107
Figure 4.6. Heart rate of mismatch control and KIAA1109 morphant nacre embryos at 2-4dpf	107
Figure 4.7. Example of PIV output.....	109

Figure 4.8. Mean arterial erythrocyte velocity in mismatch control and KIAA1109 morphant nacre embryos at 2-4dpf.....	109
Figure 4.9. Mean venous erythrocyte velocity in mismatch control and KIAA1109 morphant nacre embryos at 2-4dpf.....	111
Figure 4.10. Mean number of ISV in mismatch control and KIAA1109 morphant nacre embryos at 2-4dpf.....	113
Figure 4.11. Mean average arterial diameter in mismatch control and KIAA1109 morphant nacre embryos at 2-4dpf.....	114
Figure 4.12 Mean average venous diameter in mismatch control and KIAA1109 morphant nacre embryos at 2-4dpf.....	115
Figure 4.13 Bright field images of 3dpf mismatch control and KIAA1109 morphant nacre embryos.....	117
Figure 4.14. Mean percentage of mismatch control and KIAA1109 morphant nacre embryos with cerebral haemorrhage 2-4dpf.....	118
Figure 4.15. Percentage of haemorrhaging in variety of morpholinos at 3dpf.	119
Figure 4.16. Mean volume of mismatch control and KIAA1109 morphant nacre embryo haemorrhage 2-4dpf	120
Figure 4.17. Mean number of EC nuclei in eyes of mismatch control and KIAA1109 morphant nacre embryos 2-3dpf.....	122
Figure. 4.18. Mean number of EC nuclei in forebrain of mismatch control and KIAA1109 morphant nacre embryos 2-3dpf	123
Figure 4.19. Mean number of EC nuclei in hindbrain of mismatch control and KIAA1109 morphant nacre embryos 2-3dpf.....	124

Figure 4.20. Mean number of EC nuclei in ISV of mismatch control and KIAA1109 morphant nacre embryos 2-3dpf.....	126
Figure 4.21. Mean number of EC nuclei in artery of mismatch control and KIAA1109 morphant nacre embryos 2-3dpf.....	127
Figure 4.22. Mean number of EC nuclei in vein of mismatch control and KIAA1109 morphant nacre embryos 2-3dpf.....	128
Figure 4.23. Confocal images of 3dpf mismatch control transgenic embryos ..	130
Figure 4.24. Confocal images of 3dpf KIAA1109 morphant transgenic embryos	131
Figure 4.25. Confocal images of Dextran injected 3dpf mismatch control and KIAA1109 morphant nacre embryos	132
Figure 4.26. Brightfield images of 3dpf mismatch control and KIAA1109 morphant nacre embryo.....	134
Figure 4.27. Percentage of mismatch control and KIAA1109 morphant nacre embryos treated with GS4012 with cerebral haemorrhaging at 3dpf	135
Figure 4.28. Mean number of EC nuclei in forebrain and hindbrain of mismatch control and KIAA1109 morphant nacre embryos treated with GS4012 at 2dpf.....	136
Figure 4.29. Time taken to adhesion in mismatch control and KIAA1109 morphant nacre embryos at 3dpf.....	138
Figure 4.30. Size of thrombus in mismatch control and KIAA1109 morphant nacre embryos at 3dpf.....	139

Chapter 5.

Figure 5.1. qRT-PCR validation and STRING output of LNX1 interaction with genes.....	159
Figure 5.2. qRT-PCR validation and STRING output of Renin interaction with genes.....	161
Figure 5.3. qRT-PCR validation and STRING output of Camkg2 interaction with genes.....	163
Figure 5.4. qRT-PCR validation and STRING output of Grin1a interaction with genes.....	164
Figure 5.5. STRING output of pcdh1γ2 interaction with genes.....	166
Figure 5.6. STRING output of ndr2 interaction with genes.....	168

Index of tables

Chapter 1.

Table 1. 1. Advantages and disadvantages of morpholino technology 43

Table 2.1. Assay ID of Taqman primers 61

Chapter 2.

Table 2.2: Name and phenotype of strains of zebrafish used..... 64

Table 2.3. Morpholino sequences 64

Chapter 3.

Table 3.1. Showing genes significantly differentially expressed at day 1 in whole blood in patients with MI compared to UA..... 83

Table 3.2. Genes differentially expressed in MI compared to UA with zebrafish homology..... 86

Table 3.3. PANTHER output for genes that are differentially expressed in MI compared to UA. 89

Chapter 4.

Table 4.1. Table of KIAA1109 in human tissue from KIAA1109 EST profile..... 100

Table 4.2. Table of KIAA1109 in developmental stages from KIAA1109 EST profile..... 101

Chapter 5.

Table 5.1. Differentially expressed genes that are up regulated by KIAA1109 knockdown. 150

Table 5.2. Differentially expressed genes that are down regulated by KIAA1109 knockdown. 151

Table 5.3. PANTHER output of differentially expressed genes of KIAA1109 morphants.....	154
--	-----

Abstract

Background: I aimed to identify genes that are differentially expressed in whole blood in patients following myocardial infarction (MI) and assess these functionally in zebrafish.

Methods: We recruited patients admitted with acute coronary syndromes (MI or unstable angina). We performed whole genome microarrays on RNA extracted from whole blood at 1, 3, 7, 30 and 90d post admission, comparing the whole blood transcriptome of patients with MI with unstable angina. I then assessed the role of one such candidate (KIAA1109) in zebrafish cardiovascular development.

Results: From >54000 genes assessed, 39 genes were significantly differentially expressed in peripheral blood at 1d post MI, returning to baseline at later time points. 27 of these 39, have clear zebrafish homologues, 14 with protein similarity >50%. 9 genes were up regulated in MI, while 5 were down regulated, including a gene of unknown function; KIAA1109. I therefore knocked down KIAA1109 in developing zebrafish and assessed its role in vascular development. I also performed a microarray comparing whole embryo RNA from 36h post fertilization KIAA1109 morphants with control to assess the transcriptional effect of loss of function of KIAA1109.

KIAA1109 morphant Fli1:GFP/Gata1:dsRED transgenic zebrafish were examined by confocal microscopy for evidence of vascular abnormalities. KIAA1109 morphants developed cerebral haemorrhage (3dpf control 10%, vs. KIAA1109 morphants 50% $p < 0.05$). KIAA1109 knockdown induced a significant decrease in the number of endothelial cells (EC) in the forebrain of KIAA1109 morphants (47 ± 4 vs. 73 ± 6 in control) and hindbrain (53 ± 4 morphants vs. 95 ± 7 in control) at 2dpf. There was a significant decrease in the number of EC nuclei in the cardinal vein of KIAA1109 morphants (68 ± 6 vs. 101 ± 8 in control). The phenotype of KIAA1109 knockdown was rescued by administration of the VEGF inducer GS4012.

The microarray of total RNA from 36hpf KIAA1109 morphants identified genes that were significantly down regulated by KIAA1109 knockdown such as protocadherin 1

gamma 2, involved in the cadherin-signalling pathway and ligand of numb-protein X1, involved in the NOTCH pathway.

Conclusion: KIAA1109 is significantly down regulated in human whole blood 1d post MI. Knockdown of KIAA1109 induces severe cerebral haemorrhage in developing zebrafish and significant differential expression of important developmental genes. Functional and transcriptomic assessment in zebrafish suggests KIAA1109 is required for vascular integrity and may be a therapeutic target post MI.

Outcomes from the following work

Publications:

“Loss-of-function of kiaa1109 impairs vascular integrity and induces cerebral haemorrhage in zebrafish embryos.” Sara Solaymani-Kohal, Caroline Gray, Timothy JA Chico. (In preparation)

Presentations:

Oral presentations:

- **17th International Vascular Biology Meeting 2012, Wiesbaden, Germany**

“KIAA1109 is differentially expressed in whole blood in humans and is required for vascular integrity in zebrafish” *Sara Solaymani-Kohal*, Dr Marta Milo and Dr TJA Chico

- **14th Imperial College London Symposium, 2011**

“KIAA1109 is differentially expressed in whole blood in humans and is required for vascular integrity in zebrafish” *Sara Solaymani-Kohal*, Dr Marta Milo and Dr TJA Chico

Poster presentations:

- **10th International conference of zebrafish development and genetics, Wisconsin, 2012**

“KIAA1109 is differentially expressed in whole blood in humans and is required for vascular integrity in zebrafish” *Sara Solaymani-Kohal*, Dr Marta Milo and Dr TJA Chico

- **BAS/BSCR Meeting. Manchester, 2012**

“KIAA1109 is differentially expressed in whole blood in humans and is required for vascular integrity in zebrafish” *Sara Solaymani-Kohal*, Dr Marta Milo and Dr TJA Chico

- **7th European Zebrafish Meeting. Edinburgh, 2011**

“KIAA1109 is differentially expressed in whole blood early after myocardial infarction in humans and is required for vascular integrity in zebrafish” *Sara Solaymani-Kohal*, Dr Marta Milo and Dr TJA Chico

Abbreviations

ACS	Acute coronary syndrome
ACV	Anterior cardinal vein
BA	Basilar artery
CAD	Coronary artery disease
CADi	Coronary artery disease index
CAMK2g2	Calcium/calmodulin-dependent protein kinase
CCV	Common cardinal vein
CHD	Coronary heart disease
CK	Creatine kinase
CtA	Central artery
cTn	Cardiac troponins
DAVID	Database for annotation, visualisation and integrated discovery
DIG	Digoxigenin
DLV	Dorsal longitudinal vein
dpf	Days post fertilization
EC	Endothelial cell
ECG	electrocardiograph
FC	Fold change
fli-1	Friend leukaemia integration 1
fps	Frames per second
FSA	Fragile site associated
GFP	Green fluorescent protein
GRIN1a	Glutamate receptor, ionotropic, N-methyl D-aspartate 1a
dpf	Hours post fertilization
HYB-	Hybridization mix minus tRNA
ICAM	Intracellular adhesion molecule
IOC	Inner optic circle
IPH	Interplaque haemorrhage
IVT	in vitro transcription
LDA	Lateral dorsal artery
LDL	Low density lipoprotein
LNX1	Ligand of numb protein X-1
MCeV	Mesencephalic vein
MCP-1	Monocyte chemotactic protein 1
MCV	Middle cerebral vein
MI	Myocardial infarction
mib	Mindbomb
miRNA	Micro RNA
MMP	Matrix metalloproteinases
mRNA	Messenger RNA

Msv	Mesencephalic vein
MtA	Mesencephalic artery
NCA	Nasal ciliary artery
NDR2	Nodal related 2
NGH	Northern general teaching hospital
NIHR	National institute of health research
NSTEMI	Non ST elevation myocardial infarction
OV	Optic vein
Ox-LDL	Oxidised LDL
PAK2A	p21-activated kinase 2a
PANTHER	Protein analysis through evolutionary relationships
PBT	Phosphate buffered saline + tween 20%
PCDH1y2	Protocadherin 1 gamma 2
PCeV	Posterior (caudal) cardinal vein
PCI	Percutaneous coronary intervention
PHBC	Primordial hindbrain channel
PHS	Primary head sinus
PIV	Particle image velocimetry
PMBC	Primordial hindbrain channel
PPLR	Probability of positive log ratio
PPrA	Primitive prosencephalic artery
PrA	Prosencephalic artery
PUMA	Propagating uncertainty in microarray analysis
qRT-PCR	Quantitative real time polymerase chain reaction
RA	Rheumatoid arthritis
RAS	Renin-angiotensin system
rcf	Relative centrifugal force
Ren	Renin
ROS	Reactive oxygen species
RT	Room Temperature
SMC	Smooth muscle cell
SSC	Saline-sodium citrate
STEMI	ST elevation myocardial infarction
STRING	Search tool for the retrieval of interacting genes/proteins
T1D	Type 1 diabetes
TPM	Transcripts per million
UA	Unstable angina
VA	Ventral aorta
VCAM	Vascular cell adhesion molecule
VE-cadherin	Vascular endothelial cadherin
VEGF	Vascular endothelial growth factor
VEGFR	Vascular endothelial growth factor receptor
WISH	Whole mount <i>in situ</i> hybridization
YSL	Yolk syncytial layer

Chapter 1. Introduction

1.1. Cardiovascular disease

Coronary heart disease (CHD) is the leading cause of adult mortality in the UK, killing one in four men and one in six women. In the UK, approximately 94,000 deaths occur each year due to CHD with an estimated 2 million people living with angina (NHS).

1.1.1. Atherosclerosis

Atherosclerosis is a progressive disease that starts at an early age and develops at a rate dependent upon factors such as exercise, diet and genetic predisposition (Glass and Witztum, 2001).

Endothelial dysfunction is the initial trigger for atherosclerosis arising due to events such as vessel injury or changes in haemodynamic force (Papaioannou et al., 2006). This leads to up-regulation of adhesion molecules/receptors such as vascular cell adhesion molecule (VCAM) and intracellular adhesion molecule (ICAM). This allows monocytes to adhere to the endothelium and with the help of monocyte chemoattractant protein 1 (MCP-1) differentiate into macrophages (Hansson, 2009), (Tiwari et al., 2008). These then accumulate oxidised low-density lipoprotein (Ox-LDL) leading to formation of foam cells.

Simultaneous to these events, smooth muscle cells (SMCs) migrate from the medial portion of the arterial wall and with the foam cells form a fibrous plaque within the intima. Plaque formation leads to an inflammatory response in which macrophages undergo apoptosis leading to their phagocytic clearance, inducing release of metalloproteases which alongside neovascularization leads to plaque instability and rupture (Moulton, 2007). Following plaque rupture, blood is

exposed to the lipid rich necrotic plaque core, stimulating a coagulation cascade of platelet activation leading to thrombus formation (Croce and Libby, 2007) which can precipitate disease such as stroke or myocardial infarction. Figure 1.1 summarises the processes of atherogenesis.

1.1.2. Plaque Neovascularization

In a healthy state neovascularization is essential for maintaining haemostasis and restoration of healthy tissue (Moreno et al., 2012). In a normal vessel wall oxygen diffuses through the lumen to the intima; however when an atherosclerotic lesion evolves, luminal surface increases and exceeds the oxygen diffusion threshold, causing local hypoxia and inducing neovascularization (Moreno et al., 2012). The presence of neo-vessels makes the plaque prone to rupture due to their fragile structure, making them susceptible to interplaque haemorrhage. This neo-vessel haemorrhaging releases red blood cells into the plaque, increasing lipid peroxidation and macrophage activation. The presence of neo-vessels in plaques provides potential therapies using anti angiogenic therapy to prevent erythrocyte accumulation in the plaque (Jain et al., 2007).

1.1.3. Acute coronary syndromes

Acute coronary syndrome (ACS) is a term used which encompasses a wide range of presentations induced by acute plaque rupture, including myocardial infarction and unstable angina (UA). Diagnosis of disease is based on electrocardiographic (ECG) changes and biochemical cardiac markers.

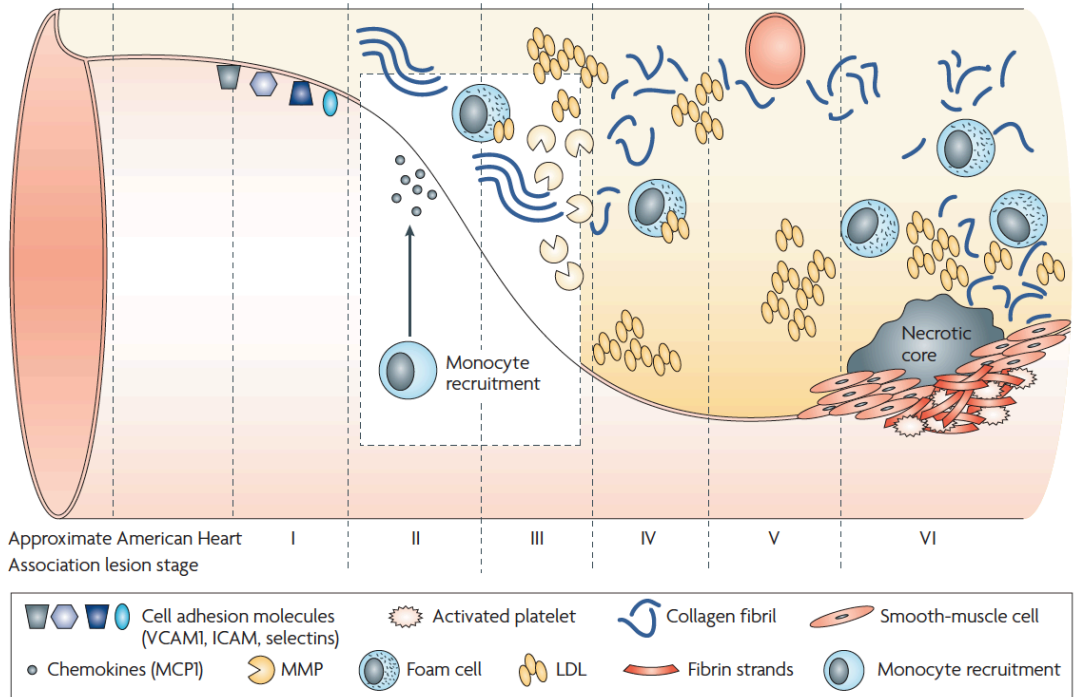


Figure 1.1. Simplified summary of mechanisms and processes in plaque formation
 Adapted from (Lindsay and Choudhury, 2008). Reprinted by permission from Macmillan Publishers Ltd: *Nature Reviews Drug Discovery* 7, 517-529 (June 2008) | doi:10.1038/nrd2588

1.1.3.1. Myocardial infarction

Upon plaque rupture the contents of the plaque are released into the blood and a coagulation cascade is triggered leading to complete or partial obstruction of an epicardial coronary artery, diminishing the availability of oxygen to cardiac muscle causing necrosis.

Upon admission to hospital with chest pain the standard diagnostic investigation is an electrocardiograph. A normal ECG reading is shown in figure 1.2.

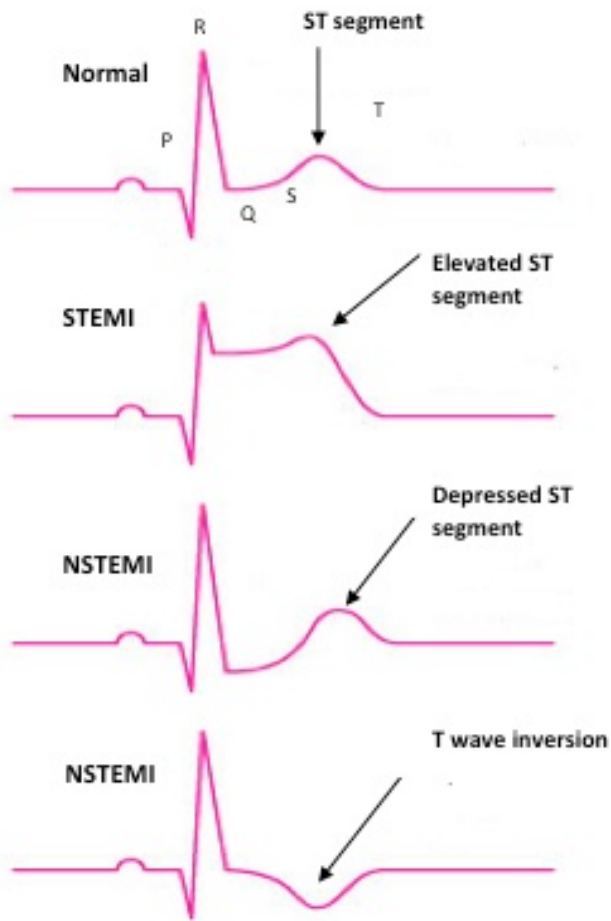


Figure 1.2. Electrocardiographic changes seen in ACS

Single lead ECG readings in different disease states, normal, ST-elevation and Non-ST elevation myocardial infarctions. (Clinical diagnosis requires at least a 12-lead ECG, where these features may be seen in only one or two leads.)

An ECG with an elevated ST segment demonstrates that the patient has suffered an ST elevation myocardial infarction (STEMI), which is generally the most severe form of ACS. An elevated ST segment indicates a significant amount of the heart has been compromised.

When the ECG displays either a depressed ST segment or an inverted T wave a diagnosis of Non-ST elevation myocardial infarction (NSTEMI) is made, although NSTEMI can occur with no ECG abnormalities. Such patients have suffered damage to the heart but the coronary artery is usually not completely occluded, with myocardial necrosis often the consequence of microvascular obstruction due to thrombus embolization from the ruptured plaque (Abbate et al., 2012)

Although diagnosis of STEMI is usually obvious due to typical ECG changes, diagnosis of both STEMI and NSTEMI requires evidence of myocardial necrosis, typically by elevation or serum troponin levels. In the absence of myocyte necrosis, patients are generally considered to be suffering from unstable angina. (Antman et al., 1996).

Unstable angina increases the risk of suffering a subsequent MI with 12% of patients with unstable angina progressing to myocardial infarction within 2 weeks (Gazes et al., 1973, Rahimtoola et al., 1983). One-year mortality of patients with unstable angina ranges from 5-14% with approximately half of deaths occurring within 4 weeks (Rahimtoola et al., 1983). Unstable angina patients are prescribed aspirin, which reduces the risk of thrombosis by inhibiting platelet aggregation and decreases cardiac death or nonfatal MI by 30-51% (Verheugt et al., 1990).

1.2. Role of peripheral blood components in Acute Coronary Syndromes

As described above, the interaction between circulating blood and the ruptured plaque is central to development of ACS. Blood is a complex mixture of cellular and soluble factors, many of which play a proven or potential role in both atherogenesis and ACS. Below, I outline these components.

1.2.1. Platelets

The first step of thrombus formation includes platelet adhesion, activation and aggregation. Platelet adhesion is triggered by exposure of plaque components to the blood. Upon platelet adhesion the thrombotic response is amplified and inflammatory cells such as monocytes are recruited to the site of injury. This increases secretion of adhesion molecules, sometimes leading to occlusion of the artery and tissue death. Due to the important role of platelets in MI Trip *et al* suggested that the use of platelet aggregation markers could be used to predict future coronary events in MI survivors (Trip *et al.*, 1990). Preventive approaches using therapies to prevent platelet aggregation reduce the risk of sudden death or non-fatal MI (Wada *et al.*, 2010). Patients with angina have elevated circulating thrombin (Abbate *et al.*, 2012) and in unstable angina an increased expression of monocyte pro-coagulant activity may be the cause of augmented thrombin formation (Neri Sernerri and Modesti, 1991). Neri *et al* found that increased monocyte tissue factor activity was not due to coronary artery disease (CAD) but unstable angina as they are not detectable in the same patients restudied 8-12 weeks later (Neri Sernerri *et al.*, 1997).

1.2.2. Leukocytes

Leukocytes are white blood cells and have many subsets including monocytes and macrophages. Total peripheral leukocyte count correlates with severity of coronary atherosclerosis and can be used as a predictor of cardiovascular outcome (Grimm et al., 1985). Endothelial dysfunction triggers an inflammatory response, attracting monocytes and macrophages to the site of injury. Monocytes are actively involved in atherosclerotic progression and lesions contain a large number of lipid-laden macrophages, known as foam cells, derived from circulating monocytes (Shimada, 2009). The interaction between monocytes, neutrophils and platelets leads to leukocyte activation and cell-adhesion molecule expression, and activates release of enzymes such as Matrix Metalloproteinases (MMPs), which degrade the subendothelial basement membrane, leading to plaque rupture or thrombogenicity.

The formation of monocyte-platelet aggregates is important in constituting a pro-coagulant state in ACS patients (Shantsila and Lip, 2009) and has been shown to be an early marker of acute myocardial infarction and to cause complications after percutaneous coronary intervention (PCI) (Shantsila and Lip, 2009).

1.2.3. Erythrocytes

Interplaque haemorrhage (IPH) is defined as red blood cell extravasation admixed with fibrin and platelet matrix within the plaque (Moreno et al., 2012). IPH also contributes to increase in plaque burden. Erythrocyte membranes are very rich in cholesterol, contributing to lipid expansion (Kolodgie et al., 2003).

This may explain the rapid progression of advanced, high-risk plaques, in which up to 40% display IPH (Moreno et al., 2012). Red blood cell lysis releases free haemoglobin (Hb), generating reactive oxygen species (ROS) and increases lipid peroxidation and macrophage activation within the atherosclerotic plaque (Moreno et al., 2009). Plaques with IPH are associated with rapid progression of disease, recurrent haemorrhage, and clinical events (Takaya et al., 2005).

1.2.4. Plasma Factors

The main role of plasma is to transport components of the blood throughout the body. It is 55% of blood volume and contains antibodies and clotting factors.

The higher concentrations of plasma tissue factor in unstable angina patients are related to a marked increase of thrombin generation, suggesting a key role of this glycoprotein in initiating coagulation (Abbate et al., 2012).

Fibrinogen is a key player in blood coagulation and there is compelling evidence indicating that raised plasma fibrinogen level is a major risk predictor for myocardial infarction and stroke. Furthermore, raised fibrinogen level predisposes to the development of advanced atherosclerotic plaques (Motterle et al., 2012). Thrombin interacts with fibrinogen, forming fibrin and inducing activation of factors V, VIII and XII that amplify the coagulation cascade, until clot formation and cross-linking with factor XIIIa. Thrombin formed during the initial phases of coagulation is increased by a positive feedback loop and platelet activation (Abbate et al., 2012).

1.3. Use of microarrays for gene expression profiling

Alongside the sequencing of the human genome, advances in microarray technology permit large-scale genomic studies in clinical medicine. Previously methods such as northern blotting were used to measure individual gene expression, but could only examine a few genes at a time. Microarrays permit expression of thousands of genes to be quantified simultaneously; so-called *transcriptional profiling*. In this approach, changes in gene expression that occur normally or as a response to disease are determined through quantification of thousands of individual cDNAs in a single sample. Under certain physiological and pathologic conditions, gene expression can alter and this can be investigated by transcriptomic analysis (Burgess, 2001).

Microarrays consist of a chip or slide that contains thousands of antisense DNA sequences, which bind complementarily to cDNA, which has been labelled to allow quantification of binding. The initial, and most important step is RNA isolation. Acquiring a high quality, reproducible concentration of RNA is essential for sensitivity and therefore accuracy of the microarray results. Lander *et al* showed that differential expression can be detected between batches of cultured cells with the only difference being the media in which they are cultured (Lander, 1999). Expression profiling of blood samples require additional treatment in order to remove globin mRNA as it can reduce the sensitivity of the hybridization results. Kits have been designed to stabilize RNA in order to increase sensitivity. If RNA levels are low techniques such as linear

amplification are used to enhance the quantity of RNA to allow accurate gene expression profiling.

Affymetrix GeneChips use a single fluorescent probe, which is attached to the cDNA through a series of washes, designed to increase the intensity of the signal upon imaging. To further increase gene specificity they also have a unique design printed with a pair of probes for each target called a probe set, which is made of 11-22 oligonucleotides and is 25 base pairs long. One is a perfect match (PM) probe, and the other a mismatch (MM) probe. PM probes are complementary strands to the RNA of interest; MM probes are created by alteration of the 13th base pair in the PM probe (Irizarry et al., 2003). The mismatch probe measures the level of *cross hybridization*, and so the more targets hybridized to the MM probe, the greater the error at that point and genes with significant MM intensities can be excluded by analysis software to provide a more significant list of genes that are differentially expressed.

1.3.1. Whole blood gene expression profiling in cardiovascular disease

When investigating human disease researchers have used peripheral blood as a high throughput, non-invasive and practical source of RNA that can provide insight into subtle changes in the body in response to disease as well as treatments (Taurino et al., 2010).

The rationale for using peripheral blood in investigating CHD is that after a myocardial infarction for example, there is a well-characterized inflammatory response to the event and initially, polymorphs migrate into the ischemic tissue

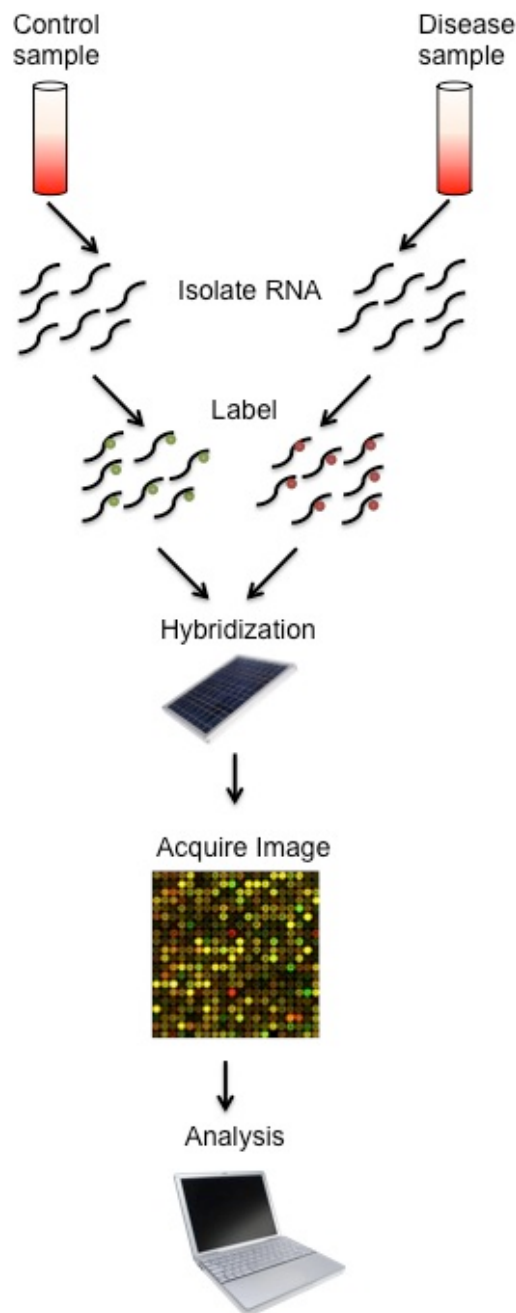


Figure 1.3. A summary of the microarray process

RNA is isolated from control and sample cells, fluorescently labelled and hybridized into a microarray chip. The chip is then imaged and then normalized and analysed accordingly.

followed by a more prolonged and extensive monocyte–macrophage infiltration (Sinnaeve et al., 2009). Taurino *et al* carried out a microarray using microRNA (miRNA) and mRNA extracted from whole blood of coronary artery disease patients before and after completion of cardiac rehabilitation programme following surgical coronary revascularization (Taurino et al., 2010). They identified several differentially expressed miRNA such as Has-miR-92, which modulates neointima formation in a rat model of vascular injury (Cheng et al., 2006). This approach may identify and can help identify other genes and pathways that play a role in the pathogenesis and progression of coronary artery disease (CAD) (Taurino et al., 2010).

Sinnaeve *et al* selected patients according to their coronary artery disease index (CADi), a validated angiographical measure of the extent of coronary atherosclerosis that correlates with outcome (Sinnaeve et al., 2009). They found 160 differentially expressed genes involved in apoptosis, cell adhesion and inflammatory and immune response processes known to modulate atherosclerosis. The identified differentially expressed gene expression correlated with the severity of angiographically documented coronary artery atherosclerosis validated by *in situ* expression. This supports the concept that peripheral blood expression may reflect pathophysiology in the vascular wall. In addition to the studies in cardiovascular disease, whole blood gene expression profiling has identified specific gene expression signatures associated with the development of autoimmune type 1 diabetes (Reynier et al., 2010).

1.4. Zebrafish are a useful tool for gene function assessment

The zebrafish is being increasingly used as a genetic model for the assessment of disease. Although less homologous to the human genome than mammalian models, its high fecundity, low maintenance cost and ease of genetic manipulation makes it a very good candidate for gene function assessment. In regards to cardiovascular research its greatest asset is optical clarity, in which organogenesis, cardiac contraction and circulation can be directly observed. The zebrafish embryo can survive and develop without circulation, as shown by the *gridlock* mutant, which suffers an aortic occlusion, since the embryo can oxygenate via diffusion (Jia et al., 2007). Vascular development can be visualised using transgenics that label specific cell types (Lawson and Weinstein, 2002, Asakawa and Kawakami, 2008, Jin et al., 2005).

1.4.1. Vascular formation in the zebrafish

Blood vessels in a zebrafish embryo are composed of a single endothelial cell layer surrounded by supporting mural cells (Santoro et al., 2009). Vasculogenesis is the primary process in which blood vessels form from the coalescence of angioblasts. The second process, angiogenesis, is the formation of new vessels from pre-existing ones. Lawson *et al* developed a *fli1:EGFP* transgenic embryo, in which endothelial cells express enhanced green fluorescent protein (GFP), to better visualize embryonic angiogenesis during vascularization of the developing zebrafish brain (Lawson and Weinstein, 2002). At approximately 24 hours post fertilization (hpf), circulation commences and the lateral dorsal aorta (LDA) is formed (Isogai et al., 2001).

The LDA helps supply cranial blood flow by forming serial connections with the aortic arches (Fujita et al., 2011). At 2 days post fertilization (dpf) the middle cerebral vein (MCV) in the brain and mesencephalic vein (MCeV) in the hindbrain form. From 2-3dpf the complex central artery network, which forms via sprouting angiogenesis, forms in the hindbrain (Fujita et al., 2011). 1-3dpf brain vascular formation can be seen in figure 1.4.

1.4.2. Vascular Endothelial Growth Factor (VEGF)

Vascular Endothelial Growth Factor (VEGF) is a major driver of vasculogenesis, angiogenesis and vascular permeability. It has also been implicated in vascular protection and maintenance (Zachary et al., 2000). Mammalian VEGFs bind to VEGF receptor (VEGFR) tyrosine kinases. VEGFA and B bind to VEGFR1, VEGFA and E bind to VEGFR2 and VEGFC and D bind to VEGFR3 (Olsson et al., 2006).

Buchner *et al* identified the *redhead* mutant, which displays cerebral haemorrhages between 2-3dpf due to a mutation in the p21-activated kinase 2a (*pak2a*), part of the PAK family which is activated by VEGF and has been implicated in angiogenesis *in vitro*. Gene knockdown of *pak2a* resulted in normal vessel patterning and cerebral haemorrhaging, indicating that loss of *pak2a* leads to a vascular integrity defect without affecting vascular patterning (Buchner et al., 2007).

Formation of the vasculature can be abolished by VEGF disruption. Fujita *et al* treated embryos with SU5416, a VEGF inhibitor drug, and found that embryos had a disruption in the primordial hindbrain channel formation (Fujita et al., 2011). Conversely, Peterson *et al* used GS4012, a VEGF inducer, to rescue

circulation in *gridlock* mutants, by correcting the aortic coarctation of the mutant (Peterson et al., 2004). Examining neovascularization in a zebrafish tumour model Zhao *et al* found the presence of VEGFR2 positive endothelial cells during formation of the tumour vascular network and that treatments with

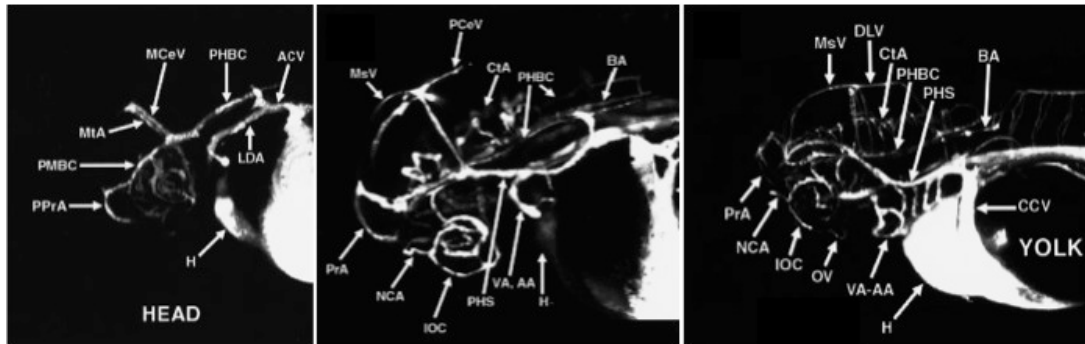


Figure 1.4. An illustration of brain vascular formation in 1-3dpf zebrafish

The illustrations show brain vasculature formation as of 1dpf (left panel), 2dpf (middle panel) and 3dpf (right panel).

Abbreviations are as follows: **ACV** Anterior cardinal vein, **BA** Basilar artery, **CCV** Common cardinal vein, **CtA** Central artery, **DLV** Dorsal longitudinal vein, **IOC** Inner optic circle, **LDA** Lateral dorsal artery, **MCEV** Mesencephalic vein, **MCV** Middle cerebral vein, **MtA** Mesencephalic artery, **NCA** Nasal ciliary artery, **OV** Optic vein, **PCeV** Posterior (caudal) cardinal vein, **PHBC** Primordial hindbrain channel, **PHS** Primary head sinus, **PMBC** Primordial hindbrain channel, **PPrA** Primitive prosencephalic artery, **PrA** Prosencephalic artery, **VA** Ventral aorta.

Adapted from Isogai et al.

Adapted and Reprinted from The vascular anatomy of the developing zebrafish: an atlas of embryonic and early larval development. *Dev Biol*, 230, 278-301, with permission from Elsevier

SU5416 significantly inhibited vascularization and growth of melanoma xenografts, but had little effect on normal vessels (Zhao et al., 2011).

1.4.3. Vascular integrity

Blood vessels consist of two main cell types, endothelial cells lining the vessel and peri-endothelial cells. EC survival is promoted by a number of factors the most prominent being VEGF. ECs are linked together by adherens junctions, vascular endothelial (VE)-cadherin that interacts with catenins, namely beta-catenin, as a binding partner to ensure vessel integrity. The zebrafish *VE-cadherin* gene is specifically expressed in the vascular endothelial cell lineage beginning with the differentiation and migration of angioblasts and persists throughout vasculogenesis, angiogenesis, and endocardium development (Larson et al., 2004). In addition, an elegant study on lumen formation in zebrafish demonstrated the presence of β -catenin, a binding partner of VE-cadherin, in EC-EC contacts (Jin et al., 2005).

Several signalling mechanisms are involved in vascular formation. Notch signalling plays an important role in blood vessel development as well as arterial-venous formation, inducing an arterial specific fate. Disruption in Notch signalling in the zebrafish mutant *mindbomb* (*mib*) induces severe cerebral haemorrhage as well as the reduction of expression of venous specific markers (Lawson et al., 2001). Using Tg(*fli1*:EGFP);*mib* mutant embryos Lawson *et al* found that the severe haemorrhaging was due to the disorganization of the structure of the hindbrain (Lawson and Weinstein, 2002).

1.5. Genetic manipulation in zebrafish

One of the advantages of zebrafish is ease of genetic manipulation. Notably, transgenic embryos can greatly help in delineating the effects of gene manipulation on organogenesis and development, while morpholino antisense allows rapid and efficient temporary knockdown of gene function.

1.5.1. Transgenesis

Transgenic embryos have been utilised for visualisation of gene expression in different cell types within the embryo. In these embryos the promoter region of the gene of interest is used to drive expression of an exogenous protein, such as green fluorescent protein. Double transgenesis or the crossing of two transgenic lines allows simultaneous visualisation of multiple components.

Although creating a stable transgenic line can be time consuming, it is extremely useful for investigations in adult fish as well as during embryonic development.

Targeted vascular reporter expression was established by Lawson *et al* by expressing GFP in *friend leukaemia integration 1 (fli-1)* positive cells which are specific to endothelial cells (Lawson and Weinstein, 2002). Long *et al* used the *GATA-1* promoter (an erythroid- specific transcription factor) to produce a transgenic (Long et al., 1997) that labels erythrocytes with dsRED.

1.5.2. Use of antisense oligonucleotides for gene knockdown

Use of antisense oligonucleotides for gene knockdown was developed by Izant and Weintraub in 1984 and first used on *xenopus* oocytes (Izant and Weintraub, 1984). Morpholino antisense oligonucleotides are synthetic ~25 base pair

oligos designed to block translation by targeting the 5'UTR or modifying pre-mRNA splicing by targeting splice junctions and preventing expression of the gene of interest. Morpholinos are injected at the 1-4 cell stage for optimum gene function knockdown. Morpholinos are similar to DNA and RNA nucleotides however have a morphine ring as opposed to a ribose ring. They also do not carry a negatively charged backbone and are therefore less likely to interact non-specifically (Eisen and Smith, 2008). Quantification of the effectiveness of the knockdown can be carried out by western blotting for the translational blocking morpholino and RT-PCR for splice blocking morpholinos. A morpholino oligo is different from natural nucleic acids, with morpholine rings replacing the ribose or deoxyribose sugar moieties and non-ionic phosphorodiamidate linkages replacing the anionic phosphates of DNA and RNA. Each morpholine ring suitably positions one of the standard DNA bases (A,C,G,T) for pairing, so that a 25-base morpholino oligo strongly and specifically binds to its complementary 25-base target site in a strand of RNA via Watson-Crick pairing. Because the uncharged backbone of the morpholino oligo is not recognized by enzymes or signalling proteins, it is not degraded by nucleases and does not trigger an innate immune response through the Toll-like receptors (Eisen and Smith, 2008). This avoids the problems of oligo degradation, inflammation and interferon induction, which are commonly encountered with other gene knockdown reagents (Summerton, 2007). Table 1.1. outlines the main advantages and disadvantages of morpholino technology.

Table 1. 1. Advantages and disadvantages of morpholino technology

Advantages	Disadvantages
<ul style="list-style-type: none"> • Resistant to nucleases and therefore stable (Eisen and Smith, 2008) • Can inhibit both zygotic and maternal transcripts (Nasevicius and Ekker, 2000) • No negatively charged backbone therefore less likely to interact non-specifically (Eisen and Smith, 2008) • Rapid phenotype observation • Ease of use 	<ul style="list-style-type: none"> • Off-target effects (Nasevicius and Ekker, 2000) • Difficult to quantify knockdown • Effect wears off in 3-5dpf (Bill et al., 2009)

1.6. Hypotheses

- I hypothesise that peripheral blood gene expression will differ in patients who present with a myocardial infarction compared to those presenting with unstable angina.
- I further hypothesise that examination of the phenotype of zebrafish embryos with induced loss-of-function of the candidates identified above will provide novel data on their role in cardiovascular development.

1.7. Aims

1. Characterise differentially expressed genes in whole blood following ACS
2. Assess function of differentially expressed genes using a zebrafish model

Chapter 2: Materials and Methods

2.1. Patients and Blood Collection

2.1.1. Recruitment criteria

Patients were recruited by the Sheffield NIHR Cardiovascular Biomedical Research Unit, which sought to establish a resource of well phenotyped patients with a range of cardiovascular diseases for basic science and translational research. Patients were approached and consented by research nurses under ethical approval granted to Dr Allison Morton. All patients recruited to the study detailed in this thesis presented to the Northern General Hospital (NGH) in Sheffield with acute onset chest pain of cardiac nature, without evidence of non-cardiac causes for the pain (such as pulmonary embolism or infection, musculoskeletal features, etc). Inclusion criterion for subjects were; acute cardiac sounding chest pain, <48 hours from onset of symptoms. Exclusion criteria were; age <18, years old, serious co-morbidities, end stage renal disease requiring renal replacement therapy, pregnancy.

2.1.2. Patient demographics

50 patients with typical ACS symptoms were recruited from The Northern General Hospital (NGH) Sheffield from April 2009.

Due to the on going and prospective nature of this study, 19 patients with data from each time point up to 3 months have currently been analysed. This is the cohort, which will be described throughout the rest of this thesis. We recruited five patients with UA, ten with NSTEMI and four with STEMI. No patients died during the follow-up. Of these patients, fifteen were men and four were women. Three were aged between 40-50 years old, four were aged between 51-60 years

old, 10 were aged between 61-70 years old and two were aged between 71-80 years old. Fourteen had a positive family history of CAD and 5 had a negative family history of CAD, which was defined as one or more first degree relative affected by CAD. Four were current smokers, nine were ex smokers and six were non-smokers. Nine patients did not suffer from diabetes, six patients suffered from impaired glucose tolerance, two suffered from non-insulin dependent diabetes mellitus and two suffered from insulin dependent diabetes mellitus. All participants were of white British ethnicity. Further details can be found in appendix 1.

2.1.3. Blood collection

Blood was collected from 146 donors. Blood samples were frozen at minus 20°C until transported. RNA was isolated within a week and kept at minus 80°C after extraction. RNA quality was assessed by examining UV absorbance ratios of 260/280 and 260/230 using a NanoDrop® ND-1000 UV-Vis Spectrophotometer (Labtech, East Sussex, UK).

2.2. RNA extraction from human blood

2.2.1. Tempus™ Blood RNA Tube

Protocol was carried out as described by the Tempus™ Blood RNA Tube protocol by Applied Biosystems. 3mL of blood was drawn directly into a Tempus Blood RNA Tube. Immediately after the Tempus tube was filled, the blood was stabilised by vortexing for 20 seconds to ensure that the Applied

Biosystems Stabilising Reagent made uniform contact with the sample. The samples were kept at minus 20°C and transported in dry ice containers. The samples were thawed in the Tempus tube at room temperature (18 to 25 °C) for approximately 20 minutes. The contents were poured into a clean 50mL tube making sure that all the contents were transferred. 1× phosphate-buffered saline (PBS; Ca²⁺/Mg²⁺-free) was added to the transferred blood to bring the total volume to 12mL. The tube was then vortexed vigorously for at least 30 seconds to ensure proper mixing of the contents. The sample was then centrifuged at 4 °C at 3,000 x *g* relative centrifugal force (rcf) for 30 minutes. The supernatant was carefully poured off into a bleach bucket. The tube was inverted on absorbent paper for 2 minutes. The remaining drops of liquid were cleared off the rim of the tube with clean absorbent paper and the inside of the tube was cleaned with medical tissue wrapped around a pipette tip, treated with RNase Zap (Ambion, Warrington, UK). 400µL of RNA Purification Re-suspension Solution was added into the tube, and the sample vortexed briefly to re-suspend the RNA pellet. The re-suspended RNA was kept on ice. The RNA purification filters were pre-wet by adding 100µL of RNA Purification Wash Solution 1 into the purification filter and then left to stand for 1 minute. The re-suspended RNA was transferred from the 50 mL tube into the purification filter, and then centrifuged at 4 °C at 3,000 x *g* (rcf) for 30 sec. The flow-through was discarded and 500µL of RNA Purification Wash Solution 1 was added onto the purification filter, then centrifuged at 4 °C at 3,000 x *g* (rcf) for 30 sec. The flow-through was discarded and 500µL of RNA Purification Wash Solution 2 was added onto the purification filter, then centrifuged at 4 °C at 3,000 x *g* (rcf) for

30 sec. The flow-through was discarded and the sample centrifuged for an additional minute to dry the membrane. The purification filter was transferred to a new collection tube and labelled. 100µL of Nucleic Acid Purification Elution Solution was added into the purification filter and the tube incubated in a heat block for 2 minutes at a temperature of 70°C, then centrifuged for 30 seconds at 3,000 x *g* (rcf). The collected RNA was eluted back into the purification filter, and then centrifuged for 2 minutes at 3,000 x *g* (rcf). The purification filter was discarded and 90µL of the RNA was transferred to a labelled cryovial and the remaining RNA was stored at minus 80°C for long-term storage.

2.3. RNA treatment

2.3.1. Using GLOBINclear™ to deplete haemoglobin RNA

Protocol was carried out as described by the GLOBINclear™ protocol (Ambion, Warrington, UK). Before beginning the experiment a dry incubator was set to 50°C. 2X Hybridization Buffer and the Streptavidin Bead Buffer were warmed to 50°C for at least 15 min before starting the procedure, making sure to vortex well before use. 30µL of Streptavidin Magnetic Beads were used for each sample. The tube of the Streptavidin Magnetic Beads was vortexed to suspend the settled beads, and the volume needed transferred into a 1.5mL non-stick tube provided with the kit. Up to 20 reactions can be processed in a single tube. The tube was briefly centrifuged (<2 sec) at low speed (<1000 x *g*) to collect the mixture at the bottom of the tube. The tube was then placed on a magnetic stand

to capture the Streptavidin Magnetic Beads. The tube was left in the magnetic stand until the mixture became transparent (~3–5 min), indicating that capture was complete. The capture time will depend on the magnetic stand used. The supernatant was carefully aspirated using a pipette without disturbing the Streptavidin Magnetic Beads. The supernatant was discarded, and the tube removed from the magnetic stand. Streptavidin Bead Buffer was added to the Streptavidin Magnetic Beads. The beads were vortexed vigorously until resuspended. The prepared Streptavidin Magnetic Beads were kept at 50°C, the beads should remain at 50°C for at least 15 min before they are used in additional steps. 1–10µg of human whole blood total RNA was added to 1µL of Capture Oligo Mix in a 1.5mL non-stick tube. 15µL of 50°C 2X Hybridization Buffer was added to the sample and vortexed briefly to mix and centrifuged briefly at low speed to collect the contents in the bottom of the tube. The sample was placed in a pre-warmed 50°C incubator which allows the Globin Capture Oligo Mix to hybridize to the globin mRNA for 15 min. The previously prepared Streptavidin Magnetic Beads were removed from the 50°C incubator, and resuspended by gentle vortexing. The sample was then briefly centrifuged (<2 sec) at low speed (<1000 x g) to collect the mixture at the bottom of the tube. 30µL of prepared Streptavidin Magnetic Beads was added to each RNA sample. The RNA bead mixture was placed at 50°C and incubated for 30 min. The sample was removed from the incubator, and vortexed briefly to mix. The sample was then centrifuged briefly at low speed to collect the contents in the bottom of the tube. The Streptavidin Magnetic Beads were captured on a magnetic stand. The tube was left on the magnetic stand until the mixture

became transparent (~3–5 min), indicating that capture is complete. 100µL of pre-prepared RNA Binding Buffer was added to each enriched RNA sample. The Bead Resuspension Mix was vortexed and 20µL immediately dispensed to each sample. The sample was vigorously vortexed for 10 sec to fully mix the reagents, and to allow the RNA Binding Beads to bind the RNA. The sample was then briefly centrifuged (<2 sec) at low speed (<1000 x g) to collect the mixture at the bottom of the tube. The RNA Binding Beads were captured by placing the tube on a magnetic stand. The tube was left in the magnetic stand until the mixture became transparent (~3–5 min), indicating that capture was complete. The supernatant was carefully aspirated using a pipette without disturbing the RNA Binding Beads, discarding the supernatant. 200µL RNA Wash Solution was added to each sample removed from the magnetic stand and vortexed for 10 sec. The RNA Binding Beads may not fully disperse during this step; this is expected, and will not affect RNA purity or yield. The sample was briefly centrifuged (<2 sec) at low speed (<1000 x g) to collect the mixture at the bottom of the tube. The RNA Binding Beads were captured in a magnetic stand as in the previous magnetic bead capture steps and carefully aspirated with the supernatant discarded. Remove the tube from the magnetic stand and briefly centrifuge the tube as in previous steps and place it back on the magnetic stand. Any liquid in the tube was removed with a small-bore pipette tip. The tube was removed from the magnetic stand and the beads were allowed to air-dry for 5 minutes with the caps left open. 30µL of pre-warmed (58°C) Elution Buffer was added to each sample and vortexed vigorously for ~10 sec to thoroughly re-suspend the RNA Binding Beads. The mixture was then incubated at 58°C for 5

minutes. The sample was vortexed vigorously for ~10 sec to thoroughly re-suspend the RNA Binding Beads and centrifuged briefly at low speed as in previous steps to collect the mixture at the bottom of the tube. The RNA Binding Beads were captured in a magnetic stand as in the previous magnetic bead capture steps. The supernatant containing the RNA was collected into a 1.5mL Non-stick tube and stored at minus 20°C.

2.3.2. Agilent Bioanalyzer™ Assessment

The Agilent 2100 Bioanalyzer™ used in conjunction with the Agilent 6000 Nano Kit™ assessed the quality, quantity and integrity of extracted and GLOBINcleared mRNA. This assessment was used as a screening tool to prevent badly degraded samples continuing to Microarray.

The Agilent 2100 Bioanalyzer™ uses Lab-on-a-chip technology to run micro-capillary electrophoresis. This is similar to using standard agarose gel and ethidium bromide capillary electrophoresis but on a much smaller scale. Importantly, as the samples after GLOBINclear™ are only approximately 30µL in volume, this technique requires only 1µL for assessment. The additional information the Bioanalyzer provides is a RNA Integrity Number (RIN). A RIN is achieved based on comparisons made across several regions of the whole electropherogram trace rather than 18s and 28s peaks alone. A RIN is a quantitative assessment of RNA integrity that allows us to compare between data sets. It can therefore provide a numerical benchmark for samples that can continue into further processing. A RIN less than 7 indicates samples that are badly degraded or contaminated and these samples do not continue to

Microarray. As the extraction protocol binds all RNA non-specifically to the filter, there are always small amounts of small RNA such as microRNA present in the samples. These are not contaminants and will not be detected at array as the probes are only designed to bind to mRNAs. All reagents described in this protocol are provided with the Agilent 6000 Nano Kit™. The gel for the analyser was prepared by spinning 550µl of RNA 6000 Nano gel matrix in a spin filter (provided) at 1500g for 10 minutes at room temperature (RT). 1µl of RNA 6000 Nano Dye concentrate was added to 65µl of the filtered gel in an RNase-free microfuge tube forming a gel-dye mix. The solution was vortexed well and centrifuged at 13000g for 10 minutes at room temperature. 9µl of this gel-dye mix was pipetted onto the chip and put under pressure via a syringe and plunger. The plunger was pushed until held by the clip and left in position for exactly 30sec. The clip was released and timed for 5 seconds; the plunger was then gently moved back to its original position. 9µl of gel-dye mix was then added to the two wells marked **G**. 5µl of RNA 6000 Nano Marker was added to each sample well (up to 12 sample wells) and also in the well marked by the ladder symbol. 1 µL of Ladder was added to the well marked by the ladder symbol. 1µl of sample was added to each of the wells. 1µl of RNA 6000 Nano Marker was added to each unused well. The chip was vortexed using the adapter provided for the IKA vortexer for 1 min at 2400rpm. After completion the chip was run in the Bioanalyzer within 5 minutes. mRNA samples achieving a RIN \geq 7 progressed to amplification and labelling.

2.3.3 Linear Amplification and labelling

The Affymetrix GeneChip® 3' IVT Express Kit was used to amplify and label RNA samples before hybridising to Microarray chips. For input samples of RNA 50-500ng, a complimentary DNA strand is synthesized using an oligo(dT) primer with a T7 promoter attached. A second complimentary DNA strand is synthesized from this to produce double stranded cDNA (completing the two reverse transcription stages). Using T7 RNA polymerase, which recognises the T7 promoter, the cDNA is amplified whilst simultaneously incorporating a Biotinylated nucleotide into the sequence (the in vitro transcription step). Labelled aRNA (amplifiedRNA) is gained as output. It is this anti-sense aRNA that will hybridize to the array. Exogenous Poly-A control genes are added at an early stage of this protocol and are amplified and labelled alongside the RNA sample. Analysis of the hybridisation intensities of the poly-A controls enables quantification of the success of the labelling process. This protocol required mRNA to have a starting quantity of 100ng in 3µL of eluate. Some samples however despite satisfactory RINs had a lower concentration than the required 33µL. A protocol was included with the GLOBINclear for mRNA precipitation and concentration; however this involved another interaction with the mRNA and could have stimulated more degradation. The Eppendorf vacuofuge concentrator was used instead to remove some of the supernatant. Running the machine for 7.5 minutes removed approximately 4µL of supernatant and concentrated most of the poorer samples to acceptable levels. Smaller volumes of samples with a higher concentration were aliquoted and brought up to 100ng/3µL with nuclease-free water.

2.3.4 Linear IVT

2.3.4.1. Assembling the first-strand master mix (to synthesize the first-strand cDNA)

For a single reaction, 4 μ L of First-Strand Buffer Mix and 1 μ L First-Strand Enzyme Mix were mixed to create the First-Strand Master Mix. 5 μ L of the First-Strand Master Mix was added to each sample/Poly-A mix and incubated for 2 hours at 42°C in a PCR thermal cylinder.

2.3.4.2 Assembling the Second-Strand Master Mix (to synthesize the second-strand cDNA)

For a single sample, 13 μ L of nuclease-free water, 5 μ L Second-Strand Buffer Mix, 2 μ L second-Strand Enzyme Mix were mixed on ice. 20 μ L was added to each sample and incubated at 16°C for 1 hour, followed by 65°C for 10 minutes. After incubation, samples could be frozen at minus 20°C.

2.3.4.3 Assembling the IVT Master Mix (to label the RNA with Biotin)

For a single sample, 4 μ L Biotin Label, 20 μ L IVT Labelling Buffer and 6 μ L IVT Enzyme Mix were mixed at room temperature. 30 μ L of the IVT Master Mix was added to each sample and incubated at 40°C for 16 hours. The RNA could be frozen at minus 20°C after this incubation if required.

2.3.4.4 Purification of amplified RNA

The amplified samples were purified to remove salts, enzymes and free nucleotides using a magnetic bead method similar to the GLOBINclear protocol. The aRNA elution solution was pre-heated at 60°C for at least 10 minutes. aRNA

binding mix was prepared from 10 μ L of RNA binding beads and 50 μ L Binding Buffer Concentrate for each sample. 60 μ L of Binding Mix was then added to each sample. The samples were transferred to the bottom of a 96 well u-bottomed plate and mixed by pipetting up and down. 120 μ L of 100% ethanol was added to each sample and mixed by pipetting. The plate was *gently* shaken for 4 minutes and then placed on a magnetic stand to capture the beads for 10 minutes. The supernatant was aspirated and discarded.

With the plate removed from the magnetic stand, 120 μ L Wash solution was added to each sample and shaken at a *moderate* speed for 4 minutes to wash the beads. The beads were then recaptured on the magnetic stand for 10 minutes and the supernatant aspirated and discarded. This step was repeated one more time.

The purified RNA was eluted from the beads by adding 50 μ L of pre-heated Elution Solution to sample wells and shaking the plate *vigorously* for at least 6 minutes or until the beads dispersed. The beads were captured for 10 minutes and the supernatant containing eluted RNA was aspirated and placed in a clean PCR tube. RNA could be stored for up to 1 year at minus 80°C at this stage or temporarily stored on ice.

After amplification, aRNA was assessed using the Agilent 2100 Bioanalyzer™ to see if samples had been amplified effectively, remained high quality or if any degradation had occurred.

Samples were then tested using the NanoDrop to achieve an accurate concentration measurement and samples below 700ng/ μ L were repeated.

Different volumes of RNA added to an array can be a major source of interchip variation, which needs to be minimised to allow comparison.

2.3.5 Evaluation and Fragmentation of RNA

RNA molecules are three-dimensional and can take on different structures in space. Secondary and tertiary structures can interfere with RNA hybridization to an array by reducing a probe's ability to capture target RNA. Fragmentation reagents were provided with the 3'IVT Express Kit. 15ng of sample (concentration assessed via NanoDrop) was mixed with 8 μ L 5x Array fragmentation buffer and topped up with nuclease free water to a final volume of 40 μ L. The mixture was incubated at 94°C for 45minutes to fragment. Samples were placed on ice immediately after incubation and assessed again using the Agilent Bioanalyzer. Two distinct peaks should be seen with RNA fragments distribute in the larger peak between 25 and 200nt.

2.4. Hybridization

All reagents described in this section were provided in the GeneChip® Hybridization, Wash and Stain Kit.

A hybridization cocktail was made for each sample containing 12.5ng of fragmented and labelled RNA sample, 4.2 μ L Control Oligonucleotide B2, 12.5 μ L 20X Hybridization Controls, 125 μ L 2X Hybridization Mix, 25 μ L DMSO, and up to 50 μ L Nuclease-free water to take the total volume to 250 μ L. The cocktail was heated at 99°C for 5 minutes then 45°C for 5 minutes in a heat block. It was then spun at maximum speed in a microfuge for 5 minutes. Whilst the solution was

heating, the array was wetted with 200 μ L Pre-Hybridization mix and incubated at 45°C for 10 minutes with rotation (60rpm). The pre-hybridization mix was then removed from the chip and the hybridization cocktail injected in its place. The array was then incubated at 45°C for 16 hours at 60 rpm. After hybridization, the chip was washed using an automated machine, courtesy of Affymetrix, for 2 hours to remove un-hybridized nucleotides and salts and scanned by the computer to construct an array image.

2.5. Microarray

2.5.1. Affymetrix microarray

Human microarrays were carried out by Dr Paul Heath in the University of Sheffield Microarray Core Facility using an Affymetrix HG_U133 plus.2 GeneChip.

To construct an array image, a laser is used to scan the chip and 'excite' labelled targets that have hybridized to probes to emit light. The intensity of light emitted is proportionate to the volume of sample at that particular point and a heat map is produced. So dependable data can be extracted from the array, the array itself needs to be assessed for quality and reliability. Variations within the chip and across chips also need to be accounted for before chips can be compared. To ensure input RNA is of good quality, it is assessed at each stage of handling before array. To quantify labelling and hybridization efficiency however, specific controls are added at the RNA labelling and hybridization steps respectively. Poly-A controls are added during linear IVT to assess

labelling efficiency. These controls, lys, phe, thr and dap are spiked directly into mRNA samples before labelling. Probe sets on the chip contain 3' end probes, mid probes and 5' end probes for each control. As cDNA is synthesized from the 3' end there may be a slightly higher signal from 3' probe sets than 5' probe sets. A ratio (3'/5') in 'spike-in controls' of more than 3 indicates either a problem in the sample itself or in target synthesis. In these cases, data from the chip is questionable and for this study chips that fell below this threshold were run again with fresh mRNA from samples stored in the bio repository. 20X Eukaryotic Hybridization Controls are added to the hybridization cocktail to measure hybridization efficiency. They are comprised of a mixture of biotinylated and fragmented cRNA of the prokaryotic genes; bioB, bioC, bioD and cre. At 1.5 pM, bioB is at the detection limit for most expression arrays and is anticipated to be called 'Present' at least 70% of the time. In contrast, the other controls should be called 'Present' all of the time, with increasing Signal values (bioC, bioD, and cre, respectively). 'Absent' calls, or relatively low signal values, indicate a potential problem with the hybridization reaction or subsequent washing and staining steps. The Affymetrix Microarray scanning software produces a document on Microarray quality including assessment of the two variables above upon which any failed arrays are highlighted. These control procedures ensure that high standards are maintained across arrays to allow accurate comparisons between them. Although variability between arrays can be reduced in this way it is impossible to remove all variation. Normalisation is needed to provide an even platform of expression between chips before fair comparisons can be made.

2.5.2. Validation by quantitative Real Time-PCR

Taqman primers were ordered from the Applied Biosystems website (Biosystems)

qRT-PCR was carried out in accordance with the ABI protocol (Biosystems) using an ABI ht7900 plate reader. Table 2.1. contains the assay ID codes for the used Taqman primer used.

2.5.3. Zebrafish morphant microarray

The KIAA1109 morphant microarray was carried out by the Genome Institute of Singapore. The custom made microarray used as published by Mathavan et al. (Mathavan et al., 2005)

2.5.3.1. Whole embryo RNA extraction

Approximately 300 whole control and KIAA1109 morphant embryos were immersed in tricaine for 20 minutes at 36hpf. The solution was then removed and the embryos washed with PBS. 250µl Tri-reagent (Sigma, T9424) was added and a 25G needle used to homogenize the embryos. 50µl of chloroform was added to the sample and inverted for 15 seconds. The sample was then incubated at room temperature for 3 minutes prior to being centrifuged at 13,000 rpm for 15 minutes at 4°C. The clear supernatant that had risen to the top of the tube was then transferred to a new Eppendorf, to which 85µl of isopropanol was added

Table 2.1. Assay ID of Taqman primers

Gene name	Assay ID
pcdh1g2	AI20S9R
camk2g2	AI39RFZ
ndr2	Dr03125298_m1
grin1a	Dr03091890_m1
renin	Dr03081915_m1
Inx1	Dr03148957_m1

and inverted gently before incubating at room temperature for 10 minutes. The sample was then centrifuged at 13,000 rpm for 15 minutes at 4°C after which the supernatant was discarded and 250µl of 75% ethanol was added to the tube. The sample was then vortexed to dislodge the pellet and centrifuged for 5 minutes at 4°C. The supernatant was discarded and the pellet allowed to air dry for 5 minutes after which the RNA pellet was resuspended in DEPC-H₂O.

2.6. Zebrafish Husbandry

2.6.1. Home Office Regulations

All studies conformed to Home Office regulations for the use of animals in scientific research and were carried out in accordance with project licence number 40/3031 which was then renewed to 40/3434 held by Dr TJA Chico and personal licence number 40/9599 held by myself. Zebrafish were raised and fed by aquarium staff and following a 14:10 hour light:dark cycle.

2.6.2. Embryo Collection

Breeding tanks were set up in adult tanks the previous night consisting of a wire mesh tank with marbles placed within an opaque tank to encourage breeding. The next morning the embryos were sorted into groups of 30 fertilised offspring and placed in Petri dishes containing fresh E3 medium with added Methylene Blue. Embryos were incubated at 28°C up to a maximum of 5.2dpf at which point they were anaesthetized using tricaine and destroyed using bleach.

2.6.3. Zebrafish Strains and Lines Utilised

Listed wildtype and transgenic embryos (table 2.2.) were collected from adult tanks using a breeding trap that prevents adults from ingesting embryos by the presence of a physical mesh barrier. Embryos were sorted into groups of 40 fertilised offspring and placed in Petri dishes containing fresh E3 medium. Embryos were incubated at 28°C for use up to 5.2dpf and remaining embryos were destroyed using bleach.

2.6.4. Zebrafish anaesthesia and mounting

To immobilise embryos for observation, MS222 (Sigma) was used in E3. To observe anaesthetised embryos under a stereo microscope they were mounted on a coverslip in 1% low melting point agarose in E3 and MS222. For longer time lapse imaging an E3 bath was used to prevent the agarose drying out.

2.7 Morpholino injections

Morpholinos were custom designed and purchased from Gene Tools Inc, Oregon, USA. Morpholinos were diluted to a stock solution of 1mM and stored at minus 20°C, aliquots were defrosted and 1:1 ratio of phenyl red was added to aid observation of injection. One-cell stage embryos were injected with 0.5-1nl (0.025pmol) morpholino and kept in E3 medium at 28°C. Sequences can be found in table 2.3. For all morpholino knockdown experiments the start site ATG morpholino was used, unless stated otherwise. All reference to control embryos also refers to the mismatch control morpholino injected embryos.

Table 2.2: Name and phenotype of strains of zebrafish used

Zebrafish Line	Phenotype
Nacre wildtype	Wildtype embryo that lacks pigmentation for easier visualisation
Fli1:GFP/Gata1:dsRED	Fli1 positive cells (endothelial cells) are tagged with GFP and Gata1 positive cells (red blood cells) are tagged with dsRED.
Flk1:GFP-NLS	Flk1 positive cells are tagged with nuclear localised GFP

Table 2.3. Morpholino sequences

	Sequence 5' - 3'	Target
Control	CCTCTTACCTCAGTTACAATTTATA	Mismatch sequence
ATG	GGAGACTGTTGTTGCCTTTATCCAT	Translation blocking
ATG-2	TGCAGATAAACAGAGCGGACATCAC	Translation blocking
Splice	ACAAATCATAAATCACTTACCCACA	Intron -exon 1 boundary

2.8. RNA probe synthesis

Antisense RNA probes were synthesised for KIAA1109. Sense probes were also synthesised as controls. Primers designed using Primer3 software (Primer3Plus) was used for KIAA1109 RNA probe synthesis:

Forward sequence: 5'- TGGAGGTCTCTCATCCCTGT

Reverse sequence: 5'- TTCACACTGCCAGGACTGAG

Amplified cDNAs from reverse transcription-PCR were inserted into pCRII-TOPO cloning vector and grown in selective media. The cloning vectors were then purified using a plasmid midi kit (Qiagen) and then linearized using the appropriate restriction enzymes and purified using the QIAquick PCR purification kit (Qiagen). For KIAA1109 sense probe restriction enzymes KpnI and NEB1 were used and for KIAA1109 antisense probe NotI and NEB3 were used. The linearized plasmid template (1 µg), 2µl of 10X transcription buffer, 1µl of DIG RNA, 2µl of T7 or SP6 RNA polymerase, and RNase-free H₂O were mixed in a total reaction volume of 20 µl. The mixture was incubated at 37°C; after 2 hours, DNase I (10 µl) was added and the incubation continued for another 15 min. After stopping the reaction by adding EDTA (1 µl, 0.5M), LiCl (2.5µl, 4M) and EtOH (75µl, 100%), that had been stored in the minus 70°C for 30 minutes prior to being added. The solution was then centrifuged at 12,000rpm for 30 minutes at room temperature. The pellet was washed with 70% ethanol and then left to dry and re-suspended in 20µl of sterile H₂O and 35µl of 100% formamide and stored at minus 80°C. To dilute the probe to be

used for *in situ* hybridization it was diluted to a 1:200 solution in Hyb- and stored at minus 20°C.

2.9. Whole Mount *In-Situ* Hybridization

Whole-mount *in situ* hybridization was performed according to Thisse *et al* (Thisse and Thisse, 2008).

Embryos were previously fixed in 4% (wt/vol) paraformaldehyde (PFA) and kept in 100% methanol. *Nacre* embryos (Lister *et al.*, 1999) were utilized as they are non-pigmented due to a lack of melanophores and so the stain could be easily visualised. Embryos were then rehydrated by successive five minute incubations at RT in methanol in 1xPBS, 5 min in 75% (vol/vol) methanol; 5 min in 50% (vol/vol) methanol; and 5 min in 25% (vol/vol) methanol and then washed four times, 5 min per wash, in 100% PBT. Embryos were permeabilized by digestion with proteinase K (Roche Diagnostics, cat. no. 1092766, prepared at 10 $\mu\text{g ml}^{-1}$) at RT for 30 mins. This is to allow the probe to enter the cells. It is important to determine the right incubation time, as under-digestion would not allow the probe to get in, whereas over-digestion will alter the morphology of the embryo. The proteinase K digestion was stopped by incubating the embryos for 30 min in 4% (wt/vol) PFA in 1xPBS. Embryos were then washed four times, 5 min per wash, in 1xPBT to remove residual PFA. The embryos were then prehybridized with 700 μl of hybridization mix (HM) for 3 hrs in a 70 $^{\circ}\text{C}$ water bath. The HM was discarded and replaced with 200 μl of HM containing 700 ng of antisense DIG-labelled probe, the right amount of RNA probe should be determined to avoid background labelling. The embryos were then hybridized overnight at 70 $^{\circ}\text{C}$. This high hybridization temperature and the percentage of

formamide in the HM buffer ensure high stringency of hybridization and decrease the occurrence of cross-hybridization.

The embryos were then washed for 10 min in pre-warmed at 70 °C solutions of 75% HM, 50% HM, 25% HM and 100% 2xSSC. Embryos were then washed twice, for 30 min per wash, in 0.2xSSC at 70 °C, which prevents nonspecific hybridization of the probe. The embryos were then put through a series of 10 min washes in 75% 0.2xSSC, 50% 0.2xSSC, 25%, 0.2xSSC and 1xPBT. The embryos were then incubated for 3 hrs at RT in blocking buffer; this saturates nonspecific binding sites for the antibody. The embryos were then incubated with anti-DIG antibody solution diluted at 1/10,000 with blocking buffer at 4 °C with gentle agitation at 40 r.p.m. overnight. The antibody solution was then discarded and embryos washed briefly in PBT. Embryos were then washed six times, 15 min per wash, in PBT at room temperature with gentle agitation at 40 r.p.m. Embryos were then incubated at RT three times, 5 min per wash, in alkaline Tris buffer with gentle agitation at 40 r.p.m. The alkaline Tris buffer was replaced with freshly prepared staining solution and kept in the dark at RT with gentle agitation 40 r.p.m. Once the desired staining intensity was reached the reaction was stopped by washing embryos in 1xPBT four times, 5 min per wash, in 4%PFA for 20 min, 1xPBT for two ten min washes and finally a series of 5 min washes in 25%, 50% and 75% glycerol. For observation the embryos were mounted in 100% glycerol. A Nikon Coolpix5400 camera was attached to a Nikon SMZ1500 stereomicroscope to capture images of the embryos.

2.10. Phenotypic analysis of KIAA1109 knockdown

2.10.1. Heart rate measurements

Heart rates were measured (without the administration of tricaine) in embryos by counting heart beat number for thirty seconds. This was then multiplied by two and expressed as beats per minute.

2.10.2. Velocity calculation measurements

Embryos were mounted in 1% low melting point agarose and recorded on Video Savant 4.0 software at 300 frames per second (fps) using a high speed camera (Olympus IX81). Erythrocyte velocity in the arterial and venous circulation of the embryos was calculated using particle image velocimetry (PIV) software (LaVision - DaVis). Measurements were taken at the sites of interest (shown in figure 2.1.) of which the mean was plotted.

2.10.3. Vessel diameter measurements

Embryos were mounted in 1% low melting point agarose and recorded on Video Savant 4.0 software at 300 frames per second (fps) using a high speed camera (Olympus IX81). Images were then saved as one extended image. Measurements were taken at the sites of interest (shown in figure 2.1.) using ImageJ and the diameter calculated from pixels to μm of which the mean was plotted.

2.10.4. Haemorrhage volume quantification

Embryos were mounted in 1% low melting point agarose and z-stack images were taken through the head using a spinning disc confocal microscope (Perkin

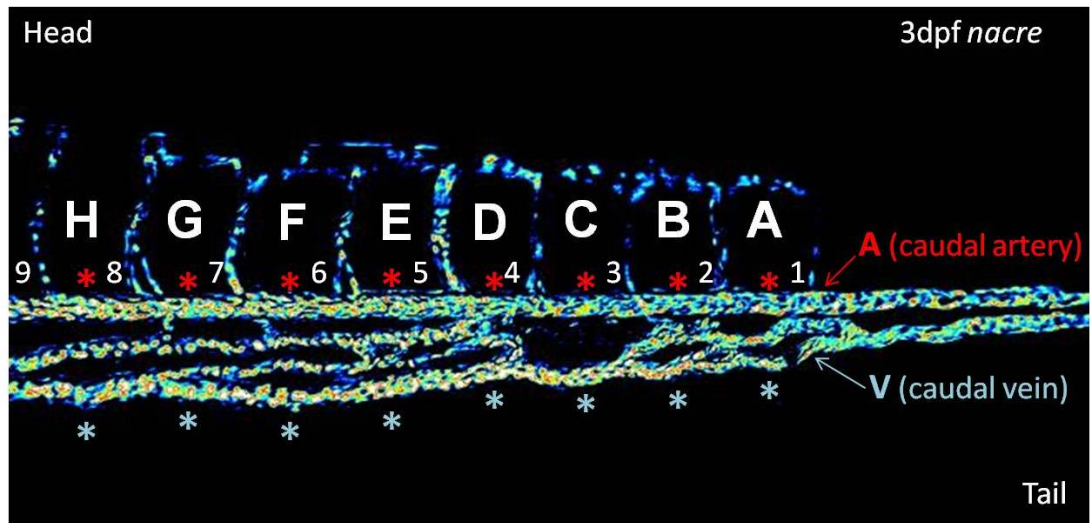


Figure 2.1. Sites of measurements of vessel size and haemodynamics.

Measurements were taken from the tail to the head. The numbers show the number of intersegmental vessels. The red stars represent the location of arterial measurements. The blue stars represent the location of venous measurements. The letters represent the space in-between the intersegmental vessels.

Elmer Ultraview VoX spinning disc confocal system running on an Olympus IX81 motorized microscope. Images were analysed as extended focus images using Volocity 6.1.1. software. The area of haemorrhage was selected and the volume calculated.

2.10.5. Endothelial cell nuclei quantification

Embryos were mounted in 1% low melting point agarose and z-stack images were taken through the whole embryos using a spinning disc confocal microscope (Perkin Elmer Ultraview VoX spinning disc confocal system running on an Olympus IX81 motorized microscope). Images were exported as extended focus images to ImageJ for analysis using the “Analyze particles” tool. The desired particle size can be selected and the software gives information on the size and area of each identified particle. This technique has been established and data reproduced within the lab and the number of calculated cell numbers compared with those calculated manually as well as compared with established normal endothelial cell numbers. Areas of interest are also comparable with established protocol.

2.10.6. Dextran injection

A high molecular weight rhodamine-dextran conjugate (2,000,000 MW TAMRA) that is normally too large to pass through the vessel wall was used to assess vessel integrity as described by Van Rooijen (van Rooijen et al., 2010). Embryos were mounted in 1% low melting point agarose and 1nl of dextran (life technologies, D-7139) was injected directly into the circulation via the common cardinal vein over the yolk sac of 2 and 3dpf embryos. Confocal images were taken after 5 minutes of which the dye had been taken up into the circulation.

2.10.7. Response to laser injury

Embryos were mounted in 1% low melting point agarose and laser injury was carried out using a Micropoint laser attached to a high-speed camera (Olympus IX81). 20 pulses of laser were administered to the arterial wall above the anus of 3dpf embryos as shown in figure 2.2. Time to adhesion was calculated as well as thrombus size after 2 minutes. ImageJ was used to measure thrombus size. Protocol adapted from Thattaliyath et al. (Thattaliyath et al., 2005)

2.11. The effect of small molecule VEGF induction

The VEGF inducer GS4012 (Calbiochem, 676491) was diluted using DMSO and 5µg/ml GS4012 was added to E3 media at 24hpf and changed daily until imaging at 3dpf. Protocol adapted from Peterson et al. (Peterson et al., 2004).

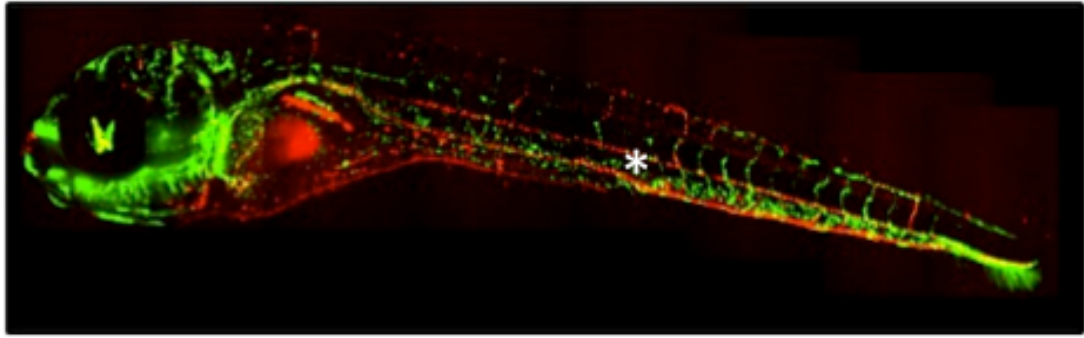


Figure 2.2. Site of laser injury

Image above is of a 5dpf double transgenic embryo, Fli1:GFP/Gata1:dsRED. Star demonstrates the site of laser injury.

2.12. Statistical Analysis

All data presented has a stated n number in its corresponding section. For the experiments in which animals were used, the number of embryos per experiment has been stated in its corresponding section. Typically data is shown as mean \pm standard error of the mean. All analysis was conducted using the GraphPad Prism statistical analysis programme and results reported as p values in corresponding sections. Statistical comparisons were made between multiple treatment groups using one-way analysis of variance (ANOVA) with a Bonferroni post-test to assess multiple comparisons between each group.

2.12.1 Microarray normalization

Dr Marta Milo, a bioinformatician in the Cardiovascular Biomedical Research Unit, carried out normalization. The first stage in normalization is to balance hybridization intensities across chips to allow meaningful comparisons to be made. To do this a set of genes that should be equally expressed in both test and control samples are identified. Affymetrix GeneChips include over 100 'housekeeping genes' which are common genes assumed to be expressed to the same level in every cell type, these genes include cytoskeleton (B actin). As these genes are expected to have the same expression, their expression ratio is set as 1. From this, a normalization factor can be applied to all genes in the chip. PUMA (Propagating Uncertainty through Microarray Analysis) is a probabilistic statistical package designed for the analysis of Affymetrix GeneChips that incorporates the measurement of uncertainty gained from the PM and MM

probes to provide an estimate of gene expression of the gene together with a credibility interval (akin to a confidence interval) (Milo et al., 2003b, Pearson et al., 2009b). This approach to probe level analysis has been shown to improve the accuracy of differentially expressed gene identification and thus increase reproducibility of the FC seen (Milo et al., 2003b).

Once accurate levels of expression have been found for each probe set on each chip, these can be compared using Principle Component Analysis (PCA).

PCA is a method of visualising data in terms of components of variability. The arrays from each patient at each time point will contain multiple variabilities for example, differences in sex gene expression, and differences as a result of phenotypic characteristics. By plotting arrays against a component accounting for maximal variability, it is possible to see the spread of patients and time points across this component. Arrays that group together are the most similar and arrays separated by a large distance are the most different in terms of the component. Adding a second component accounting for as much of the remaining variability as possible, can further distinguish between arrays and even a third component can be added.

Standard PCA assumes that the uncertainty of each gene in each comparable chip is constant. However it has been argued that this is often an unreasonable assumption when applied to highly variable biological data (Sanguinetti et al., 2005). PUMA takes a probabilistic approach utilising credibility intervals to include the variability of each gene in PCA. This approach has been shown to remove 'noise' from the dataset and lead to tighter groupings within the plot. Due to the lack of replicates in this study, statistical errors are likely to be high

and standard PCA may not show groups of similarity due to this. By taking into account the uncertainty using PUMA, patterns in array distribution may be noticed.

To determine the significance of changes in expression the expression ratio was calculated using the below equation, **g** represents gene, **Tg** the test sample and **Cg** the control sample.

$$Eg = Tg/Cg$$

When the level of **g** is the same in both the test and control samples the ratio will equal **1**. Where **g** is up regulated in the test sample the ratio will be greater than 1 and when down regulated it will be between 1 and 0. The fold change can now be calculated by multiplying the reciprocal of down regulated genes by **-1**.

We defined differential expression using a cut off of a fold change of greater than 2 or -2.

In order to improve the robust detection of differentially expressed genes the Probability of Positive Log Ratio (PPLR) uses a Bayesian hierarchical model to combine probe-level measurement error and between replicate variance and adopts the variational method to estimate the parameters. It also accounts for the variance seen between chips by using uncertainty measurements from replicate experiments to calculate point estimations and standard errors of the expression levels. This means that PUMA accounts for both within chip and across chip variance when identifying differentially expressed genes. PUMA uses the point estimate and standard error measurements to calculate a PPLR score for each probe set. This can be used to order probe sets by probability of differential expression between two events such as MI vs. UA.

Of those genes with a fold change >2 or -2 , those with a PPLR of greater than 0.8 or less than 0.2 were classed as significant. These are arbitrary values, which have been previously used as significant cut off values for up regulated and down regulated differentially expressed genes analysed using PUMA (Quackenbush, 2002).

Chapter 3: Identifying Differentially Expressed Genes in Peripheral Blood of Patients Presenting with Acute Coronary Syndrome (ACS)

3.1. Introduction

3.1.1. Expression analysis of patient peripheral blood

Gene expression profiling of RNA extracted from peripheral blood has the potential to be an informative method for identification of biomarkers, examination of disease states, stratification of patient populations and investigation of immune responses. However, the relatively high proportion of globin messenger RNA present in total RNA extracted from whole blood can reduce the efficacy of the microarray assay by interfering with the detection of less abundant gene transcripts (Feezor et al., 2004, Liu et al., 2006a). Common laboratory practice often includes fractionation of whole blood components prior to RNA extraction. Depending on the fractionation method selected, partial or complete removal of erythrocytes and reticulocytes, the primary source of globin RNA, may be achieved. However, an alternative that we used was to extract the RNA and clear the globin prior to array hybridisation.

3.2. Results

3.2.1. Defining differential expression

50 patients with typical ACS symptoms were recruited from The Northern General Hospital (NGH) Sheffield from April 2009. Blood samples were collected at days 1, 3, 7, 30, 90 and 360 after the acute event. Due to the on going and prospective nature of this study, 19 patients with data from each time point up

to 3 months have currently been analysed. This is the cohort, which will be described throughout the rest of this thesis.

We recruited five patients with UA, ten with NSTEMI and four with STEMI. No patients died during the follow-up.

My main time point of interest was 1 day post admission (visit 1), because signals arising from plaque rupture are more likely to be detected early and the confounding effects of treatment and complications such as heart failure are less likely to be apparent at this early time point. A summary of the study time points is illustrated in figure 3.1.

The microarray data was normalised and statistical analysis carried out by Dr Marta Milo (CVBRU Bioinformatician) using published protocols of open sources software Propagating Uncertainty in Microarray Analysis (PUMA) (Pearson et al., 2009a). This approach to probe level analysis has been shown to improve the accuracy of differentially expressed gene identification and thus increase reproducibility of the fold change seen (Milo et al., 2003a).

The microarray data examined expression of 54,464 transcripts. Of these, hypothetical genes as well as those that have not yet been annotated were removed, leaving 45,490. To determine the significance of changes in expression the expression ratio was calculated as described in chapter 2 (2.5.1.2.).

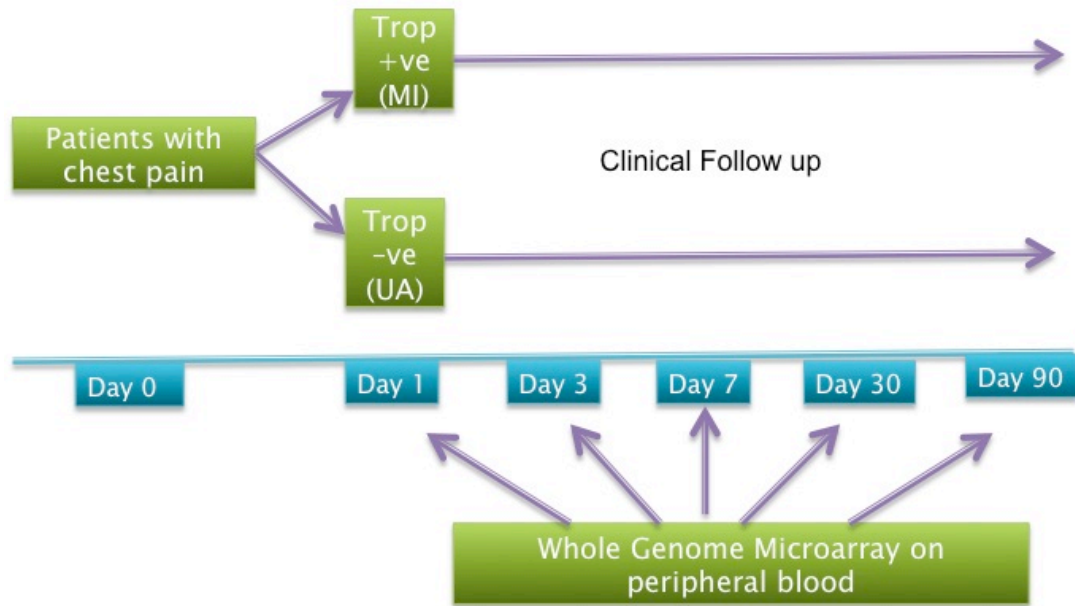


Figure 3.1. Summary of sample collection

Timeline demonstrates the process of patient recruitment and sample collection. Patients suffering with chest pains were admitted and an ECG and 12h serum Troponin measurement performed to define whether the patients had suffered UA, STEMI or NSTEMI. Blood samples were taken at 1, 3, 7, 30 and 90 days post admission, from which RNA was extracted from peripheral blood for whole genome Affymetrix microarray analysis.

3.2.2 Identifying gene expression differences in peripheral blood from patients with MI compared with unstable angina

Microarray studies generate large quantities of data that generally require interrogation in a focused manner. I sought to identify genes that are differentially expressed in peripheral blood from patients with both STEMI and NSTEMI compared with patients who present in a similar or identical manner but who have no evidence of myocardial necrosis (unstable angina). By this comparison, I sought to determine genes whose expression may be altered by the early consequences of plaque rupture, or even which have played a role in initiating plaque rupture. To identify such genes I concentrated on those that were differentially expressed in both the STEMI and NSTEMI groups compared to the UA at 1d post admission.

3461 genes were differentially expressed between NSTEMI, STEMI and UA groups at 1d post admission. 99 of these were significantly differentially expressed in both myocardial infarct (STEMI and NSTEMI) groups compared to the unstable angina group (table 3.1).

Table 3.1. Showing genes significantly differentially expressed at day 1 in whole blood in patients with MI compared to UA.

Gene Title	Gene Symbol		
7-dehydrocholesterol reductase	DHCR7	intermediate chain 1	
angiomin like 1	AMOTL1	E2F transcription factor 1	E2F1
ankylosis, progressive homolog (mouse)	ANKH	EP400 N-terminal like	EP400NL
ankyrin repeat domain 19	ANKRD19	EPH receptor B3	EPHB3
apolipoprotein B mRNA editing enzyme, catalytic polypeptide-like 3B	APOBEC3B	Ets homologous factor	EHF
ATP-binding cassette, sub-family D (ALD), member 1	ABCD1	family with sequence similarity 125, member B	FAM125B
ATPase family, AAA domain containing 4	ATAD4	family with sequence similarity 26, member F	FAM26F
beta-1,3-glucuronyltransferase 3 (glucuronosyltransferase I)	B3GAT3	family with sequence similarity 39, member D pseudogene	CXYorf1
BRCA1 interacting protein C-terminal helicase 1	BRIP1	family with sequence similarity 90, member A1	FAM90A1
calcium binding protein 1	CABP1	fibroblast growth factor receptor 2 (bacteria-expressed kinase, keratinocyte growth factor receptor, craniofacial dysostosis 1, Crouzon syndrome, Pfeiffer syndrome, Jackson-Weiss syndrome)	FGFR2
CD274 molecule	CD274	FRAS1 related extracellular matrix 1	FREM1
chemokine (C-C motif) ligand 23	CCL23	G antigen 1	CTD-2248C21.2
Chemokine (C-X-C motif) receptor 7	CXCR7	G protein-coupled receptor 56	GPR56
Chromosome 1 open reading frame 128	C1orf128	gamma-aminobutyric acid (GABA) B receptor, 2	GABBR2
chromosome 15 open reading frame 43	C15orf43	gelsolin (amyloidosis, Finnish type)	GSN
chromosome 16 open reading frame 55	C16orf55	guanine nucleotide binding protein, alpha transducing 3	GNAT3
chromosome 17 open reading frame 47	C17orf47	guanylate cyclase activator 1C	GUCA1C
Chromosome 19 open reading frame 6	C19orf6	immunoglobulin heavy variable 7-81	IGHV7-81
chromosome 21 open reading frame 34	C21orf34	interleukin 20	IL20
Coiled-coil domain containing 85B	CCDC85B	KIAA1109	KIAA1109
collagen, type VIII, alpha 1	COL8A1	KIAA1632	KIAA1632
CTD (carboxy-terminal domain, RNA polymerase II, polypeptide A) small phosphatase-like	CTDSPL	Leber congenital amaurosis 5	LCA5
cyclin-dependent kinase-like 1 (CDC2-related kinase)	CCNG2	leucine rich repeat containing 16	LRRC16
cytoskeleton associated protein 2-like	CKAP2L	leucine-rich repeats and transmembrane domains 2	LRTM2
dishevelled associated activator of morphogenesis 2	DAAM2	lipoma HMGIC fusion partner-like 4	LHFPL4
dynein, cytoplasmic 2, light	DYNC2LI1	M-phase phosphoprotein 8	MRPS18C
		Meis homeobox 1	MEIS1
		microcephalin 1	MCPH1

netrin G1	NTNG1
NIMA (never in mitosis gene a)- related kinase 9	NEK9
nitric oxide synthase 3 (endothelial cell)	NOS3
otoancorin	OTOA
p21(CDKN1A)-activated kinase 6	PAK6
PDGFA associated protein 1	PDAP1
phosphodiesterase 1A, calmodulin-dependent	PDE1A
potassium inwardly-rectifying channel, subfamily J, member 5	KCNJ5
POU class 2 associating factor 1	POU2AF1
proline rich, lacrimal 1	PROL1
Protein kinase C, zeta	PRKCZ
protocadherin 21	PCDH21
protocadherin beta 5	PCDHB5
pyroglutamyl-peptidase I	PGPEP1
recombination activating gene 1	RAG1
retinal G protein coupled receptor	RGR
ribonuclease P/MRP 25kDa subunit	RPP25
Scavenger receptor class A, member 5 (putative)	SCARA5
selenoprotein P, plasma, 1	SEPP1
SET binding factor 2	SBF2
signal-regulatory protein alpha	SIRPalpha
similar to Alu subfamily SX sequence contamination warning entry	LOC646736
SMAD family member 3	SMAD3
SMAD specific E3 ubiquitin protein ligase 1	SMURF1
solute carrier family 1	SLC1A1

member 1	
solute carrier family 2 (facilitated glucose transporter), member 13	SLC2A13
solute carrier family 6 (neutral amino acid transporter), member 19	SLC6A19
sperm flagellar 2	SPEF2
spermatogenesis associated 12	SPATA12
Src homology 2 domain containing adaptor protein B	SHB
suppressor of Ty 16 homolog (S. cerevisiae)	SUPT16H
synovial sarcoma translocation, chromosome 18	SS18
tetratricopeptide repeat, ankyrin repeat and coiled-coil containing 2	TANC2
transcription factor Dp family, member 3	TFDP3
transmembrane protein 117	TMEM117
transmembrane protein 62	TMEM62
tumor protein p53 binding protein 1	TP53BP1
unc-5 homolog B (C. elegans)	UNC5B
WD repeat domain 42A	WDR42A
WD repeat domain 60	WDR60
WD repeat domain 63	WDR63
YY1 transcription factor	YY1
zinc finger protein 397	ZNF397
zinc finger protein 416	ZNF416
zinc finger protein 668	ZNF668

The table above displays the genes that are differentially expressed in both STEMI and NSTEMI groups compared to the UA group.

Since I planned to perform functional assessment of differentially expressed genes in zebrafish, it was necessary to identify which of these genes have zebrafish orthologues. 54,464 transcripts were analysed by the microarray, of which the 'hypothetical genes' were removed from the data set. From the remaining genes those that were differentially expressed (a fold change of ≥ 2) were separated. From genes that were significantly statistically differentially expressed (defined as a PPLR higher than 0.8 or lower than 0.2) were identified. The genes that were significantly differentially expressed in both MI groups vs. UA were selected and BLASTed using Ensembl for zebrafish orthologues, of which 27 were found to possess clear zebrafish homologues (table 3.2.). From these 27 genes that were present in zebrafish only 14 had a genetic similarity of $>50\%$; shared between zebrafish and humans.

Of these 14 conserved genes, 5 were down regulated and 9 up regulated in MI compared with UA (Figure 3.2). Although there are some minor differences between NSTEMI and STEMI groups, all genes are significantly differentially up- or down regulated at 1d, which resolves at later time points. Figure 3.3 shows a heat map of expression of these genes combining all patients with MI compared with UA, indicating clearly their early expression differences that return rapidly to similar levels as in UA. These candidates are therefore potentially implicated in the processes leading to, or the early response to, plaque rupture.

Table 3.2. Genes differentially expressed in MI compared to UA with zebrafish homology

Gene Symbol	% Homology to zebrafish
SMURF1	88
KIAA1109	74
C19orf6	73
DAAM2	72
UNC5B	66
SLC2A13	62
SLC1A1	62
WDR42A	61
COL8A1	59
CXCR7	54
FREM1	50
SBF2	50
SCARA5	49
POU2AF1	43
E2F1	42
PCDHB5	42
GUCA1C	40
AMOTL1	38
WDR60	38
MPHOSPH8	36
C15orf43	35
IL20	35
LRTM2	34
OTOA	31
LCA5	31
CKAP2L	18
LRRC16	16



Figure 3.2: Heat maps of genes differentially expressed in MI compared to UA

A) Genes that are differentially expressed in the STEMI group compared to the UA group.

B) Genes that are differentially expressed in the NSTEMI group compared to the UA group.

Heat map demonstrates the down (green map) or up (red map) regulation of differentially expressed genes, as indicated by the scale.

I next performed Gene Ontology analysis using the online database **Protein ANalysis THrough Evolutionary Relationships** (PANTHER). This is a classification system that classifies genes by their functions, using published scientific experimental evidence and evolutionary relationships to predict function even in the absence of direct experimental evidence. A summary of the PANTHER analysis can be seen in table 3.4.

The PANTHER output table shows genes that are differentially down regulated are mostly involved in the cell communication biological processes as well as extracellular matrix structural molecular process and G protein coupled receptor and other receptor protein classes.

Up regulated genes are involved in immune response, macrophage activation and response to stimulus biological processes. Molecular processes such as receptor and transmembrane activity are also involved as well as being part of transporter protein class. These findings link accordingly to known gene function and other processes that occur during a response to a myocardial infarction. An up regulation of macrophage activation and immune response is part of the coagulation response to a MI. As endothelial dysfunction plays a large role in precession to MI a down regulation in cell communication might be anticipated as well as the G protein coupled receptors. The heat map in figure 3.3 shows the significant differentially expressed genes that also have a homology of greater than 50% with the human genes.

Table 3.3. PANTHER output for genes that are differentially expressed in MI compared to UA.

Gene Symbol	CXCR7
Regulation	Up
Biological process	Cell communication Cellular process Immune response Immune system process Response to stimulus Signal transduction Cell motion
Molecular process	G protein coupled receptor activity Receptor activity
Protein class	G protein coupled receptor Receptor
Gene Symbol	C19orf6
Regulation	Up
Molecular process	Structural cellular activity
Gene Symbol	COL8A1
Regulation	Down
Biological process	Carbohydrate transport Cell communication Cellular process Immune response Immune system response Macrophage activation Response to stimulus Signal transduction Skeletal system development Transport
Molecular process	Receptor activity Structural cellular activity Extracellular matrix structural constituent
Cellular process	Extracellular matrix Extracellular region
Gene Symbol	DAAM2
Regulation	Down

Biological process	Cellular process Cell motion
Molecular process	Structural cellular activity
Gene Symbol	FREM1
Regulation	Up
Biological process	Cell communication Cellular process Immune system process Macrophage activation Response to stimulus Signal transduction Transport Vesicle mediated transport
Molecular process	Receptor activity
Cellular process	
Protein class	Receptor
Gene Symbol	KIAA1109
Regulation	Down
Gene Symbol	RGR
Regulation	Down
Biological process	Cell communication Cellular process Immune response Immune system process Response to stimulus Signal transduction Cell motion
Molecular process	G protein coupled receptor activity
Protein class	G protein coupled receptor Receptor
Gene Symbol	SCARA5
Regulation	Up
Biological process	Cell communication Cellular process Immune system process Macrophage activation Response to stimulus Signal transduction Transport Vesicle mediated transport

Molecular process	Receptor activity Structural cellular activity Extracellular matrix structural constituent Transporter activity
Cellular process	Extracellular matrix Extracellular region
Protein class	Transporter
Gene Symbol	SBF2
Regulation	Up
Biological process	Transport Vesicle mediated transport
Gene Symbol	SMURF1
Regulation	Up
Biological process	Skeletal system development
Gene Symbol	SLC1A1
Regulation	Up
Biological process	Cell communication Cellular process Signal transduction Transport
Molecular process	Transmembrane transport Transmembrane activity
Protein class	Transporter
Gene Symbol	SLC2A13
Regulation	Up
Biological process	Carbohydrate transport Transport
Molecular process	Carbohydrate transmembrane transporter activity Transmembrane transport Transporter activity
Protein class	Carbohydrate transporter Transporter
Gene Symbol	UNC5B
Regulation	Down
Biological process	Cell communication Cellular process Signal transduction
Molecular process	Receptor activity
Protein class	Receptor
Gene Symbol	WDR42A
Regulation	Up
Biological process	Cell communication Cellular process

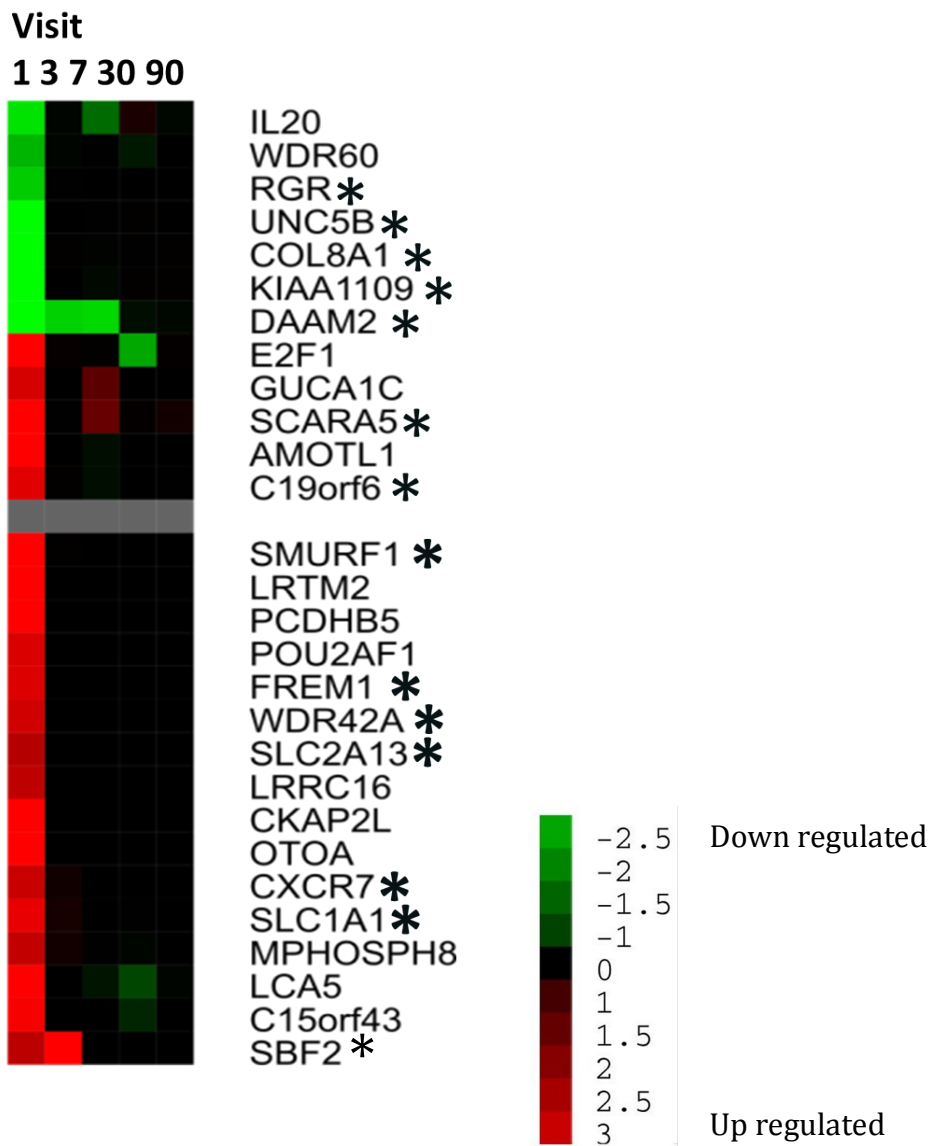


Figure 3.3. Heat map illustrating expression patterns at different time points. Heat map demonstrates the down (green map) or up (red map) regulation of differentially expressed genes conserved in zebrafish. The gene names that are starred represent genes that have a protein homology >50% with zebrafish.

3.3. Discussion

The data presented in this chapter confirm my hypothesis that the peripheral blood transcriptome differs in patients with MI compared with UA. Due to the large amount of data generated by the time course of expression profiling, I restricted my focus to genes that were differentially expressed between groups at the earliest time point examined (1d post admission). Despite this narrow focus I identified 99 genes that were differentially expressed between MI and UA, even using stringent cut offs for fold change (≥ 2) and statistical significance ($P_{\text{PLR}} \geq 0.8$ or ≤ 0.2).

Although these data are purely observational and do not support any causal link between the differentially expressed genes and the initiation of an ACS, it is interesting that the most significantly differentially expressed genes were those involved in the immune response, cell communication and macrophage activation, all processes known to be involved in plaque rupture and coagulation.

Although peripheral whole blood has previously been used in cardiovascular research (Sinnaeve et al., 2009, Taurino et al., 2010) one of its major disadvantages is the inability to tell which cell type the signal comes from. Peripheral whole blood transcriptomic changes might include differential expression signatures from leukocytes, reticulocytes, platelets or even rare hematopoietic progenitors (Sinnaeve et al., 2009). My data cannot determine which of these cells are giving rise to the signal detected. However, since this is the first work attempting to identify a transcriptomic “signature” of MI, the use of the most comprehensive (and most easily obtained and processed) source of

RNA seems justified as a first step. Further work profiling the transcriptome of isolated components of peripheral blood is necessary to identify the source of the differentially expressed genes.

We used microarrays for this study due to their sensitivity and cost effectiveness. Serial analysis of gene expression (SAGE) and massively parallel signature sequencing (MPSS) are well-established alternatives to microarrays. More recently, direct sequencing of transcripts by high-throughput sequencing technologies (RNA-Seq) has become a growing alternative to microarray and like SAGE and MPPS does not depend on genome annotation for prior probe selection. The main challenges of RNA-Seq are that they present novel algorithmic and logistic challenges, and current RNA-Seq strategies require lengthy and time-consuming library preparation procedures. Microarrays are still widely used due to their robust sample processing and analysis pipelines, in particular for projects that involve large numbers of samples for profiling transcripts in model organisms with well-annotated genomes (Baginsky et al., 2010).

The output of the microarray analysis was normalised and fold change (FC) between groups calculated. Filtering genes by FC has been shown to select genes that can be reliably and consistently compared across experiments (Mutch et al., 2002). Filtering by FC alone does not assure significance as FC measurements themselves do not account for measurement error or fluctuations in absolute gene expression level (Newton et al., 2001). These

changes/errors can render results un-reproducible which reduces the significance of findings. To improve the reproducibility of results expression results can be filtered again by P-value (Shi et al., 2008). This is how the majority of expression studies obtain testable gene lists. Our analysis however has been conducted using novel probabilistic methods and requires filtering by different means. PUMA computes PPLR values for each gene/probe and takes into account probe level measurement error and (particularly important due to the small cohort being assessed) variance across replicates (i.e. between chips and individuals). This approach has improved detection of differentially expressed genes (Liu et al., 2006b) and due to the inclusion of sources of variation, can be a more accurate way of filtering than by P-value. PPLR however can be seen as analogous to P-values when considering the most and least significant genes. Although the insignificant genes were discarded before further analysis.

In-silico methods were used to further analyse the list of significantly differentially expressed genes in order to determine a candidate gene. PANTHER is a widely used database for high throughput protein analysis. *In-silico* analysis provides important information on gene function and pathway processes providing a more in-depth knowledge of the group as well as individual genes involved in myocardial infarctions. It can also provide insight as to the causative or responsive involvement of the genes compared to controls.

From the 99 differentially expressed genes identified, only 14 were found to possess a highly conserved zebrafish homologue. Although reducing the

stringency of the cut off used (for example accepting less protein homology) would increase the number of zebrafish orthologues, it is clear that unbiased genomic techniques in humans will yield a significant number of targets that would be difficult to functionally assess in zebrafish. However, it can be argued that the more evolutionarily conserved a gene is, the more fundamental is its likely role in both development and potentially in disease related mechanisms. It is noteworthy that many biological agents that therapeutically target specific molecules in human disease (anti-TNF, anti-IL1, anti-VEGF) inhibit gene products that are highly conserved between zebrafish and humans.

In search for a novel gene that is differentially expressed in MI patients compared to UA to further functionally assess, the most significant differentially expressed gene at 1 day post admission as well as having the highest sequence homology to zebrafish was selected. KIAA1109 was selected not only due to its high homology to zebrafish, most significant differential expression at 1 day post admission and novelty but also due to its presence in endothelial cells and leukocytes as shown by previous microarrays. In this next chapter I will assess the functional role of KIAA1109 using a zebrafish model.

Chapter 4: An examination of the role of KIAA1109 in vascular development in zebrafish

4.1. Introduction

4.1.1. Role of KIAA1109 in humans

KIAA1109, identified as part of the Kazusa ORFeome Project (Project) was first described as encoding a novel G8 domain, related to other human disease related proteins (He et al., 2006) such as PKHD1 and KIAA1199, up regulation of which is associated with cellular mortality (Michishita et al., 2006). KIAA1109 was later described as part of a linkage disequilibrium block KIAA1109/TENR/IL-1/IL-21 (van Heel et al., 2007). Van Heel *et al* found that the 4q27 celiac disease associated region which they had identified contained KIAA1109, which was widely expressed as multiple splice variants in various tissue types. They also found that although no difference in KIAA1109 expression could be observed between normal and celiac disease duodenal tissue, in the presence of inflammation KIAA1109 expression was reduced (van Heel et al., 2007).

KIAA1109 has further been associated with type 1 diabetes (T1D) and rheumatoid arthritis (RA) by Zhernakova *et al*. The authors carried out a genome wide association study and found the region to be associated with T1D and RA in Dutch patients (Zhernakova et al., 2007). In consideration of the Van Heel findings they concluded that the KIAA1109/TENR/IL-1/IL-21 linkage disequilibrium block might be a locus for autoimmune disease.

Tindall *et al* also looked at the 4q27 region in association with prostate cancer risk and found that genetic variation within the region might be associated with

susceptibility to the disease in men with family history and suggested that KIAA1109 may play a potential role in conferring this risk (Tindall et al., 2010). KIAA1109 is also known as Fragile Site Associated (FSA) and is reported by Kuo *et al* to play an important role in regulating mammalian epithelial growth and differentiation and tumour development (Kuo et al., 2006).

These findings implicate KIAA1109 in a range of human diseases, but without demonstrating its function either in normal processes or pathology. Since I had demonstrated KIAA1109 is down regulated in peripheral blood following myocardial infarction (Chapter 3) I sought to examine its role in cardiovascular development.

The KIAA1109 gene is located on chromosome 4 in humans and on chromosome 13 in zebrafish. The human gene has 83 exons and is 15000 base pairs long. It has 99% homology with the murine gene and 74% homology with the zebrafish gene and encodes a protein that contains a transmembrane helix domain and is hypothesised to be integral to the membrane by UniProtKB-KW electronic annotation. The protein has a predicted molecular weight of 555519.38 daltons. The isoelectric point of KIAA1109 protein is predicted to be 6.12.

The EST profile for KIAA1109 as can be seen on the NCBI website (NCBI) KIAA1109 is expressed in 34 human tissues at all developmental stages other than infancy (Table 4.1 and 4.2.).

Using Search Tool for the Retrieval of Interacting Genes/Proteins (STRING) known and predicted protein-protein interactions can be observed (figure 4.1).

Table 4.1. Table of KIAA1109 in human tissue from KIAA1109 EST profile.

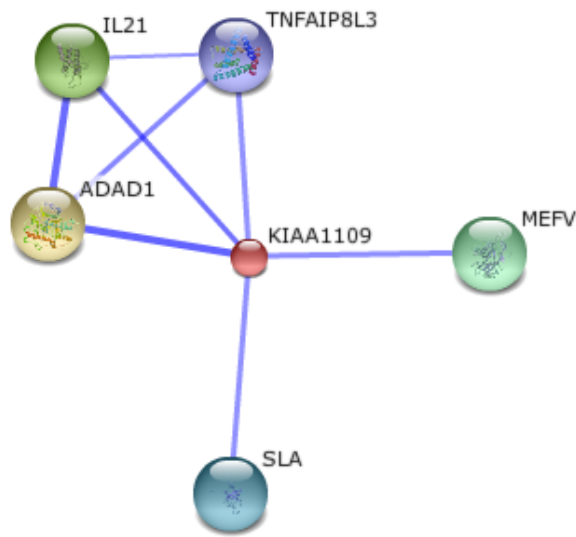
Body sites	transcripts per million (TPM)	Body sites	transcripts per million (TPM)
adipose tissue	77	mouth	15
adrenal gland	30	muscle	150
ascites	0	nerve	64
bladder	0	ovary	0
blood	65	pancreas	65
bone	69	parathyroid	242
bone marrow	41	pharynx	0
brain	76	pituitary gland	60
cervix	0	placenta	70
connective tissue	13	prostate	52
ear	124	salivary gland	0
embryonic tissue	51	skin	18
esophagus	0	spleen	18
eye	90	stomach	31
heart	33	testis	27
intestine	25	thymus	62
kidney	14	thyroid	64
larynx	0	tonsil	0
liver	24	trachea	38
lung	23	umbilical cord	0
lymph	0	uterus	30
lymph node	89	vascular	38
mammary gland	99		

Table above demonstrates the transcripts per million (TPM) of KIAA1109 expression in healthy tissue.

Table 4.2. Table of KIAA1109 in developmental stages from KIAA1109 EST profile

Developmental stage	transcripts per million (TPM)
embryoid body	57
blastocyst	81
foetus	52
neonate	64
infant	0
juvenile	17
adult	64

Table demonstrates the transcripts per million (TPM) of KIAA1109 expression in developmental stages.



Protein	Description
ADAD1	<i>adenosine deaminase domain containing 1 (testis-specific)</i> ; Plays a role in spermatogenesis.
IL21	<i>interleukin 21</i> ; Cytokine with immunoregulatory activity.
MEFV	<i>Mediterranean fever</i> ; Probably controls the inflammatory response in myelomonocytic cells at the level of the cytoskeleton organization
SLA	<i>Src-like-adaptor</i> ; Adapter protein, which negatively regulates T-cell receptor (TCR) signaling. Inhibits T-cell antigen-receptor induced activation of nuclear factor of activated T-cells. Involved in the negative regulation of positive selection and mitosis of T-cells.
TNFA1P8L3	<i>tumour necrosis factor, alpha-induced protein 8-like 3</i>

Figure 4.1. STRING output of KIAA1109 interaction with genes.

Diagram shows the genes that strongly interact or are predicted to interact with KIAA1109. The table also contains a list of gene names included in the diagram.

There is no data on the effect of KIAA1109 loss of function in any model, no KIAA1109 knockout mouse has been generated and no functional role has ever been ascribed to this gene, aside from the genetic associations detailed above.

Since KIAA1109 was differentially expressed in peripheral blood following ACS. I therefore wished to determine its function. I chose to examine this in zebrafish, since this model possesses many advantages for rapid functional assessment of uncharacterized genes (see section 1.3).

4.2. Results:

4.2.1. qRT-PCR validation of KIAA1109 down regulation

In order to validate the differential expression of KIAA1109 in patients with MI compared to UA, quantitative RT-PCR was carried out alongside the housekeeping gene, *DECR1* (Stamova et al., 2009). The patterns of KIAA1109 expression in STEMI, NSTEMI and UA patients follow that of the microarray as shown in figure 4.2. There is a reduced expression of KIAA1109 in the MI patients (STEMI and NSTEMI) compared to the UA group, however this was not statistically significant. This could be due to the quality of the RNA, which had been stored for a long time. It could also be due to the use of inappropriate housekeeping genes.

4.2.2. Expression of KIAA1109 in zebrafish

To determine the normal expression pattern of KIAA1109 in zebrafish, gene specific primers were designed to produce an 800bp product. Figure 4.3 shows expression of this partial KIAA1109 transcript at 1-5dpf in wildtype *nacre* embryo cDNA.

KIAA1109 transcript could be detected at all time points, suggesting it is expressed throughout these stages of development. Although expression appears to be lower

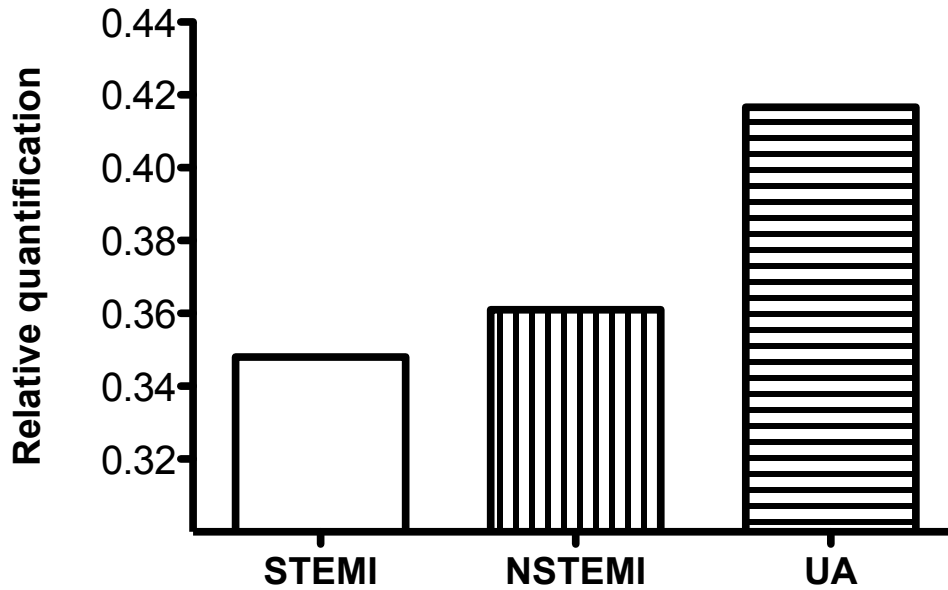


Figure 4.2. qRT-PCR validation of KIAA1109

The graph above shows qRT-PCR expression of KIAA1109 in STEMI (N=4), NSTEMI (N=10) and UA (N= 5) patient samples. Plotted relative to housekeeping gene DECR1.

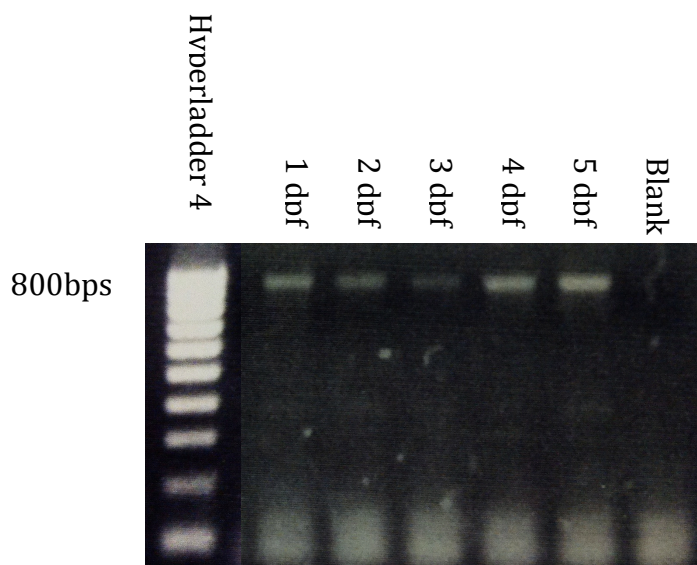


Figure 4.3. Expression of KIAA1109 in 1-5dpf cDNA

Image of gel electrophoresis demonstrates the expression of KIAA1109 at 1-5dpf wildtype embryo cDNA. Pooled 300 embryos per sample.

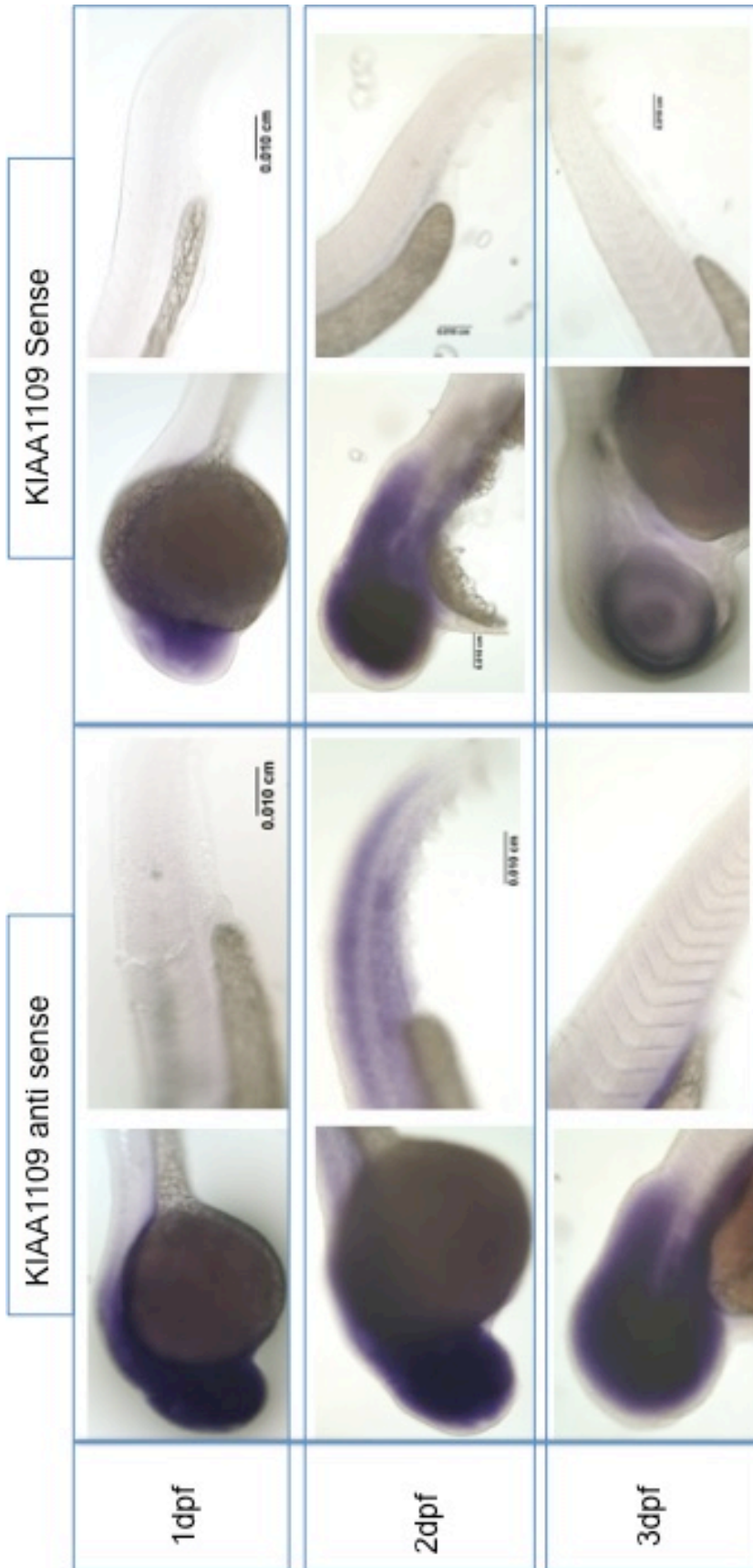


Figure 4.4. Whole mount *in-situ* hybridization of 1-3dpf nacre embryos for KIAA1109. Panel demonstrates expression pattern of KIAA1109 in 1-3dpf wildtype nacre embryos in the head and tail. KIAA1109 antisense column represents expression pattern of the antisense probe. KIAA1109 sense column represents expression pattern of sense probe. Scale bar = 0.010cm

at the earlier time points with least expression at 3dpf increasing to a maximum at 5dpf, gel based PCR is semi-quantitative at best. Bands were extracted and purified for sequencing which confirmed these bands do indeed represent amplification of KIAA1109 at all time points.

Using this purified KIAA1109 PCR product a RNA KIAA1109 *in situ* hybridisation probe was synthesised as described in chapter 2 (2.8). KIAA1109 expression within whole embryos was observed at 1-3dpf in *nacre* embryos (figure.4.4). *Nacre* embryos are advantageous for whole mount *in situ* hybridization as they lack melanocytes and allow for better visualisation of the localisation of the probe. A sense probe was also synthesised as a control. At 1dpf there was non-specific expression in the brain and less in the tail. This expression increased at day 2 in both the head and the tail, and remained the same in the head at 3dpf however it was reduced in the tail. These results have to be interpreted with caution, since developing the sense probe for the same period of time leads to staining in the head, but not the trunk (figure 4.4). Later time points could not be performed due to the inability of the *in situ* probe to penetrate the tissue at older time points. From these data, I concluded that KIAA1109 is ubiquitously expressed in zebrafish at 2dpf, in particular in the trunk, and possibly also the head though the staining with the sense probe makes this uncertain. Ubiquitous or near ubiquitous expression might be expected given the data presented in table 4.1.

4.2.3. Survival of KIAA1109 morphant embryos

In order to ascertain an optimum dosage of the KIAA1109 morpholino, embryo survival was observed after injection of a range of concentrations. Initially the embryos were injected with 0.05pmol morpholino (figure 4.5).

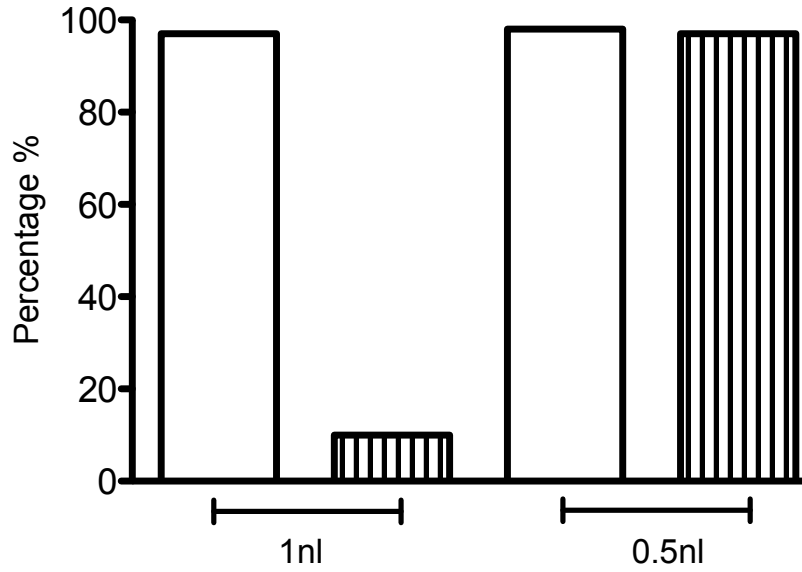


Figure 4.5. Survival of mismatch control and KIAA1109 morphant nacre embryos
Survival percentage of mismatch control (clear bars) and KIAA1109 morphant (lined bars) wildtype nacre embryos.

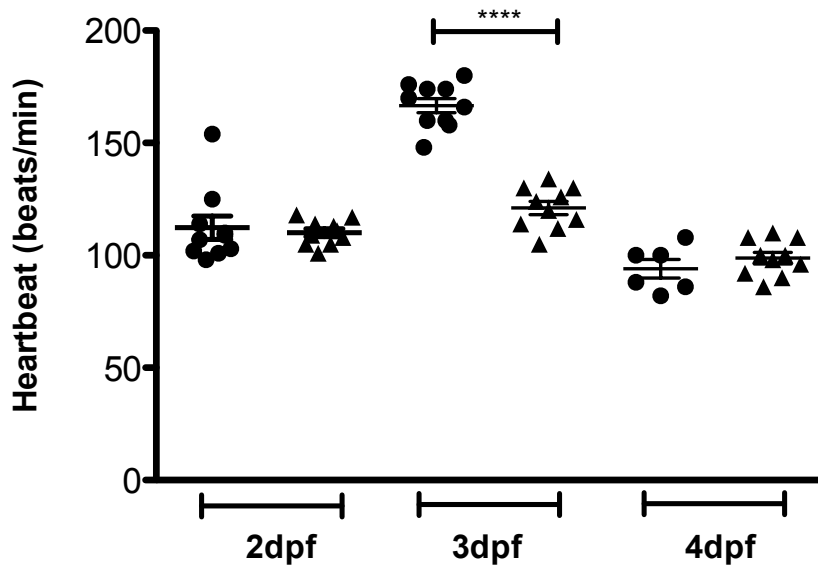


Figure 4.6. Heart rate of mismatch control and KIAA1109 morphant nacre embryos at 2-4dpf

Graph demonstrates heartbeat per minute of mismatch control (circles) and KIAA1109 morphant (triangles) embryos from 2-4dpf.

Mean \pm SEM. One-way ANOVA, Bonferroni post test. $P < 0.05$. $N = 10$, 30 embryos per group.

As shown in figure 4.5 there was a high death rate at a 1nl concentration and so the dose was halved which increased the survival rate significantly and was therefore used for subsequent injections. “Optimisation” of morpholino dose according to mortality is usual, however, it is possible that the mortality seen was due not to toxicity but a specific and lethal effect of KIAA1109 deficiency, and that the lower dose induced less KIAA1109 knockdown to allow survival. As discussed in chapter 1 (1.5.2), use of morpholino antisense does suffer a number of disadvantages, though these are balanced by their general efficiency and rapidity of use.

4.2.4. Effect of KIAA1109 morpholino knockdown on cardiovascular performance

Once I had determined a dose of morpholino that did not induce significant mortality, I characterised the effect of KIAA1109 knockdown on a range of cardiovascular parameters.

4.2.4.1. Heart rate

Heart rates were measured (without the administration of tricaine) in embryos by counting heart beat number for thirty seconds. Figure 4.6 shows that there was no significant difference in the heart rate of control and KIAA1109 morphant embryos at 2dpf. However the heart rate of the morphant embryos was significantly lower than control at 3dpf with no significant difference again at 4dpf. Schwerte *et al.* examined heart rate in zebrafish and found that average heartbeats per minute in zebrafish were approximately 140bpm at 2dpf, 170bpm at 3dpf and 190bpm. My findings correspond to these readings for the control at 2 and 3dpf however heart rate decreases at 4dpf. In KIAA1109 morphants heart rate is significantly lower than those reported by Schwerte at 3 and 4dpf (Schwerte, 2009). The reasons for

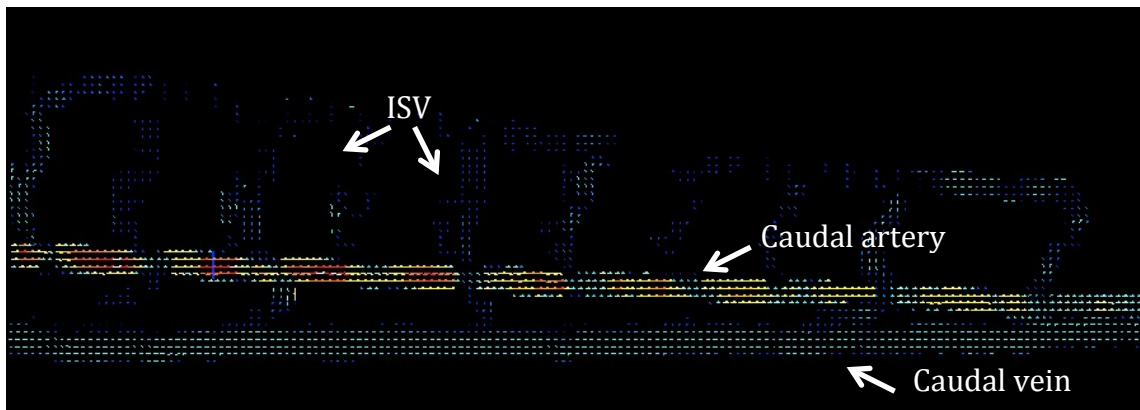


Figure 4.7. Example of PIV output.

The screenshot above demonstrates particle velocimetry (PIV) output in order to measure erythrocyte velocity. The software assigns arrows to moving particles over the time of the video according to their direction and the colour correlates with the velocity of the moving particle, red being the fastest and blue the slowest. A line is drawn over the area of interest and the mean velocity is noted and plotted.

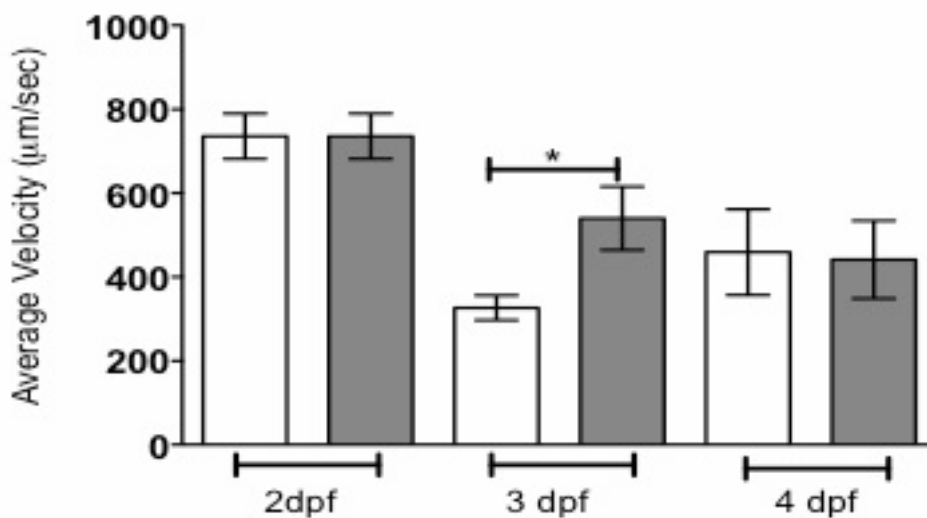


Figure 4.8. Mean arterial erythrocyte velocity in mismatch control and KIAA1109 morphant nacre embryos at 2-4dpf

Graph demonstrates average arterial erythrocyte velocity in the mismatch control (white bars) and KIAA1109 morphant (grey bars) at 2-4dpf.

Mean \pm SEM. One-way ANOVA, Bonferroni post test. $P < 0.05$. $N = 10$, 30 embryos per group.

these discrepancies may lie in strain differences or the fact that I measured heart rate in non-temperature controlled conditions (Denvir et al., 2008).

4.2.4.2. Arterial velocity

I next measured aortic erythrocyte velocity to ascertain whether KIAA1109 knockdown had any effect on cardiac output. Average arterial erythrocyte velocity was measured by using particle image velocimetry technology, in which arrows show direction of flow and the colours represent the erythrocyte velocity of the area of interest as shown in figure 4.7. For arterial erythrocyte velocity, measurements along the caudal artery were obtained at regular intervals, of which the mean is shown in figure 4.8.

At 2dpf no significant difference can be observed between control and morphant embryos. However at 3dpf morphant embryos had a significantly higher arterial erythrocyte velocity compared to the control which decreased at 4dpf, showing no significant difference between the two groups.

4.2.4.3. Venous velocity

I next measured the effect of KIAA1109 knockdown on erythrocyte velocity in the caudal vein. Average venous erythrocyte velocity was measured by using PIV technology, taking measurements along the caudal vein at regular intervals, of which the mean is plotted as shown in figure 4.9.

No significant difference was detected in venous erythrocyte velocity between the groups over these time points. Generally, venous erythrocyte velocity is lower than arterial erythrocyte velocity at all time points, as expected given the greater diameter of the vein.

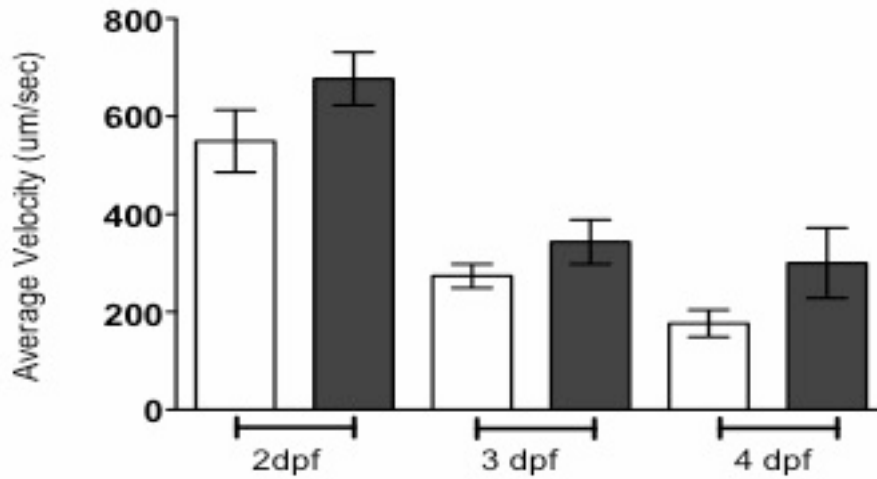


Figure 4.9. Mean venous erythrocyte velocity in mismatch control and KIAA1109 morphant nacre embryos at 2-4dpf

Graph demonstrates average venous erythrocyte velocity in the mismatch control (white bars) and KIAA1109 morphant (grey bars) at 2-4dpf.

Mean \pm SEM. One way ANOVA, Bonferroni post test. P=NS. N=10, 30 embryos per group.

4.2.5. Effect of KIAA1109 morpholino knockdown on embryonic vascular development

4.2.5.1. ISV formation

To ascertain the effect of KIAA1109 knockdown on angiogenesis, the number of intersegmental vessels was counted within a region of interest, defined as the number of intersegment vessels from the caudal loop, as illustrated in chapter 2 (figure 2.1). No significant difference in the number of ISVs between control and KIAA1109 morphant groups were detected at 2, 3 or 4dpf (figure 4.10). Although this does not exclude a minor effect on ISV angiogenesis, it excludes a major effect; for example VEGF knockdown or inhibition greatly impairs ISV number and formation (Covassin et al., 2006, Herbert et al., 2009).

4.2.5.2. Axial vessel formation

To ascertain the effect of KIAA1109 knockdown on development of the axial vessels, arterial formation was observed and arterial diameter measured using PIV images. No abnormality was observed in the KIAA1109 morphant group compared to control morphants. There was also no significant difference in the mean arterial diameter between the two experimental groups across all time points. Similarly, no abnormal venous formation could be observed in the morphant group compared to the control. There was also no significant difference in the mean venous diameter between the two experimental groups across all time points shown in figure 4.12.

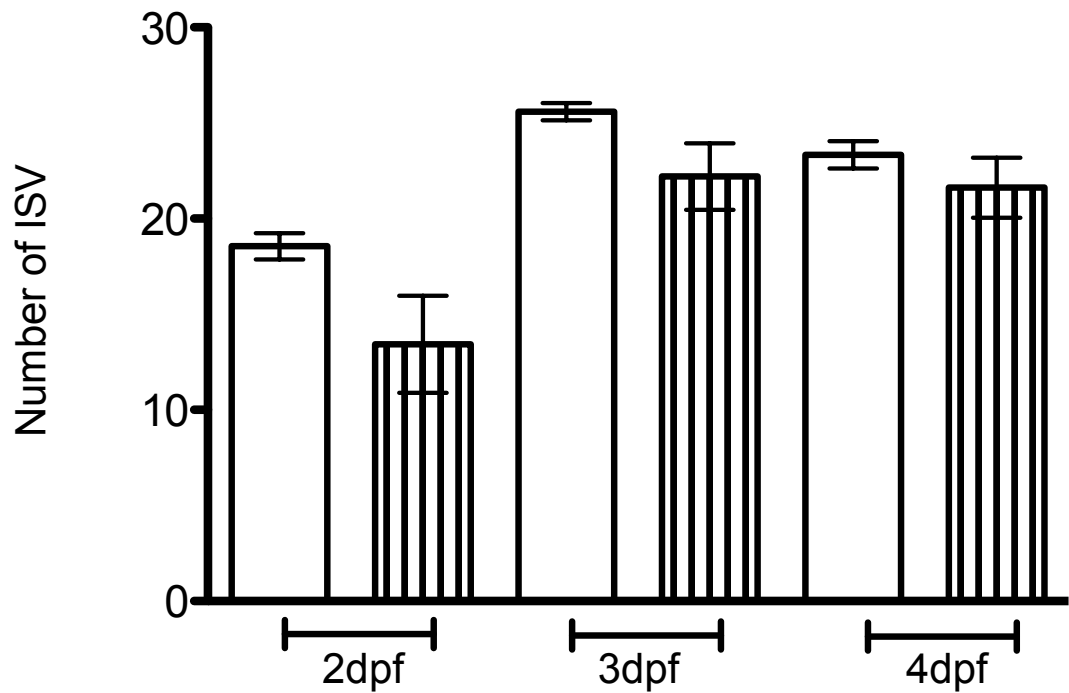


Figure 4.10. Mean number of ISV in mismatch control and KIAA1109 morphant nacre embryos at 2-4dpf

Graph demonstrates average number of ISVs in the mismatch control (white bars) and KIAA1109 morphant (lined bars) at 2-4dpf.

Mean \pm SEM. One way ANOVA, Bonferroni post test. P=NS. N=10, 30 embryos per group.

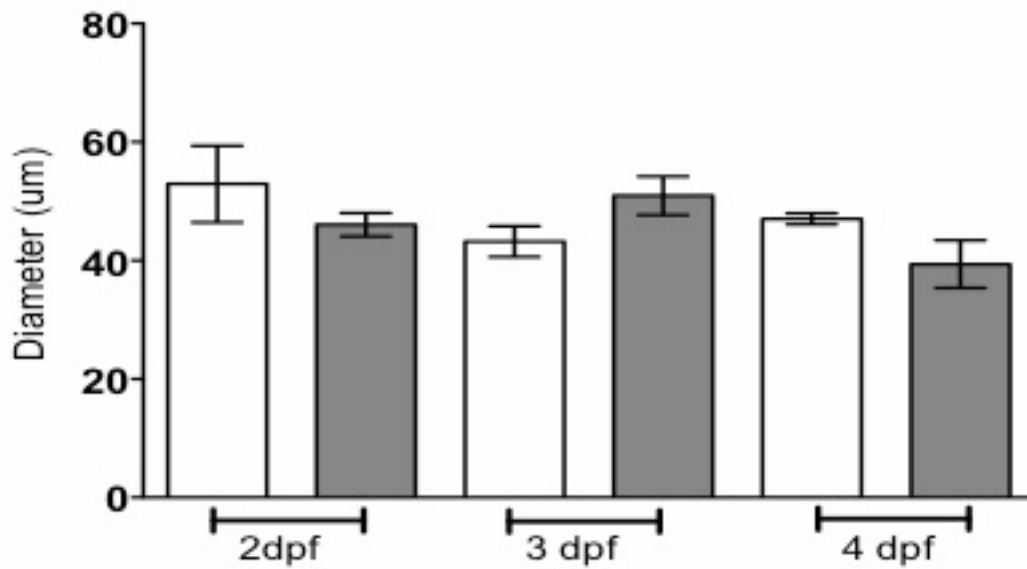


Figure 4.11. Mean average arterial diameter in mismatch control and KIAA1109 morphant nacre embryos at 2-4dpf

Graph demonstrates average arterial diameter in the mismatch control (white bars) and KIAA1109 morphants (grey bars) at 2-4dpf.

Mean \pm SEM. One way ANOVA, Bonferroni post test. P=NS. N=10, 30 embryos per group.

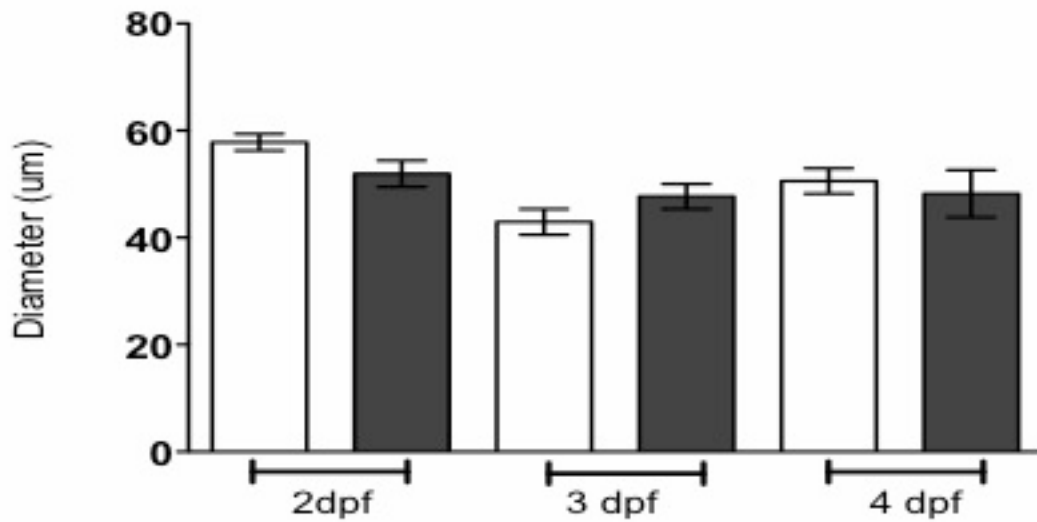


Figure 4.12 Mean average venous diameter in mismatch control and KIAA1109 morphant nacre embryos at 2-4dpf

Graph demonstrates average venous diameter in the mismatch control (white bars) and KIAA1109 morphants (grey bars) at 2-4dpf.

Mean \pm SEM. One way ANOVA, Bonferroni post test. P=NS. N=10, 30 embryos per group.

4.2.5.3. The effect of KIAA1109 morpholino knockdown on the cerebral vasculature

While performing the phenotypic assessments detailed above, I observed a number of embryos with cerebral haemorrhage in the KIAA1109 morphant group (figure 4.13). To ensure that the phenotype was specific to KIAA1109 knockdown splice and non-overlapping morpholinos were designed (chapter 2.7.1).

To quantify the incidence of cerebral haemorrhage, several plates of embryos were injected and observed at 2-4dpf (figure 4.14). There were significantly more embryos with cerebral haemorrhage in the KIAA1109 morphant group compared to the control at all time points. The most significant difference was at 3dpf with approximately 50% of morphant embryos suffering from cerebral haemorrhage. Figure 4.15 shows that there is no significant difference in the percentage of embryos with cerebral haemorrhaging between the three different KIAA1109 morpholinos. For the remainder of this thesis KIAA1109 morphants refers to those injected with a ATG start site blocking morpholino.

During these studies it was also observed that some control morphants occasionally had cerebral haemorrhages. However these appeared to be smaller compared to those in the morphant group. It was also observed that KIAA1109 morphants frequently had several sites of haemorrhaging, consistently in the forebrain and hindbrain. To quantify the volume of haemorrhage in the groups confocal images were taken of morpholino injected *fli1:GFP;GateDsRed* transgenic embryos and using Volocity software z-stack images were taken and volume of haemorrhages measured. If an embryo had several sites of haemorrhage, as was common in the KIAA1109 morphant group, individual volumes would be calculated and summed for a total volume (figure 4.16). These studies showed that KIAA1109 morphant embryos had significantly larger volume of haemorrhage at all time points

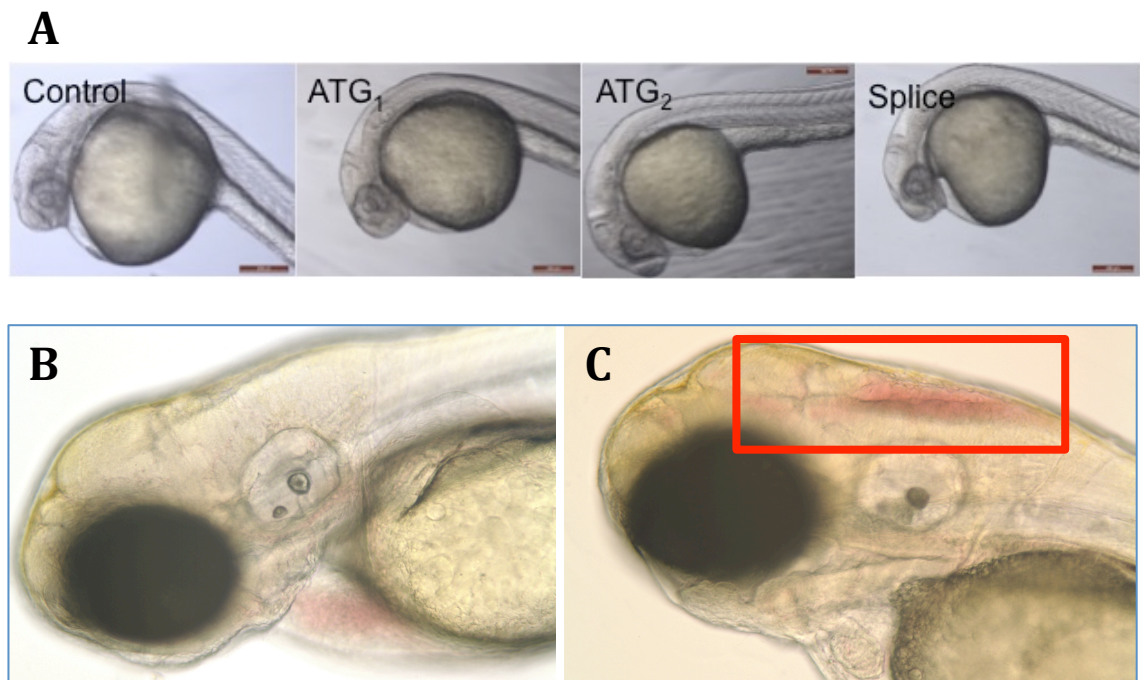


Figure 4.13 Bright field images of 3dpf mismatch control and KIAA1109 morphant nacre embryos

A) Illustrates 1dpf mismatch control, ATG₁, ATG₂ and splice morpholino injected embryos, demonstrating the lack of non-specific, off target, effects in the knockdowns, and a control.

B) Illustrates 3dpf mismatch control *nacre* embryo with no cerebral haemorrhaging. C) Illustrates 3dpf KIAA1109 morphant *nacre* embryo with cerebral haemorrhaging in the hindbrain. Red box illustrates location of cerebral haemorrhaging in hindbrain.

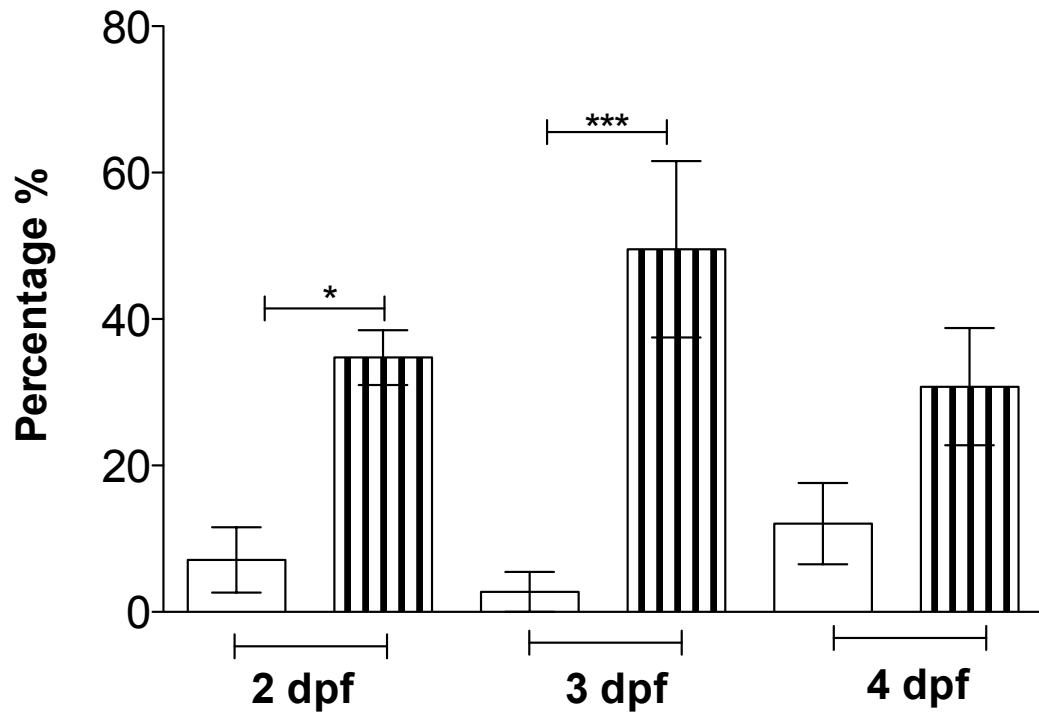


Figure 4.14. Mean percentage of mismatch control and KIAA1109 morphant nacre embryos with cerebral haemorrhage 2-4dpf
 Graph demonstrates mean percentage of mismatch control (white bars) and KIAA1109 morphant groups (lined bars) with cerebral haemorrhage 2-4dpf. Mean \pm SEM. One way ANOVA, Bonferroni post test. $P < 0.05$. $N = 10$, 100 embryos per group.

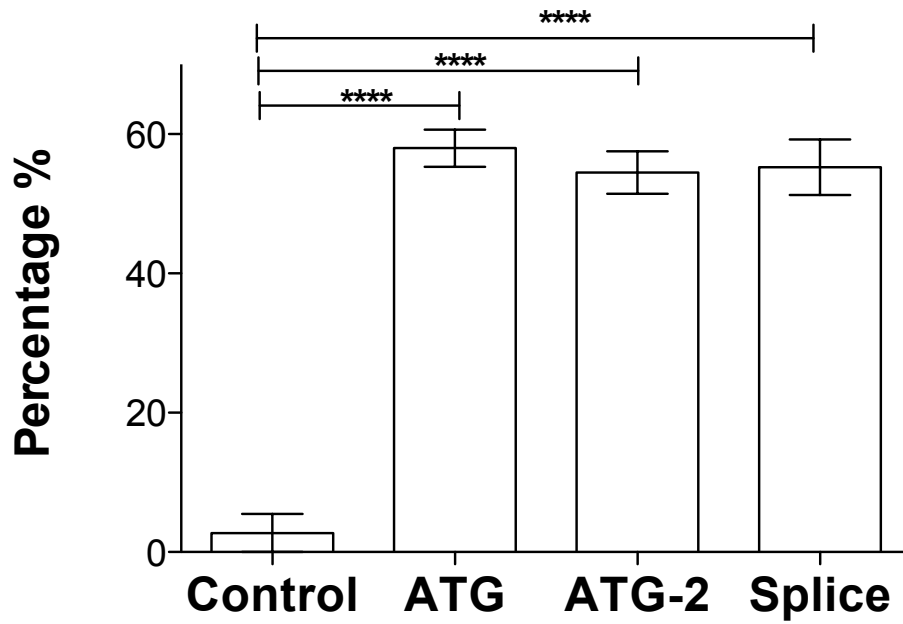


Figure 4.15. Percentage of haemorrhaging in variety of morpholinos at 3dpf.

Graph above demonstrates the number of embryos with cerebral haemorrhages at 3dpf using a start blocking morpholino (ATG MO), non-overlapping morpholino (ATG-2 MO) and splice morpholino (Splice MO) compared to mismatch control injected embryos.

Mean ± SEM. One way ANOVA, Bonferroni post test. $P < 0.05$. $N=3$, 100 embryos per group.

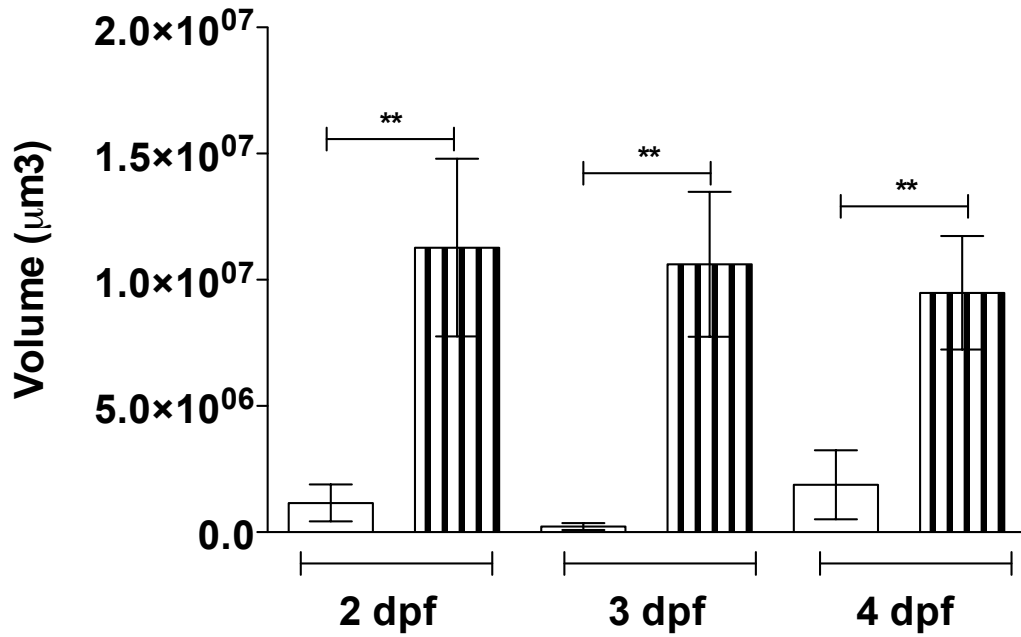


Figure 4.16. Mean volume of mismatch control and KIAA1109 morphant nacre embryo haemorrhage 2-4dpf

Graph demonstrates average volume of haemorrhage in mismatch control (white bars) and KIAA1109 morphant (lined bars) 2-4dpf.

Mean ± SEM. One way ANOVA, Bonferroni post test. P<0.05. N=10, 30 embryos per group.

compared to the control, even at 4dpf when there was no statistically significant difference in percentage of embryos with cerebral haemorrhage.

4.2.5.4. The effect of KIAA1109 morpholino knockdown on endothelial cell number

The haemorrhagic phenotype described above raised the possibility that KIAA1109 knockdown induced a defect in vascular formation that was not detected in the previous assessments. I therefore quantified the number of endothelial cells present within the embryo. Transgenic embryos *flk1:GFP-NLS* were used as they express GFP in the endothelial cell nuclei (Blum et al., 2008). Morphant and control *flk1:GFP-NLS* embryos were imaged at 2 and 3dpf using a spinning disc confocal microscope. The z-stack images were exported as an extended focus, and particle image analysis was carried out using ImageJ. Endothelial cell nuclei were measured in the forebrain, eye, hindbrain, ISV, caudal artery and caudal vein. Figure 4.17 shows the number of endothelial cell nuclei in the eye of control and KIAA1109 morphants at 2 and 3dpf. There was no significant difference in the number of endothelial cell nuclei in the eye between groups.

Figure 4.18 shows the number of endothelial cells in the forebrain of control and KIAA1109 morphant embryos at 2 and 3dpf. There were significantly fewer endothelial cell nuclei in the forebrain of KIAA1109 morphants compared to the controls at 2dpf. Although the same trend was apparent at 3dpf it was not statistically significant. Very similar results were seen when I quantified the number of endothelial cells in the hindbrain (Figure 4.19).

Figure 4.20 shows the number of endothelial cells in the ISV of control and KIAA1109 morphant embryos at 2 and 3dpf. There was no significant difference in

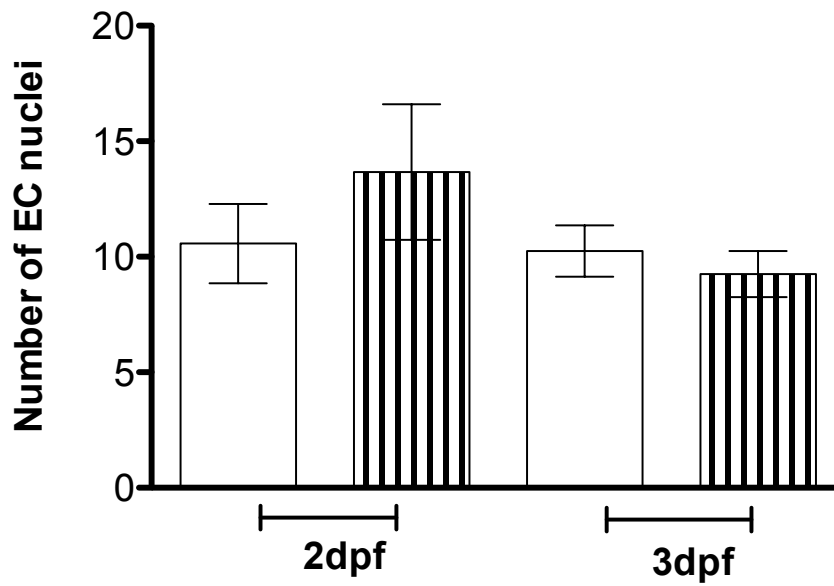
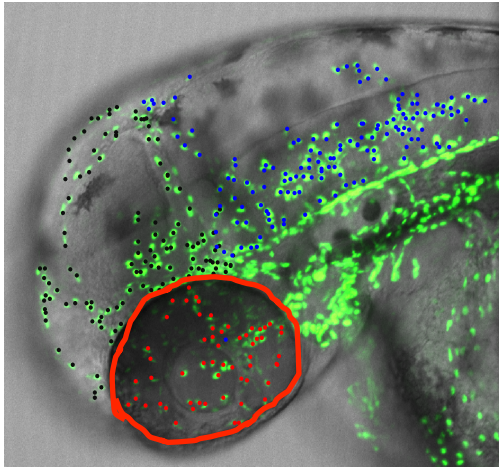


Figure 4.17. Mean number of EC nuclei in eyes of mismatch control and KIAA1109 morphant nacre embryos 2-3dpf

Graph demonstrates average number of EC nuclei in eyes of mismatch control (white bars) and KIAA1109 morphant (lined bars) at 2-3dpf.

Mean \pm SEM. One way ANOVA, Bonferroni post test. P=NS. N=10, 10 embryos per group.

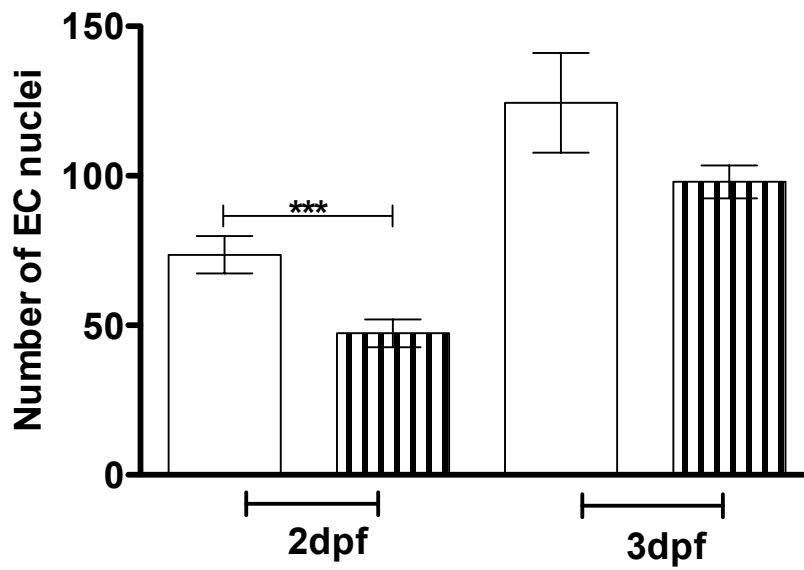
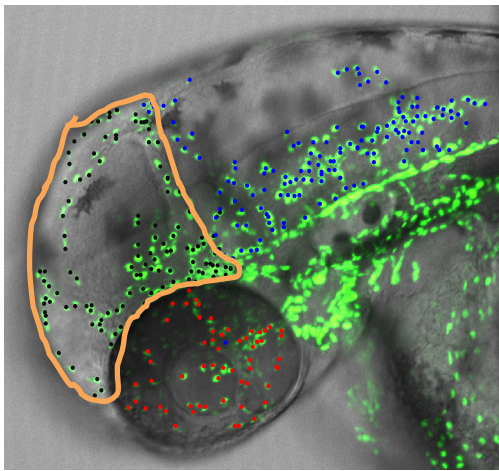


Figure. 4.18. Mean number of EC nuclei in forebrain of mismatch control and KIAA1109 morphant nacre embryos 2-3dpf.

Image above graph demonstrates area of interest, circled in orange.

Graph demonstrates average number of EC nuclei in forebrain of mismatch control (white bars) and KIAA1109 morphant (lined bars) at 2-3dpf.

Mean \pm SEM. One way ANOVA, Bonferroni post test. $P < 0.05$. $N = 10$, 10 embryos per group.

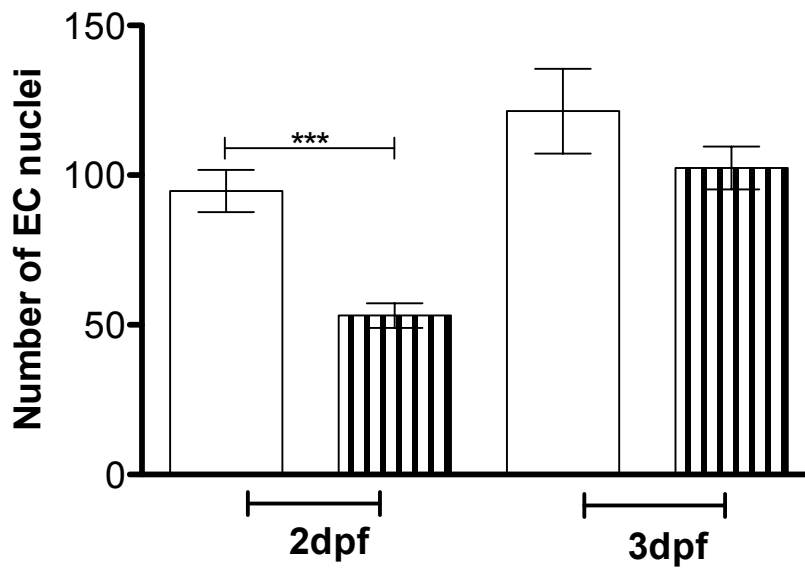
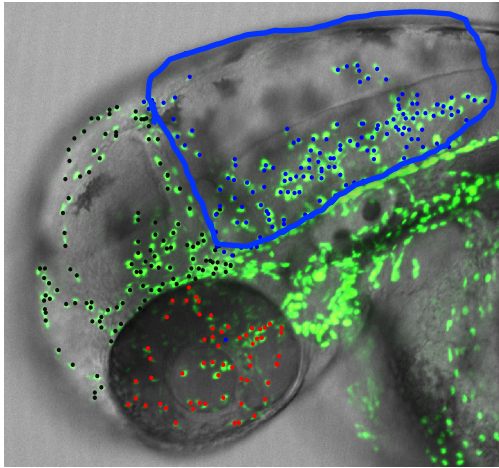


Figure 4.19. Mean number of EC nuclei in hindbrain of mismatch control and KIAA1109 morphant nacre embryos 2-3dpf

Image above graph demonstrates area of interest, circled in blue.

Graph demonstrates average number of EC nuclei in hindbrain of mismatch control (white bars) and KIAA1109 morphant (lined bars) at 2-3dpf.

Mean \pm SEM. One way ANOVA, Bonferroni post test. $P < 0.05$. $N = 10$, 10 embryos per group.

the number of endothelial cell nuclei in the ISV of KIAA1109 morphants compared to the control embryos at either time point.

Figure 4.21 shows the number of endothelial cells in the caudal artery of control and KIAA1109 morphant embryos at 2 and 3dpf. There was no significant difference in the number of endothelial cells in the caudal artery of KIAA1109 morphants compared to the control embryos at either time point.

Figure 4.22 shows the number of endothelial cells in the caudal vein of control and KIAA1109 morphant embryos at 2 and 3dpf. There were significantly fewer endothelial cell nuclei in the caudal vein of KIAA1109 morphants compared to the control embryos at 2dpf. Although the same trend was apparent at 3dpf it was not statistically significant. Thus, KIAA1109 knockdown induces a reduction of endothelial cell number selectively in hindbrain, forebrain and vein but not eye, artery or intersegmental vessels at 2dpf.

4.2.5.5. Vascular integrity

In order to better visualise vascular patterning as well as the site of haemorrhaging, morphant *fli1:GFP;GataDsRed* embryos were imaged using spinning disc confocal microscopy (figure 4.23). As early as 2dpf a pooling of erythrocytes can be visualised in the KIAA1109 embryos compared to the control embryos of the same age. At 3dpf there is a substantial accumulation of erythrocytes in the forebrain and hindbrain. However vascular patterning seems to occur normally. At 4dpf there are residual erythrocytes remaining in the hindbrain of the KIAA1109 morphant with normal circulation observed compared to the control. To better visualise the site of haemorrhage, high magnification images were taken using transgenic *fli1:GFP;GataDsRed* at 3dpf, as this is the time point at which there is the greatest proportion of embryos with haemorrhage and

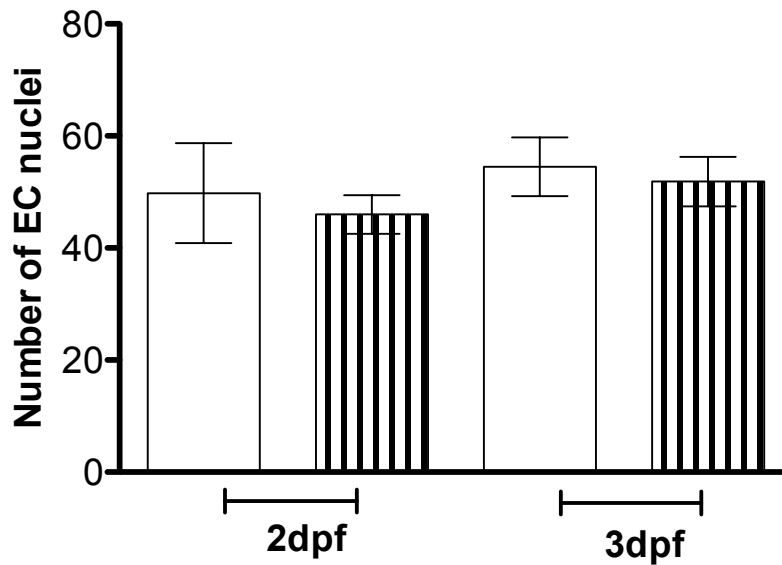
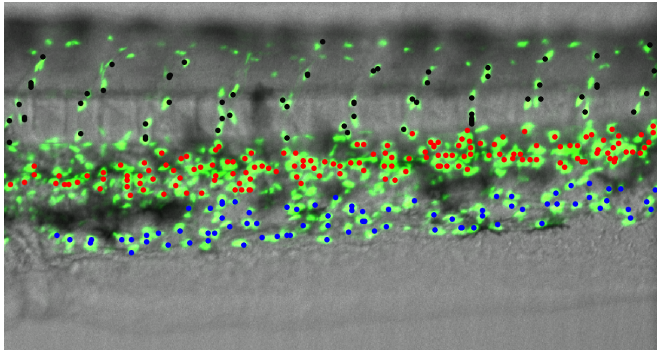


Figure 4.20. Mean number of EC nuclei in ISV of mismatch control and KIAA1109 morphant nacre embryos 2-3dpf

Image above graph demonstrates intersegmental vessels in black dots.
 Graph demonstrates average number of EC nuclei in ISV of mismatch control (white bars) and KIAA1109 morphant (lined bars) at 2-3dpf.
 Mean \pm SEM. One way ANOVA, Bonferroni post test. P=NS. N=10, 10 embryos per group.

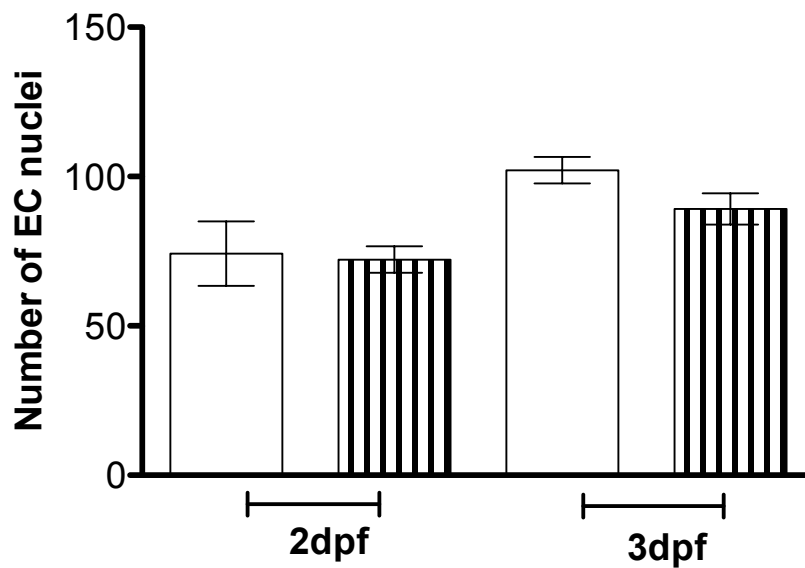
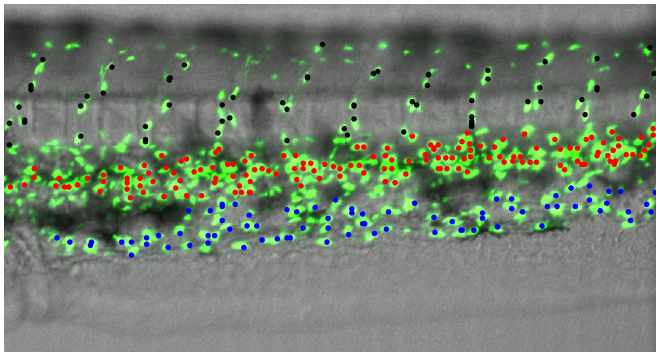


Figure 4.21. Mean number of EC nuclei in artery of mismatch control and KIAA1109 morphant nacre embryos 2-3dpf

Image above graph demonstrates artery in red dots.

Graph demonstrates average number of EC nuclei in artery of mismatch control (white bars) and KIAA1109 morphant (lined bars) at 2-3dpf.

Mean \pm SEM. One way ANOVA, Bonferroni post test. P=NS. N=10, 10 embryos per group.

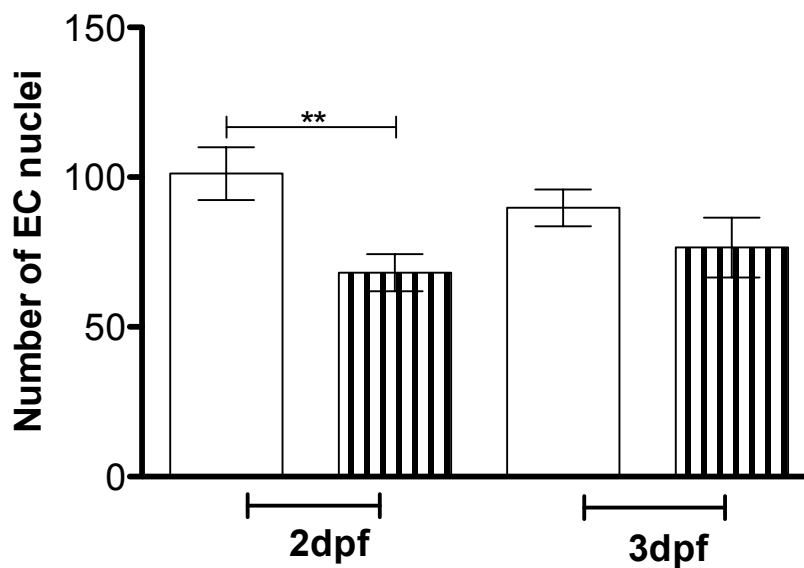
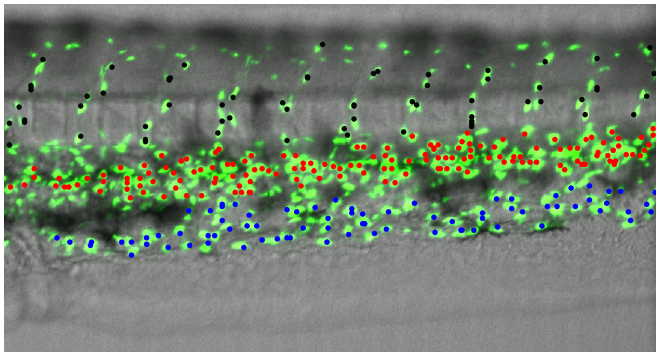


Figure 4.22. Mean number of EC nuclei in vein of mismatch control and KIAA1109 morphant nacre embryos 2-3dpf

Image above graph demonstrates vein in blue dots.

Graph demonstrates average number of EC nuclei in vein of mismatch control (white bars) and KIAA1109 morphant (lined bars) at 2-3dpf.

Mean \pm SEM. One way ANOVA, Bonferroni post test. $P < 0.05$. $N = 10$, 10 embryos per group.

with the largest volume. Figure 4.23 shows a magnified region of the hindbrain of a control embryo. The subsequent panels show that the red erythrocytes are contained within the green vessel. However as can be seen in figure 4.23 the same region in the KIAA1109 morphant embryo shows a pooling of erythrocytes around the vessel but also a gap within the vasculature from which an erythrocyte can be seen leaving the inside of the vessel towards the outside.

This suggests that there is an increase in vascular permeability, in order for the erythrocytes to be able to move to the outside of the vessel.

A red hydrophilic polysaccharide dye, Dextran, was injected into the bloodstream of embryos at 3dpf via the vena cava. After 10 minutes post injection the localization of the dextran can be visualized using a fluorescent microscope. Z-stack time-lapse videos were carried out every 3 minutes for one hour. A snapshot of the extended focus was exported and displayed as figure 4.25.

The dextran injections further demonstrate the increased permeability of vessels within the hindbrain of KIAA1109 morphant embryos, by leaking out of the vessel, an effect that was not seen in control embryos.

4.2.6. VEGF rescue of cerebral haemorrhaging

My finding that the cerebral vessels in KIAA1109 morphants had less endothelial nuclei and appeared more permeable raised the possibility of defective VEGF function to account for these phenotypes. As detailed in section 1.4.2 VEGF is an essential angiogenic growth factor that also induces vascular permeability. I therefore examined what affect the small molecule VEGF inducer GS4012 had on the phenotype in KIAA1109 morphants. Control and morphant embryos were treated with GS4012 at 24hpf and observed at 2 and 3dpf. I used a 5µg/ml concentration, at which there was minimal embryo lethality.

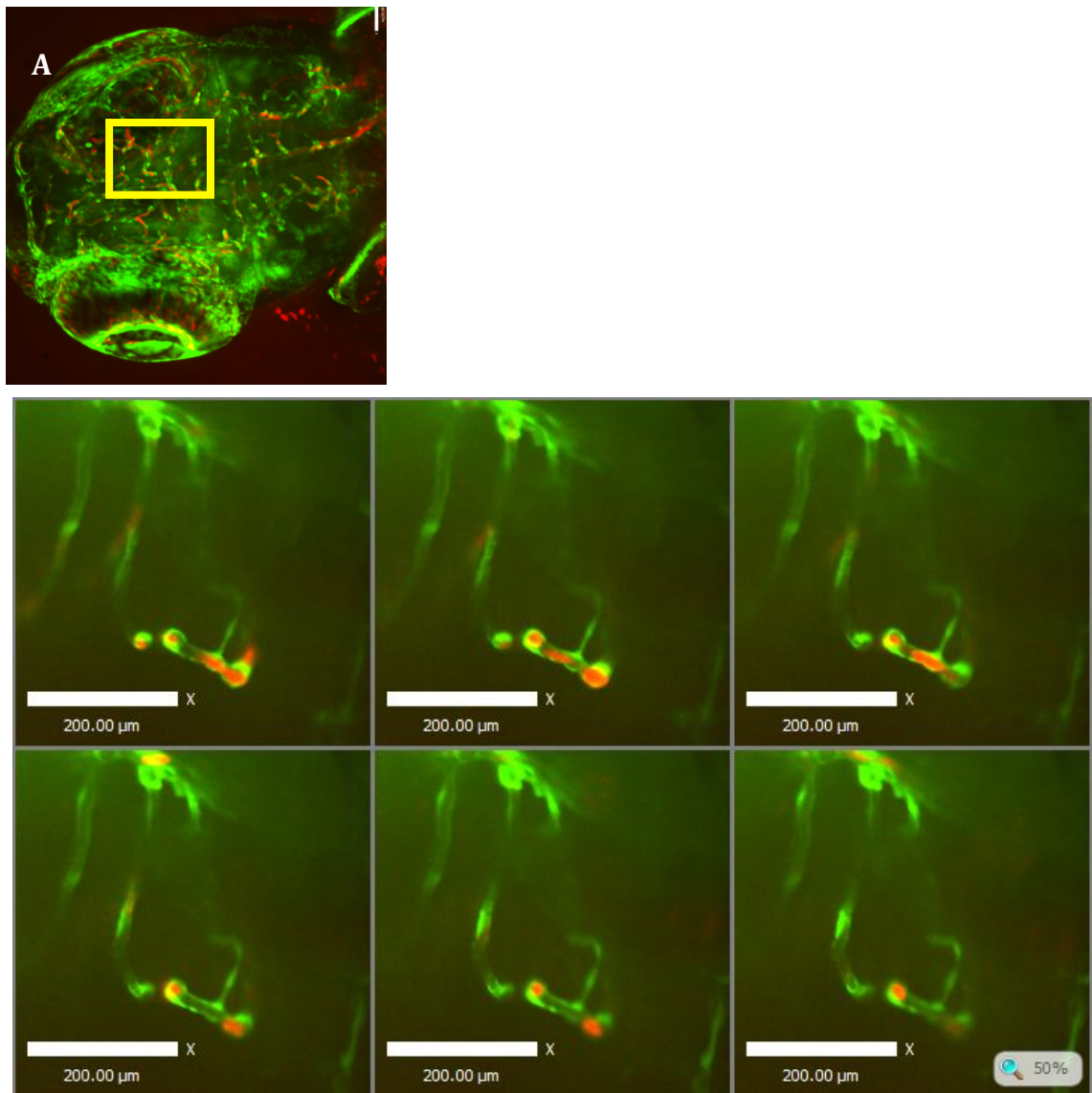


Figure 4.23. Confocal images of 3dpf mismatch control transgenic embryos

All images using Fli1:GFP; Gata:dsRed. A) 3dpf control dorsal view of the head demonstrating normal vasculature and flow. Yellow box demonstrates site of lower panel. B) 3dpf control magnification of the hindbrain demonstrating erythrocyte movement confined within the vessel.

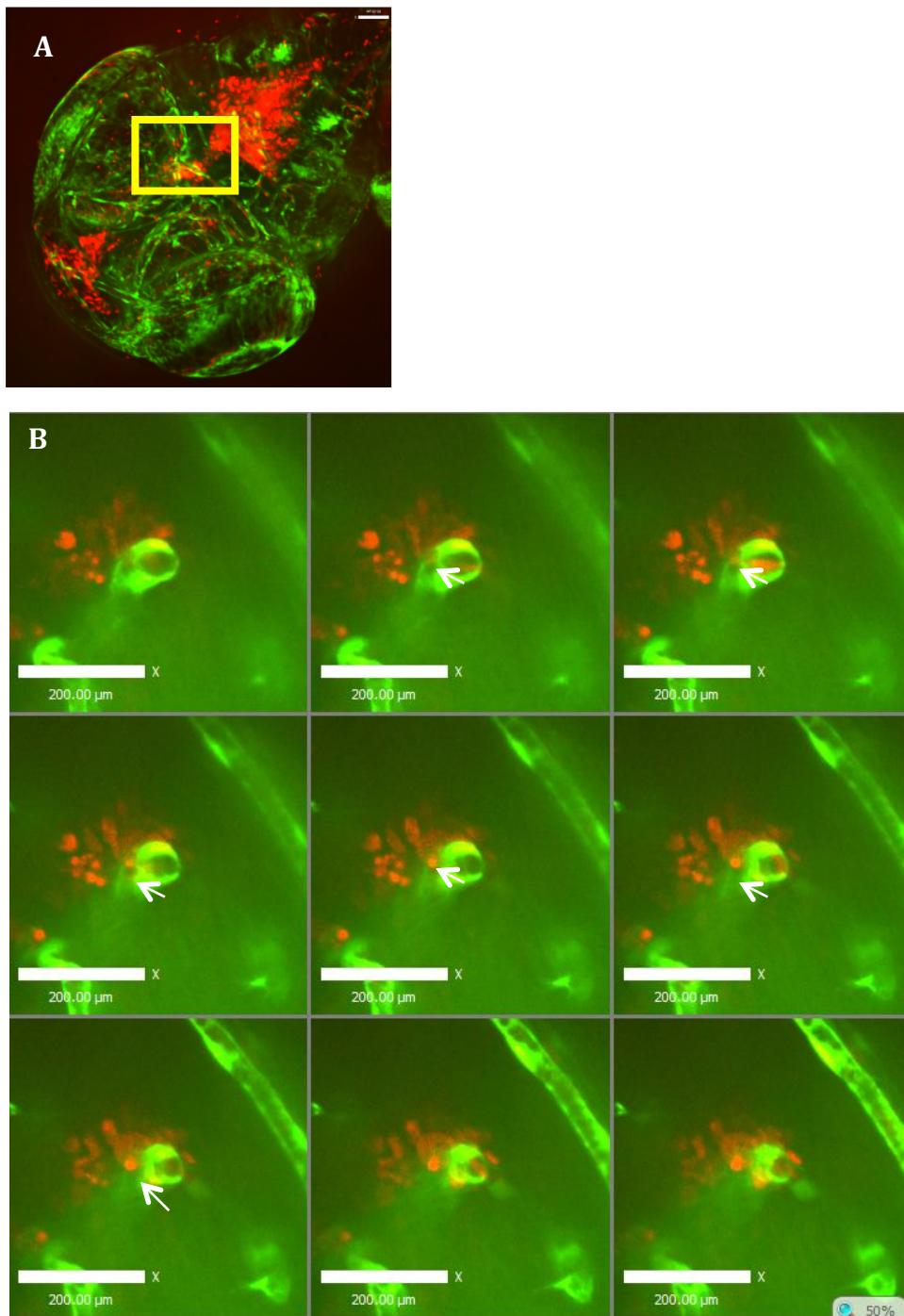


Figure 4.24. Confocal images of 3dpf KIAA1109 morphant transgenic embryos
 All images using Fli1:GFP;Gata:dsRed. A) 3dpf control dorsal view of the head demonstrating normal vasculature and flow. Yellow box demonstrates locality of magnification. B) 3dpf control magnification of the hindbrain demonstrating erythrocyte movement from within to outside the vessel. White arrow shows tracked erythrocyte.

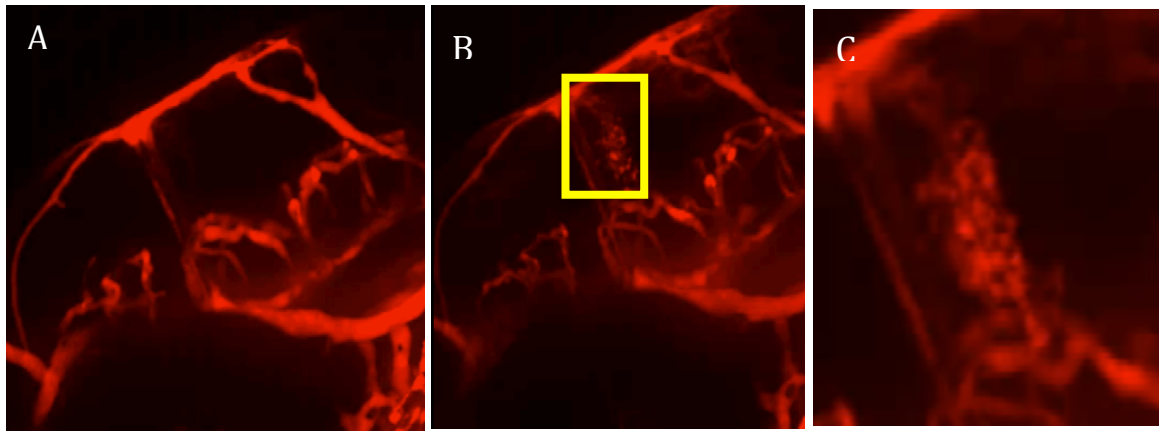


Figure 4.25. Confocal images of Dextran injected 3dpf mismatch control and KIAA1109 morphant nacre embryos

A) Illustrates 3dpf mismatch control *nacre* embryo injected with Dextran. B) Illustrates 3dpf KIAA1109 morphant *nacre* embryo injected with Dextran displaying vascular leakage. Yellow box illustrates location of cerebral haemorrhaging in hindbrain. C) Magnification of the leakage area in the KIAA1109 morphant embryos, as indicated by the yellow box on panel B.

KIAA1109 morphant embryos treated with GS4012 displayed a statistically significant reduction in cerebral haemorrhage in comparison to untreated KIAA1109 morphants (figure 4.26 and 4.27). There are also a significantly lower number of morphant embryos with cerebral haemorrhaging in the GS4012 group compared to the control in the same treatment group. Treatment with GS4012 also rescued the reduction of endothelial cells in the forebrain and hindbrain at 2dpf (figure 4.28) seen in KIAA1109 morphants (figure 4.19, 4.20).

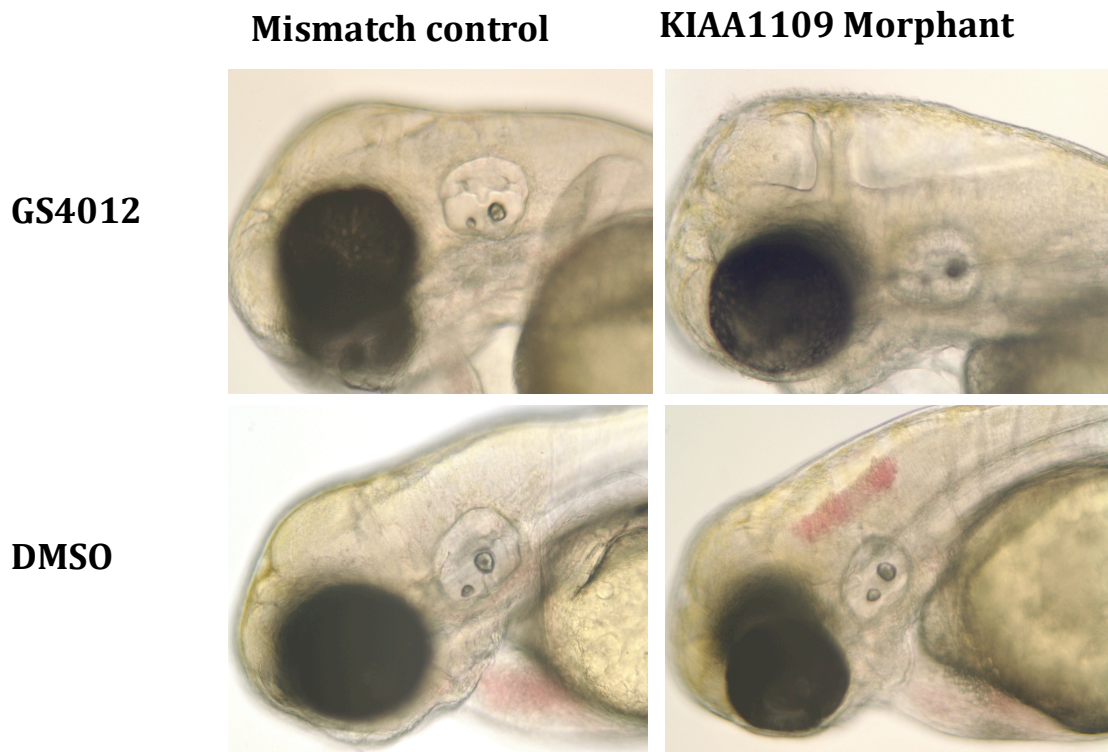


Figure 4.26. Brightfield images of 3dpf mismatch control and KIAA1109 morphant nacre embryo

Image illustrates 3dpf mismatch control and KIAA1109 morphant *nacre* embryos treated with GS4012 and DMSO.

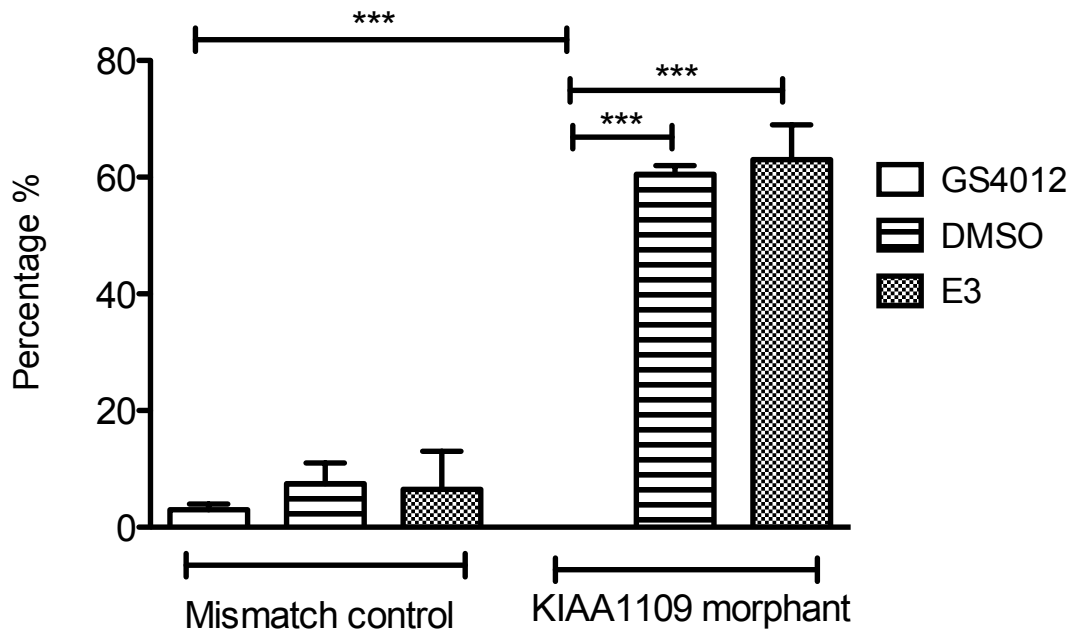


Figure 4.27. Percentage of mismatch control and KIAA1109 morphant nacre embryos treated with GS4012 with cerebral haemorrhaging at 3dpf
 Graph demonstrates the average percentage of mismatch control and KIAA1109 morphant nacre embryos that have cerebral haemorrhaging after incubation with GS4012, DMSO and E3 at 3dpf. N=3, 60 embryos per group.

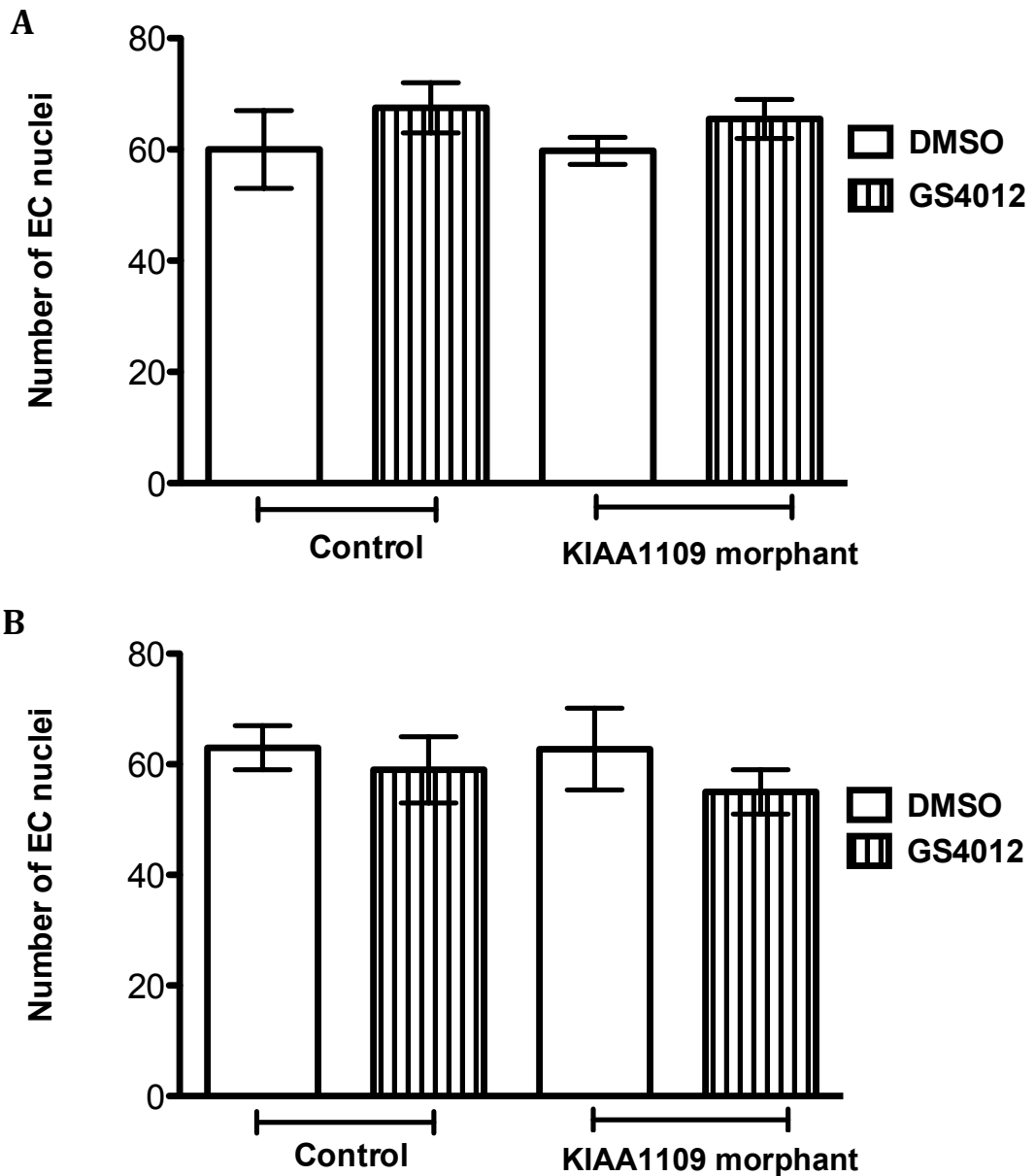


Figure 4.28. Mean number of EC nuclei in forebrain and hindbrain of mismatch control and KIAA1109 morphant nacre embryos treated with GS4012 at 2 dpf. Graph demonstrates average number of EC nuclei in A) forebrain and B) hindbrain of mismatch control and morphant embryos at 2 dpf. Mean \pm SEM. One way ANOVA, Bonferroni post test. P=NS. N=3, 60 embryos per group.

4.3. Thrombocyte adhesion and thrombosis

Since haemorrhage may be a consequence of impaired thrombostasis, I examined whether KIAA1109 knockdown impairs thrombocyte adhesion and thrombosis at a site of endothelial injury. An established laser injury technique in our lab was used to cause a small injury at the arterial wall above the anus using a laser and the time to adhesion was measured for two minutes (figure 4.29).

The results show that thrombocytes (the zebrafish equivalent of platelets) of KIAA1109 morphants take significantly longer to adhere to the site of injury compared to controls. Although there is no statistically significant difference in the size of the thrombus, KIAA1109 morphants showed a trend towards less thrombus formation. The lack of significance could be due to a too small group size, as this method of measurement of thrombus formation can be technically challenging. It is noteworthy however; that in our group we have shown that knockdown of the P2Y₁₂ receptor induces highly significant inhibition of thrombus formation, without inducing cerebral haemorrhage. It is unlikely therefore that impaired haemostasis is the sole cause for the haemorrhagic phenotype observed in KIAA1109 morphants.

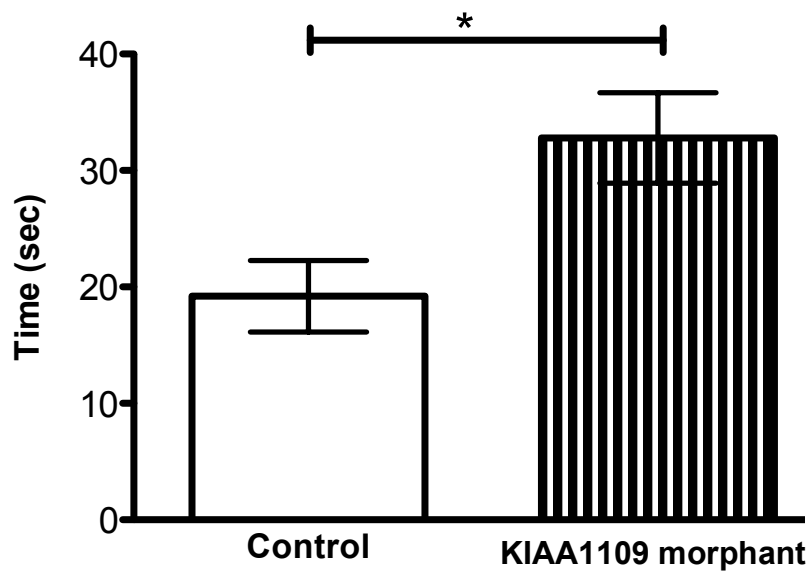


Figure 4.29. Time taken to adhesion in mismatch control and KIAA1109 morphant nacre embryos at 3dpf

Graph demonstrates time taken to adhesion of thrombocytes in mismatch control (clear bars) and KIAA1109 morphant (lined bars) at 3dpf.

Mean ± SEM. T-test. $*= < 0.05$. N=3, 10 embryos per group.

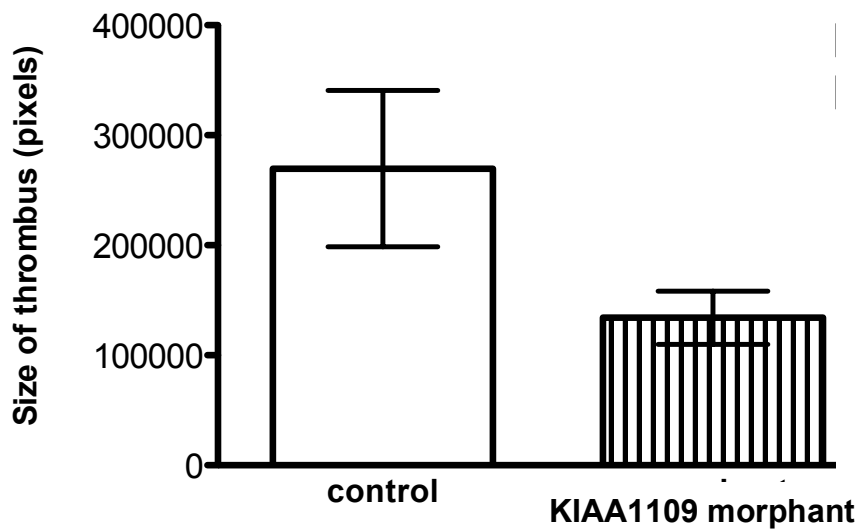


Figure 4.30. Size of thrombus in mismatch control and KIAA1109 morphant nacre embryos at 3dpf

Area under the curve graph demonstrates size of thrombus in mismatch control (white bar) and KIAA1109 morphant (lined bar) at 3dpf.

Mean \pm SEM. T-test. $p=NS$. $N=3$, 10 embryos per group.

4.4. Discussion

Since KIAA1109 is significantly down regulated in human peripheral blood following MI (Chapter 3) and no direct evidence exists for the function of KIAA1109 in any system, I sought to characterize its role in cardiovascular development in zebrafish. Although bioinformatics based on genome sequencing provided us with a zebrafish homolog of KIAA1109, this was yet to be proven to be expressed *in vivo*. Sequence specific primers were designed in order to amplify the gene using PCR, but due to the large size of the gene only exons 6-13 were amplified and confirmed to be KIAA1109 by sequencing. rt-PCR showed that KIAA1109 was detectable in zebrafish cDNA 1-5dpf. However KIAA1109 could not be detected in maternal cDNA. Once I had established that KIAA1109 was expressed at these early stages of zebrafish development, I used whole mount *in-situ* hybridization to characterize the spatial expression of KIAA1109. Within the limitations of the technique, it appeared that KIAA1109 was ubiquitously expressed in the trunk at 2dpf. Such expression might be expected from the available data in other systems, but since optimization of *in situ* hybridization is biased (overdeveloping will always suggest ubiquitous expression, whereas under developing leads to an impression of limited expression) I consider these data preliminary.

To establish the function of KIAA1109, I attempted to induce KIAA1109 loss-of-function. Within the zebrafish community morpholino antisense is by far the most commonly used technique for this purpose, despite the disadvantages

listed in Chapter 1 (1.5.2). Morpholinos generally do not cause degradation of their RNA targets; instead, they block translation of the target mRNA until that RNA is degraded naturally. This means that RT-PCR is not suitable for assaying translation blocking by morpholinos. By blocking sites involved in splicing pre-mRNA, morpholinos can be used to modify and control normal splicing events. This activity can be assayed by RT-PCR, with successful splice-modification appearing as changes in the RT-PCR product band on an electrophoretic gel. The band might shift to a new mass or, if splice-modification triggers nonsense-mediated decay of the transcript, the band will lose intensity or disappear. Nevertheless, confirming aberrant splicing does not confirm that the phenotype is due to specific gene knockdown. Although western blotting to confirm KIAA1109 protein knockdown is the best way to confirm the morpholino effect, there are no antibodies available to zebrafish KIAA1109, and cross-reactivity with other species is unlikely. There is however a human KIAA1109 antibody available. It would be possible to use the human antibody on zebrafish morphants, as well as using monoclonal antibodies to fragments of the protein, or using a combination of monoclonal antibodies instead of a polyclonal. Although this work was not carried out, it would be worth trying in the future. Even if morpholino induced protein knockdown is confirmed, this does not confirm that the phenotype observed is specific to this effect, and it can still be due to off target effects. Ideally, this should be confirmed by rescuing the phenotype by injection of the mRNA. However, this is technically challenging, and I was unable to clone the entire KIAA1109 transcript, due to its large size. In addition, unrestricted overexpression from the earliest time points is not

necessarily the reverse of inducing knockdown specifically in KIAA1109 expressing cells (the morpholino effect) and mRNA overexpression and the morpholino antisense effect have different kinetics. Therefore, a failure to rescue the morpholino effect is not clear evidence that the phenotype is due to off-target effects. Some groups have used co-injection with a p53 morpholino (since many off-target effects are deemed to be due to p53 activation) and if I had had sufficient time I would have performed these studies, or examined the effect of the KIAA1109 morpholinos in p53 stable mutants.

Withstanding these reservations, it seems most likely that the cerebral haemorrhage induced by KIAA1109 knockdown was a specific effect. This is supported by the fact that three separate morpholinos induced the same phenotype, that our group has used dozens of morpholinos and not observed similar phenotypes, and that the effect can be rescued by small molecule VEGF induction, which seems less likely in the case of off-target or non-specific effects. The initial observation of gene knockdown experiments is the general development and survival of the embryos. Upon finding a morpholino concentration in which embryos exhibited healthy behaviour and motility, KIAA1109 gene function was knocked down using a ATG morpholino. However what was very noticeable in the KIAA1109 morphant group was the presence of haemorrhages in consistent locations within the head of the embryos. Before the development of haemorrhage, morphants are indistinguishable from control embryos and establish a robust circulation and the window of time in which haemorrhages appear corresponds to a period of active angiogenesis.

Cerebral haemorrhage is a phenotype observed in several mutant lines generated in forward genetic studies such as a *redhead*, which has a mutation in the *pak2a* gene (Buchner *et al.*, 2007), *mindbomb* which carry mutations on the *mib* gene, which encodes a RING E3 ligase required for Notch activation (Itoh *et al.*, 2003) and *bubblehead* which carry a mutation in the *βpix* gene (Liu *et al.*, 2006a). These mutants, even where the causative mutation has not been isolated, show that this phenotype can be associated with loss-of-function of a single gene. Buchner *et al* found cerebral haemorrhaging in *redhead* at 2 and 3dpf, which is consistent with our findings however in *redhead* haemorrhage resolved in some embryos as they got older, which was not the case for KIAA1109 morphant embryos. The *mindbomb* mutant also exhibits cerebral haemorrhaging caused by a loss of Notch signalling. Upon further investigation Lawson *et al* found that the embryos exhibit normal vascular patterning however the vessel itself lacked any structure (Lawson *et al.*, 2001). To better understand the cause of leakage of the erythrocyte from the cerebral vessels, I used the transgenic embryo, *fli1:EGFP;GataDsRed*, in which endothelial cells express GFP and the erythrocytes express GataRed. The expression of EGFP is detectable as early as the three-somite stage (Lawson and Weinstein, 2002) and therefore the transgenic lines are very useful for the study of vascular formation from an early to late time point. I used spinning disc confocal microscopy to obtain time-lapse images; microangiography has traditionally been used to observe vascularization however it only allows for visualization of patent vessels limiting the scope of investigation into defective vessels or vessels that have yet to be lumenised. Confocal imaging of the dorsal brain of embryos

revealed normal vascular patterning within the brain, as reported for *mindbomb* mutants. Upon higher magnification imaging it was obvious that KIAA1109 morphant embryos had increased permeability compared to the controls as displayed by escaping erythrocytes seen in figure 4.24. To further investigate the vascular permeability of the morphant embryos Dextran was injected into live embryos at 3dpf and embryos imaged on a spinning disc confocal microscope after 5 minutes, after which the dye was taken up into the circulation and could be visualized for time-lapse videos. The videos show the leakage of erythrocytes in the morphant embryos at the sites of haemorrhage, compared to the control embryos, which display the dye only within the vasculature. This is in comparison to the work carried out by Buchner *et al* in which they injected fluorescent quantum dots into the circulation of *pak2a* deficient embryos and found that the blood vessels were more prone to rupture rather than general leakiness, which suggests a loss of junctional integrity rather than an increase in permeability (Buchner et al., 2007).

As the confocal imaging and dextran injections suggested the haemorrhage in KIAA1109 morphants might be caused by decreased vascular integrity I treated the morphants with the VEGF inducer GS4012. VEGF is traditionally associated with angiogenesis and VEGF increases vascular permeability in order to guide tip cells (Olsson et al., 2006). VEGF is also involved in vascular maintenance and endothelial cell survival (Murakami et al., 2011). In order to not interfere with early vascular development and angiogenesis, GS4012 was added to the morphant embryos and control embryos at 24hpf, in which they were incubated until observations at 2 and 3dpf. The up regulation of VEGF in the morphant

embryos prevented the haemorrhage in the drug treated group compared to the DMSO and E3 group, implying that either the KIAA1109 phenotype was due to reduction of VEGF signalling, or that it can be overcome by up regulating VEGF signalling.

To attempt to better understand the mechanism for the KIAA1109 morphant phenotype, I next attempted to define the transcriptional effect of KIAA1109 loss-of-function. These studies are described in the following chapter.

Chapter 5: Transcriptional profiling of KIAA1109 morphants

5.1. Introduction

Having characterised differentially expressed genes in whole blood following an ACS and identifying and functionally assessing KIAA1109 function in zebrafish, I next examined the transcriptional effects of KIAA1109 knockdown in zebrafish. Although not all phenotypes are determined at a transcriptional level, such as an effect on adhesion molecule expression it is of interest to gain insight into the transcriptional changes that occur upon knockdown of the gene, which could lead to the induction of decreased vascular integrity.

5.1.1. Bioinformatic analysis of microarray datasets

Microarray studies generate a large amount of data, which often presents challenges in analysis and interpretation. Many bioinformatic tools have been developed to assist researchers in interpreting microarray datasets, and below I briefly describe those used in this chapter.

5.1.1.1. PANTHER

Protein ANalysis THrough Evolutionary Relationships (PANTHER) is an ontological system that classifies genes by their functions, using published scientific experimental evidence and evolutionary relationships to predict function even in the absence of direct experimental evidence. The database was designed for the high-throughput analysis of protein sequences (Huang da et al., 2009). (PANTHER)

5.1.1.2. STRING

Search Tool for the Retrieval of Interacting Genes/Proteins (STRING)

is a database of known and predicted protein interactions. The interactions include direct (physical) and indirect (functional) associations; they are derived from four sources: genomic context, high throughput experiments, conserved co-expression and published data. STRING quantitatively integrates interaction data from these sources for a large number of organisms, and transfers information between these organisms where applicable. The database currently covers 5,214,234 proteins from 1133 organisms. (STRING)

5.2. Results

5.2.1. RNA extraction

RNA was extracted from ~300 whole embryos at 36hpf which were injected at 1-2 cell stage with either the ATG blocking KIAA1109 or mismatch control morpholino.

4 injections and extractions were carried out on separate days, providing 4 replicates per group. The RNA was dispatched to the Singapore Institute of Genomics, and was kindly carried out by Serene Lee Gek Ping, using a custom microarray developed by the group of our collaborator Sinnakarupan Mathavan. These studies performed one microarray per group (i.e. eight arrays total) to provide estimates of variability between replicates. We then used Genespring software to analyse the data and identify genes that were differentially expressed with statistical significance ($p > 0.05$).

From this list of differentially expressed transcripts, I removed unannotated, hypothetical proteins, as although these may be mechanistically important they

are unable to provide insight into the effect of KIAA1109 as they have no identified function or participation in biological pathways. The remaining differentially expressed genes are shown in table 5.1 (up regulated in KIAA1109 morphants) and table 5.2 (down regulated in KIAA1109 morphants).

Compared with other microarray studies we have performed, the number of differentially expressed genes induced by KIAA1109 knockdown is relatively small. For example, previous studies in our group examining the effect of blood flow on transcription, or the transcriptional effect of specific mutations have yielded hundreds of differentially expressed genes. It appears therefore that KIAA1109 is unlikely to play a major role in transcriptional regulation.

Each differentially expressed gene was put through a literature search, looking for expression patterns in the zebrafish model organism database (Zfin) which showed mainly expression in the head of embryos or ubiquitous expression, as well as using PANTHER to determine if the genes are involved in any specific pathways.

5.2.2. PANTHER analysis of differentially expressed genes

A list of the PANTHER outputs can be seen for differentially expressed genes in table 5.3.

The first numerical column contains the number of genes in the uploaded list that map to the PANTHER classification category. The second numerical column contains the expected value, which is the number of genes you would expect in the reference list for the PANTHER category, based on the reference list. The

Table 5.1. Differentially expressed genes that are up regulated by KIAA1109 knockdown.

Gene name	Gene Symbol	p-value	Fold change
Cell adhesion molecule 1b	cadm1b	0.03	3.02
Glutamate receptor, ionotropic, AMPA 2a	gria2a	0.04	2.13
Leucine-rich repeat LGI family, member 2b	lgi2b	0.01	2.23
Ligand of numbe protein X1	lnx1	0.02	2.40
Neuropeptides B/W receptor	npbwr2	0.03	2.32
Solute carrier family 17 (sodium-dependent inorganic phosphate cotransporter), member 6a	slc17a6a	0.02	2.51
Renin	ren	0.01	2.17
synaptotagmin XIb	syt11b	0.01	2.04
HtrA serine peptidase 3a	htra3a-001	0.01	2.78
kelch repeat and BTB (POZ) domain containing 12	kbtbd12	0.01	2.53
proline rich 15-like b	prr15lb	0.01	2.03
zgc:136908	zgc:136908	0.03	2.19
glycine N-methyltransferase	gnmt	0.00	2.07
im:7147183	im:7147183	0.04	3.06
glutamate receptor, ionotropic, N-methyl D-aspartate 1a	grin1a	0.00	2.08
crystallin, gamma N1	crygn1	0.00	3.33
crystallin, gamma S3	crygs3	0.01	2.28

Table 5.2. Differentially expressed genes that are down regulated by KIAA1109 knockdown.

Gene name	Gene Symbol	p-value	Fold change
Otoferlin	otof	0.02	3.47
MACRO domain containing 2	macro2	0.01	2.09
protocadherin 1 gamma 2	pcdh1g2	0.01	2.02
growth regulation by estrogen in breast cancer 1	greb1	0.02	2.03
coiled-coil domain containing 120	ccdc120	0.02	2.59
zinc finger protein 729	ZNF729	0.00	2.05
late endosomal/lysosomal adaptor, MAPK and MTOR activator 2	lamtor2-001	0.01	2.14
ankyrin repeat and death domain containing 1B	ankdd1b	0.04	2.07
RNA binding motif protein 41	rbm41	0.00	2.05
ribosomal protein L21	rpl21	0.03	2.20
nodal-related 2	ndr2	0.00	2.35
ribosomal protein S23	rps23	0.03	2.44
apolipoprotein A-1	apoa1	0.02	2.51
regulator of G-protein signalling 12	rgs12	0.01	2.49
carboxyl ester lipase (bile salt-stimulated lipase)	cel.1	0.02	2.74
cerebellin 1 precursor	cbln1	0.04	2.12
si:dkeyp-59a8.1	si:dkeyp-59a8.1	0.05	2.28

third numerical column is a fold change representation of the number of genes in the reference list compared to the expected value. Of the 34 differentially expressed genes all were mapped by PANTHER however most of these were 'unclassified' and therefore removed from the table (table 5.3). The findings are also not statistically significant as there is a small list of differentially expressed genes and so there may be only one gene involved in a pathway.

The Notch signalling pathway has the highest fold representation, which is for the gene *LNK1*. This is of particular interest as the role of Notch in vascular remodelling and integrity is well established. *Gria2a* also has a high fold representation in both metabotropic and ionotropic glutamate receptor pathways. The metabotropic glutamate receptor group III pathway is a G-protein coupled receptor that is activated by L-AP-4 and inhibits adenylate cyclase activity. The ionotropic glutamate receptor pathway is a series of molecular signals initiated by glutamate binding to a glutamate receptor on the surface of the target cell, followed by the movement of ions through a channel in the receptor complex.

The highest fold representation for biological processes are asymmetric protein localization, protein localization and dorsal/ventral axis specification, which also involve *LNK1*. The highest fold represented molecular function was glutamate receptor activity for *gria2a* and aspartic type endopeptidase activity.

Interestingly the highest fold represented in the cellular component is cell junction for the *LNK1* gene. There is an equally high fold representation of plasma membrane for the same gene. The fold representation for protein class includes over representation in cadherin protein class for *Pcdh1γ2* and cell

junction for the *LNK1* gene. Although not greatly over represented there are also many relevant processes such as cell adhesion molecule and cell junction protein.

As the phenotype was rescued using a VEGF inducer it would have been expected that there may have been some down regulation in VEGF, however VEGFaa, VEGFab and VEGFc showed no statistically significant differential expression. As the mechanism by which GS4012 up regulates VEGF is currently unknown and since the microarray was custom made, it could be that the relevant VEGF component was not included on the chip or not differentially expressed at 36hpf.

Although there is not a large list of genes that are differentially expressed genes and the fold representation of some processes are not significant, it does however provide us with a greater knowledge of the kinds of pathways and processes that may be affected by the knockdown of KIAA1109.

Table 5.3. PANTHER output of differentially expressed genes of KIAA1109 morphants

Pathways	Observed number of differentially expressed genes	Expected by chance	Fold Representation
Notch signalling pathway	1	0.04	25
Ionotropic glutamate receptor pathway	1	0.06	16.67
Metabotropic glutamate receptor group III pathway	1	0.07	14.29
Cadherin signalling pathway	1	0.11	9.09
Heterotrimeric G-protein signalling pathway-Gq alpha and Go alpha mediated pathway	1	0.13	7.69
Heterotrimeric G-protein signalling pathway-Gi alpha and Gs alpha mediated pathway	1	0.17	5.88
Wnt signalling pathway	1	0.27	3.70

Biological Process	Observed number of differentially expressed genes	Expected by chance	Fold Representation
asymmetric protein localization	1	0.03	33.33
protein localization	1	0.03	33.33
dorsal/ventral axis specification	1	0.03	33.33
localization	1	0.06	16.67
nerve-nerve synaptic transmission	1	0.09	11.11
lipid transport	1	0.12	8.33
pattern specification process	1	0.21	4.76
neurotransmitter secretion	1	0.21	4.76
synaptic transmission	2	0.45	4.44
exocytosis	1	0.23	4.35
translation	1	0.28	3.57
neurological system process	4	1.23	3.25

endocytosis	1	0.33	3.03
vesicle-mediated transport	2	0.7	2.86
visual perception	1	0.36	2.78
system process	4	1.49	2.68
cell-cell signalling	2	0.76	2.63
cell-cell adhesion	1	0.38	2.63
sensory perception	1	0.46	2.17
cation transport	1	0.47	2.13

Molecular Function	Observed number of differentially expressed genes	Expected by chance	Fold Representation
glutamate receptor activity	1	0.02	50.00
aspartic-type endopeptidase activity	1	0.02	50.00
neuropeptide hormone activity	1	0.03	33.33
lipid transporter activity	1	0.05	20.00
hormone activity	1	0.08	12.50
ligand-gated ion channel activity	1	0.11	9.09
structural constituent of ribosome	1	0.14	7.14
small GTPase regulator activity	2	0.3	6.67
calcium ion binding	2	0.34	5.88
nuclease activity	1	0.21	4.76
structural molecule activity	3	0.96	3.13
enzyme regulator activity	2	0.68	2.94
ion channel activity	1	0.36	2.78
peptidase activity	1	0.49	2.04

Cellular Component	Observed number of differentially expressed genes	Expected by chance	Fold Representation
cell junction	1	0.12	8.33
plasma membrane	1	0.12	8.33
extracellular matrix	1	0.39	2.56
extracellular region	1	0.39	2.56

PANTHER Protein Class	Observed number of differentially expressed genes	Expected by chance	Fold Representation
ionotropic glutamate receptor	1	0.02	50.00
aspartic protease	1	0.02	50.00
neuropeptide	1	0.03	33.33
apolipoprotein	1	0.05	20.00
cadherin	1	0.08	12.50
peptide hormone	1	0.08	12.50
basic helix-loop-helix transcription factor	1	0.09	11.11
ligand-gated ion channel	1	0.11	9.09
cell junction protein	1	0.12	8.33
structural protein	1	0.14	7.14
ribosomal protein	1	0.14	7.14
membrane traffic protein	2	0.3	6.67
G-protein modulator	2	0.3	6.67
nuclease	1	0.21	4.76
calcium-binding protein	1	0.26	3.85
transfer/carrier protein	1	0.3	3.33
ion channel	1	0.33	3.03
extracellular matrix protein	1	0.39	2.56
transporter	2	0.92	2.17
cell adhesion molecule	1	0.49	2.04
protease	1	0.49	2.04

5.3. Differentially expressed genes

Upon PANTHER analysis it became obvious that some genes had high fold representations in many different pathways and processes, in particular those that were related to angiogenic processes.

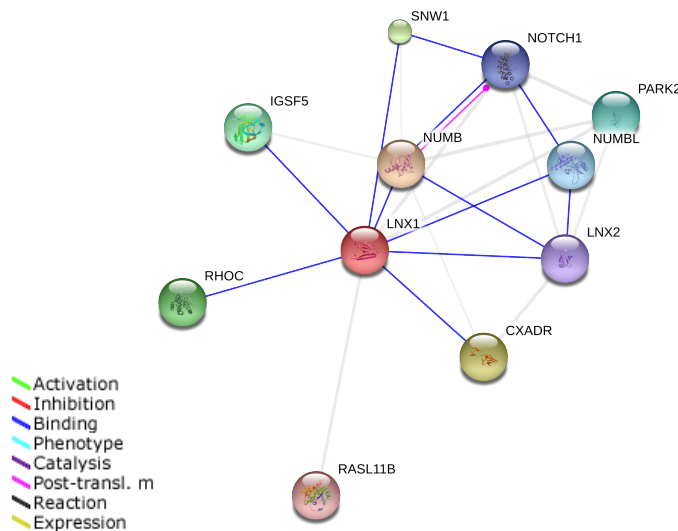
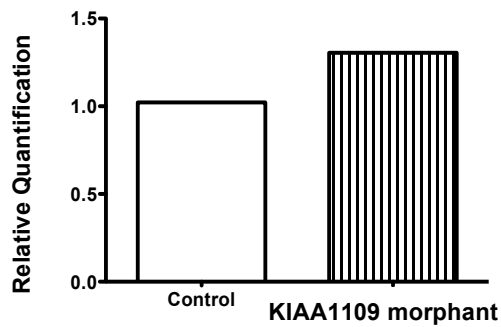
5.3.1. Ligand of numb protein X-1 (*LNK1*)

LNK1 is significantly up regulated in KIAA1109 morphants compared to controls. This was validated using quantitative RT-PCR (figure 5.1) using a commercially ready Taqman probe as described in chapter 2.4.

LNK1 has 65% homology to human LNX1. LNX1 was identified as a protein that interacts with Numb and named Ligand of Numb protein X (Nie et al., 2002) zfin showed that *LNK1* has been shown to be expressed maternally and ubiquitously (Ro and Dawid, 2009).

PANTHER analysis output showed that *LNK1* is involved in the Notch signalling pathway and can be visualized using STRING database (figure 5.1). The role played by *LNK1* is in targeting Numb, a component of the Notch pathway that functions in the specification of cell fates during development and is known to control cell numbers during neurogenesis in vertebrates (Johnson, 2003). *LNK1* ubiquitinates *Numb*, leading to proteasomal degradation and has been shown to modulate Notch signalling in cultured cells (Nie et al., 2002). Ubiquitination of *Numb* by *LNK1* is also thought to have an effect on the formation or remodelling of cell-cell junctions, as ectopic expression of *LNK1* can remove claudins from cell junction and enhance TGF β -induced epithelial to mesenchymal transition in epithelial cells (Takahashi et al., 2009). STRING analysis also shows that it

interacts with *CXADR*, which is a component of the epithelial apical junction complex that is essential for the tight junction integrity, proposed to function as a homophilic cell adhesion molecule. In zebrafish depletion of *LnX-1* using specific antisense morpholinos caused strong embryonic dorsalization (Ro and Dawid, 2009).



Gene	Gene name
LNX2	ligand of numb-protein X 2
RASL11B	RAS-like, family 11, member B
NOTCH1	Notch homolog 1
SNW1	SNW domain containing 1
NUMB	numb homolog
PARK2	Parkinson disease (autosomal recessive, juvenile) 2
NUMBL	numb homolog -like
RHOC	ras homolog gene family
IGSF5	immunoglobulin superfamily, member 5
CXADR	coxsackie virus and adenovirus receptor

Figure 5.1. qRT-PCR validation and STRING output of LNX1 interaction with genes.

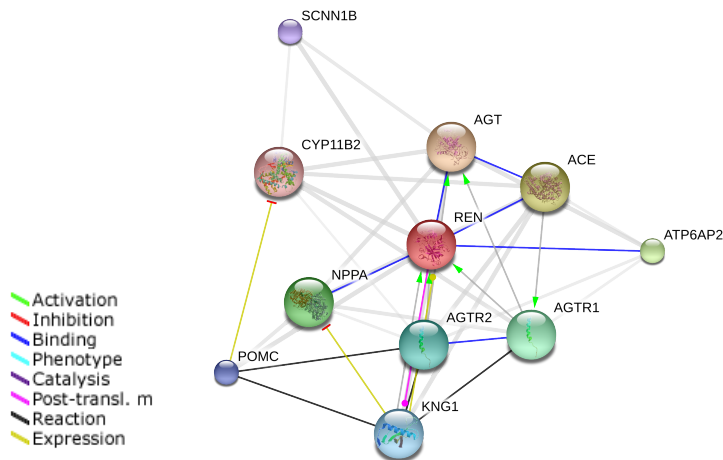
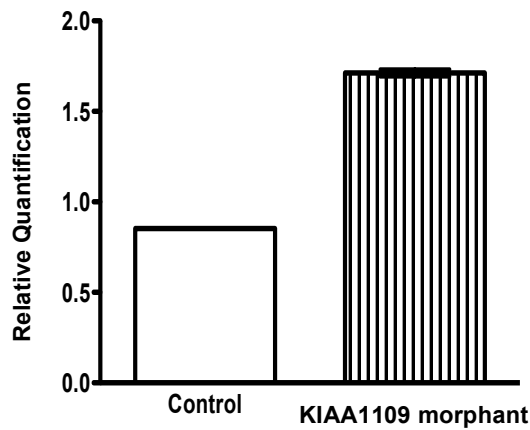
Diagram shows the genes that strongly interact with LNX1 and the colour of the lines represents the type of interaction shown in the table. The table also contains a list of gene names included in the diagram. Mean \pm SEM. T-test. $p=NS$. $N=3$, 100 embryos per group.

5.3.2 Renin (*ren*)

Renin is significantly up regulated in the KIAA1109 morphants compared to controls. This was validated using quantitative RT-PCR (figure 5.2).

Renin maintains blood pressure through vasoconstriction by generating angiotensin I from angiotensinogen in the plasma, initiating a cascade of reactions that produce an elevation of blood pressure and increased sodium retention by the kidney as part of the renin-angiotensin system (RAS) (Brown, 2007). Pathological activation of the RAS results in excessive vasoconstriction, sodium retention, abnormal vascular smooth muscle and cardiac hypertrophy and fibrosis (Ma et al., 2010). Elevated plasma *renin* activity is associated with increased morbidity and mortality in patients with cardiovascular disease (Volpe et al., 2012) and pharmacological inhibition of RAS has led to reductions on cardiovascular morbidity and mortality.

It might be expected that *renin* is significantly up regulated in the KIAA1109 morphants, as due to cerebral haemorrhaging the blood pressure would be predicted to be reduced in the KIAA1109 morphants. Liang *et al* found expression of *renin* in the kidney of zebrafish (Liang et al., 2004), in keeping with its expression pattern in humans and its role in activation of RAS.



Gene	Gene name
SCNN1B	sodium channel, nonvoltage-gated 1, beta
POMC	proopiomelanocortin
KNG1	kininogen 1
AGTR2	angiotensin II receptor, type 2
ACE	angiotensin I converting enzyme 1
CYP11B2	cytochrome P450, family 11, subfamily B, polypeptide 2
AGTR1	angiotensin II receptor, type 1
AGT	angiotensinogen
ATP6AP2	ATPase, H ⁺ transporting, lysosomal accessory protein 2
NPPA	natriuretic peptide precursor A

Figure 5.2. qRT-PCR validation and STRING output of Renin interaction with genes.

Diagram shows the genes that strongly interact with *Renin* and the colour of the lines represents the type of interaction shown in the table. The table also contains a list of gene names included in the diagram. Mean \pm SEM. T-test. $p=NS$. $N=3$, 100 embryos per group.

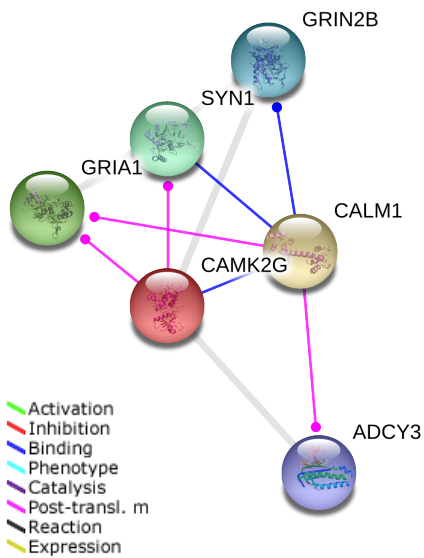
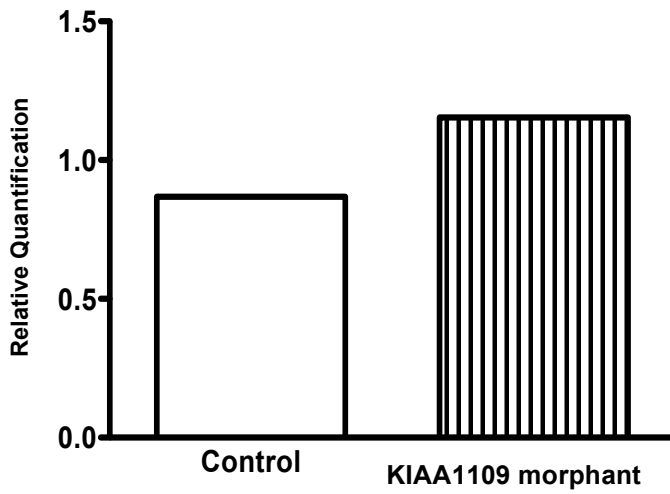
5.3.3. Calcium/calmodulin-dependent protein kinase (*camk2g2*)

Camk2g2 is significantly up regulated in the KIAA1109 morphants compared to controls. This was validated using quantitative RT-PCR (figure 5.3). *CaMK-II* is highly conserved Ca^{2+} - /calmodulin-dependent protein kinase expressed throughout the lifespan of all vertebrates. Zfin shows that *Camk2g2* is expressed in the forebrain, hindbrain and liver. During early development, *CaMK-II* regulates cell cycle progression and non- canonical Wnt-dependent convergent extension (Rothschild et al., 2007). They found that there were significant expression levels of *camk2g2* transcripts from the 8-cell through to 72hpf in the forebrain, midbrain and hindbrain and claim that this *CaMK-II* localization in the zebrafish is consistent with its involvement in non-canonical Wnt pathways (Rothschild et al., 2007)

5.3.4 Glutamate receptor, ionotropic, N-methyl D-aspartate 1a (*grin1a*)

Grin1a is significantly up regulated in the KIAA1109 morphants compared to controls. This was validated using quantitative RT-PCR (figure 5.4) using a commercially ready Taqman probe as described in chapter 2.5.4.

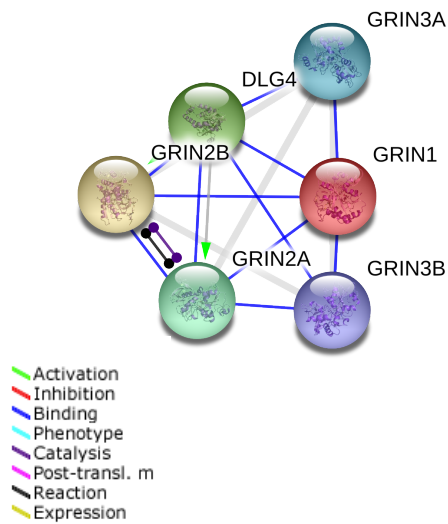
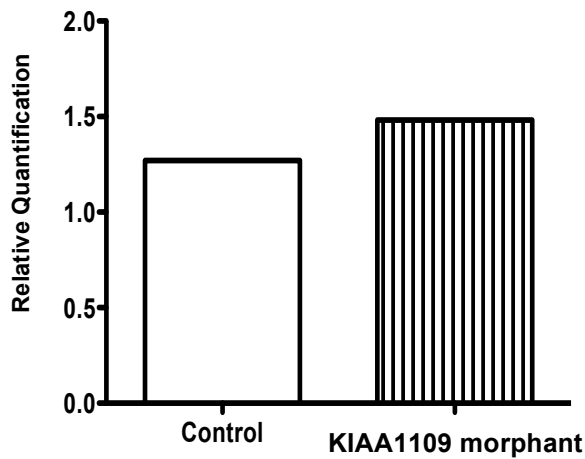
Glutamate is the main excitatory neurotransmitter in vertebrates, and its effects are mediated by means of two classes of receptors: G protein-coupled receptors (metabotropic glutamate receptors) and ligand-gated ion channels (ionotropic receptors) (Cox et al., 2005). PANTHER analysis had shown that the differentially expressed genes had a significantly larger representation of genes in both of these pathways.



Gene	Gene name
CALM1	calmodulin 1 (phosphorylase kinase, delta)
GRIA1	glutamate receptor, ionotropic
ADCY3	adenylate cyclase 3
SYN1	synapsin I
GRIN2B	Glutamate receptor, ionotropic, N-methyl D-aspartate 2B

Figure 5.3. *qRT-PCR* validation and *STRING* output of *Camk2g* interaction with genes.

Diagram shows the genes that strongly interact with *Camk2g* and the colour of the lines represents the type of interaction shown in the table. The table also contains a list of gene names included in the diagram. Mean \pm SEM. T-test. $p=NS$. $N=3$, 100 embryos per group.



Gene	Gene Name
DLG4	discs, large homolog 4
GRIN3B	glutamate receptor, ionotropic, N-methyl-D-aspartate 3B
GRIN3A	glutamate receptor, ionotropic, N-methyl-D-aspartate 3A
GRIN2B	glutamate receptor, ionotropic, N-methyl D-aspartate 2B

Figure 5.4. qRT-PCR validation and STRING output of *Grin1a* interaction with genes.

Diagram shows the genes that strongly interact with *Grin1a* and the colour of the lines represents the type of interaction shown in the table. The table also contains a list of gene names included in the diagram. Mean \pm SEM. T-test. p=NS. N=3, 100 embryos per group.

Expression analysis via in situ hybridization shows that *Grin1a* is expressed in the brain, diencephalon, hindbrain (Tzeng et al., 2007) as well as the midbrain and forebrain (Cox et al., 2005).

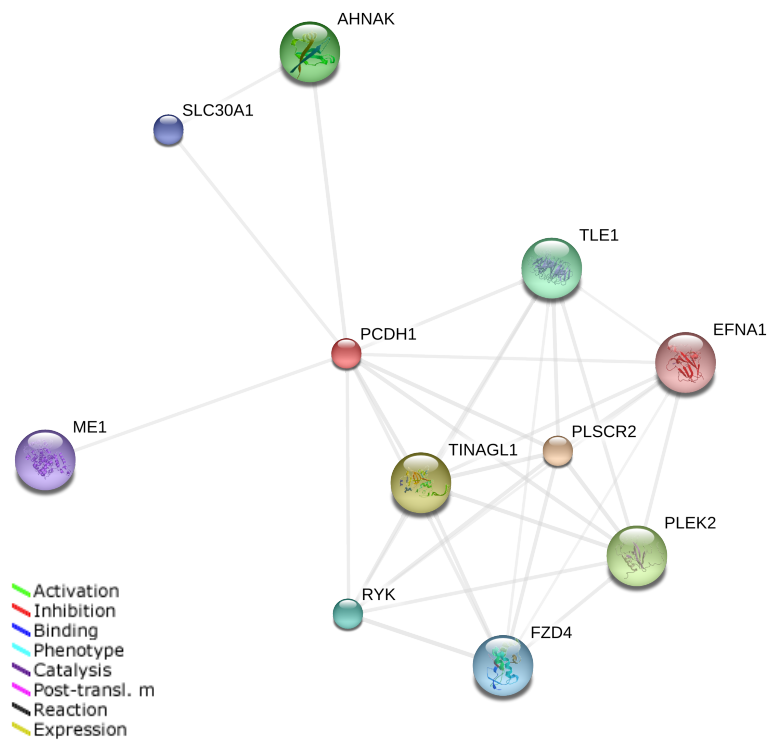
5.3.5. Protocadherin 1 gamma 2 (*PCDH1γ2*)

Pcdh1γ2 is significantly down regulated in the KIAA1109 morphants compared to controls. The clustered protocadherins are a subfamily of neuronal cell adhesion molecules that play an important role in development of the nervous systems in vertebrates (Tan et al., 2010). Zebrafish contains two independent protocadherin clusters, *Pcdh1* and *Pcdh2*, that collectively contain at least 107 genes (Noonan et al., 2003). Wu *et al* found that similar to the mammalian *Pcdh* genes, the zebrafish *Pcdh* genes are also expressed in the CNS and that expression of the *Pcdh1γ* from zebrafish brain total RNA preparations by using RT-PCR (Wu, 2005). PANTHER analysis showed that *pcdh1γ2* is involved in the cadherin signalling pathway as well as the wnt pathway. STRING analysis shows that *pcdh1γ2* interacts with many genes that interact with these pathways as well as being involved in other relevant mechanisms.

5.3.6. Nodal related 2 (*ndr2*)

Ndr2 is significantly down regulated in the KIAA1109 morphants compared to controls.

Nodal-related factors have been implicated in mesodermal and neural patterning, and left-right asymmetry, in several animal models and Erter *et al* were able to isolate and characterize the zebrafish *ndr2* and found that it



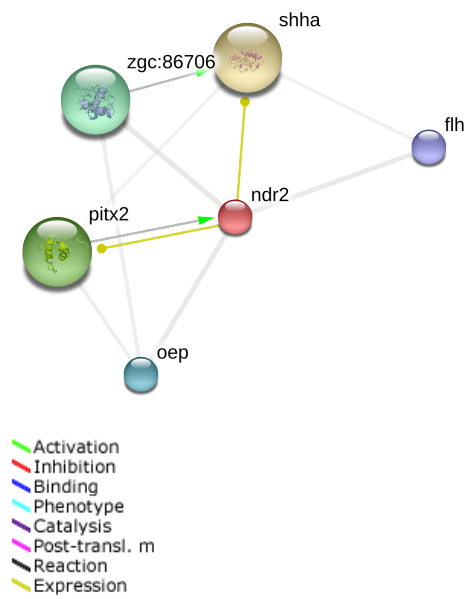
Gene	Gene Name
AHNAK	AHNAK nucleoprotein
RYK	RYK receptor-like tyrosine kinase
TLE1	transducin-like enhancer of split 1
FZD4	frizzled homolog 4
PLEK2	pleckstrin 2
ME1	malic enzyme 1
EFNA1	ephrin-A1
TINAGL1	tubulointerstitial nephritis antigen-like 1
PLSCR2	phospholipid scramblase 2

Figure 5.5. STRING output of *pcdh1γ2* interaction with genes.

Diagram shows the genes that strongly interact with *pcdh1γ2* and the colour of the lines represents the type of interaction shown in the table. The table also contains a list of gene names included in the diagram.

encodes a robust mesendodermal inducer that signals non autonomously during the earliest stages of embryonic patterning, and that part of this activity arises from within the YSL (Erter et al., 1998). PANTHER analysis showed that *ndr2* is involved in the TGF β pathway, as the nodal family of proteins is a subset of the TGF β superfamily and work as part of a positive feedback loop by interacting with other proteins to induce gene transcription. In zebrafish the *Cyclops* locus encodes *ndr2* and Rebagliati *et al* showed that in the *Cyclops* mutant, a loss of *Ndr2* signalling causes abnormal patterning and morphogenesis of mesoderm and forebrain (Rebagliati et al., 1998).

The role of *ndr2* played in patterning can also be confirmed by STRING in its interaction with genes such as *shha* which is a signal produced by the notochord that induces somite patterning, dorso-ventral patterning of the brain and early patterning of the developing eyes.



Gene	Gene Name
shha	Sonic hedgehog protein A
oep	one-eyed pinhead
flh	floating head
pitx2	Pituitary homeobox 2

Figure 5.6. STRING output of *ndr2* interaction with genes.

Diagram shows the genes that strongly interact with *ndr2* and the colour of the lines represents the type of interaction shown in the table. The table also contains a list of gene names included in the diagram.

5.4. Discussion

In this chapter I performed a microarray on KIAA1109 morphants and used *in-silico* methods to analyse the transcriptional effect of KIAA1109 knockdown, in an attempt to gain insight into the mechanisms by which KIAA1109 is involved in vascular integrity.

In-silico methods of research have been widely used by biologists to further gain information on their area of interest. The majority of bioinformatics tools available are not user friendly without a computing background and often require substantial time to familiarize oneself with the output format as well as personalizing the uploaded list to the specifications of that particular system. The output lists can also require the specialist knowledge of a bioinformatician and can be hard for biologists to analyse efficiently. Most annotational databases use numerous public sources of protein and gene annotation and are therefore dependent on vigilant and regular updates. As this is not the case in some public source databases, many genes remain unannotated and the uploaded list may need to be reanalysed at regular intervals or by several databases in order to gain a complete list of annotations, which can be very time consuming.

However there are user friendly and reliable databases used regularly for annotation, which can provide informative insight into pathways and functions of genes of interest. Using a combination of PANTHER for pathway inclusion and

STRING for protein interaction, I was able to visualize biological interactions for genes that I identified as differentially expressed by KIAA1109 knockdown.

Genes were validated using qRT-PCR and Taqman probes which were commercially available. Only two genes did not have commercially available probes which were designed using the inbuilt probe design software within the Applied Biosystems website. Of the six genes only four showed the same differential expression using qRT-PCR. The genes that were significantly down regulated, *pcdh1γ2* and *ndr2* did not show significant reduction compared to the control. This could be due to the sensitivity of the assay being less than that of a microarray and therefore not showing a significant difference. Although not validated by qPCR, *in-silico* analysis showed that suppression of some of these genes might plausibly account for the KIAA1109 knockdown phenotype. *Pcdh1γ2* is part of the cadherin family, which plays a large role in vascular integrity, which is down regulated in KIAA1109 morphants. In humans *renin* is released upon a fall in blood pressure, in particular due to haemorrhaging. This was also reflected in the KIAA1109 morphant group, with a significant up regulation of *renin* in the morphants where the main phenotype is cerebral haemorrhaging. It is also of interest that *LNK1* which is part of the Notch pathway is up regulated in KIAA1109 morphants in which the phenotype can be rescued by VEGF induction. An induction of Notch ligand *dll4* has been shown to reduce VEGF, likely via down regulation of VEGFR-2 expression, in cultured endothelial cells (Williams et al., 2006). As previously shown KIAA1109 is expressed in endothelial cells, and can be rescued with VEGF induction, however the mechanism by which GS4012 induces VEGF is unknown. The

findings using pathway analysis as well as protein interaction could shine a light on the induction pathway of VEGF in order to rescue the morphant phenotype.

The *in-silico* findings of this chapter lead to many speculations as to the mechanism by which the knockdown of KIAA1109 causes a decrease in vascular integrity as well as which pathway this gene could be involved in and proteins that it is interacting with. As mentioned these are *in-silico* findings and speculations of the function of KIAA1109 can only be fully understood by further experiments.

Chapter 6: General discussion

6.1. General discussion

Cardiovascular disease is the largest cause of death worldwide. Although useful biomarkers for diagnosis of acute coronary syndromes are well established in order to obtain more information about the pathogenesis of myocardial infarctions we investigated gene expression patterns in peripheral blood of UA patients compared to those having suffered MI.

A limitation of the study was the patient demographics. As a result of all recruited patients living within the South Yorkshire area with 100% of participants are White British; the results will be highly specific to this population and less transferable to others.

In order to investigate gene expression patterns in peripheral blood RNA was extracted from peripheral blood of UA and MI patients at serial time points, of which my results have concentrated on 1 day post admission as this is the time point at which most deaths post MI occur.

Gene expression profiling of RNA extracted from peripheral blood is a potentially informative method for identifying biomarkers, examining disease states, and investigating immune responses. In cardiovascular disease there are many advantages to studying gene expression from whole blood rather than from fractionated subpopulations such as neutrophils. Firstly, when fractionation steps are performed, α and β globin mRNA transcripts are often still rich in total RNA extracted from leukocyte-enriched populations (Feezor et al., 2004) while the fractionation itself can contribute to an increase in sample-to-sample variability in the microarray assay (Fan et al., 2007). Secondly, there

are a multitude of populations within whole blood including neutrophils, monocytes, and dendritic cells. While some studies may require analysis of individual cell types it may be advantageous in this study to investigate them as a whole so as not to exclude any potential markers, additionally it was more cost and time efficient to study these together. Finally, working with whole blood across multiple sites instead of fractionation facilitates a uniformity that is diminished with each additional step in the processing of the blood (Vartanian et al., 2009). However, the relatively high proportion of globin messenger RNA present in total RNA extracted from whole blood can reduce the efficacy of the microarray assay by interfering with the hybridization step of the microarray and therefore the detection of less abundant gene transcripts (Feezor et al., 2004). Fractionation of whole blood components prior to RNA extraction is a common occurrence and depending on the fractionation method selected, partial or complete removal of reticulocytes, the primary source of globin RNA, may be achieved. In preparing the RNA the Ambion GLOBINclear™ kit was used to remove globin from the RNA to ensure efficient hybridization.

The use of microarrays has expanded rapidly as an unbiased approach to the identification of novel genes for research. Its flexibility, reducing cost and high-throughput has allowed its use in studying a variety of human diseases. The use of Affymetrix GeneChip allows us to gain large numbers of gene expression data from large cohorts of patients for comparison. The output of a microarray can range from 4,000–50,000 measurements of gene expression per biological sample making correctly analysing the data one of the biggest challenges. This is

dependent on many different databases for annotation of probe sets and gene names, which are not always up to date and are ever changing. It can also be an overwhelming process to identify the most significant list of genes, which puts an emphasis on the parameters set, such as p values and fold change, to ensure an unbiased end-list of genes. However analysis software such as PUMA and several annotation databases have been designed to help researchers efficiently deal with large data sets. Using such software and databases I was able to identify a novel candidate gene, KIAA1109.

It is important to confirm differential expression of candidate genes using quantitative RT-PCR. qRT-PCR is a technically challenging technique, that can be time consuming and expensive. There is also no general consensus in the use of appropriate control genes as well as the accurate analysis of data, with some using the delta ct method and others the pfaffl method as well as relative quantification making validation subjective to the operator. The housekeeping genes I used were DECR1 and TRAP1 which have been published as being the most stably expressed genes needed for accurate normalization in RNA expression studies of human whole blood (Stamova et al., 2009). Although the qRT-PCR data acquired is not statistically significant, the trend does follow that seen in the microarray data.

Although RNA based biomarkers are unlikely to be amenable to direct clinical introduction given their technical difficulty and susceptibility to variability, the ability of arrays to provide whole genome level assessments (at the mRNA level) is extremely powerful. It is possible that differentially expressed transcripts (such as KIAA1109) are differentially expressed at the protein level.

I did not examine this, but such changes in protein transcription are much more practically suitable for use as biomarkers and diagnostics.

Upon selecting a candidate gene it is important to assess the function of the gene in an appropriate animal model. Zebrafish have many advantages for such a purpose due to their small size, high fecundity, genetic homology to humans and the established use of genetic manipulation for gene knockdown and over expression studies. Morpholino technology has long been used in zebrafish to temporarily knockdown target gene expression. This can provide important information as to the effect of KIAA1109 knockdown in the development of the embryo. Morpholino antisense does have its pitfalls as it is only active up to 3-4dpf and so cannot be used for long-term investigation as well as some off target effects that can be misinterpreted as a phenotype. However, it is difficult to carry out western blotting in zebrafish as there are very few antibodies that are effective and available. The creation of a stable mutant to confirm morpholino data is now possible (Buchner et al., 2007, Itoh et al., 2003, Jiang et al., 1996), however is time consuming (see future work).

Upon knocking down KIAA1109 I observed severe cerebral haemorrhaging, which was not present in control morphants. To increase my confidence in the specificity of the phenotype to KIAA1109 knockdown two other morpholinos were designed, a splice site and non-overlapping morpholino, both of which induced a similar percentage of cerebral haemorrhaging. I was unable to perform mRNA rescue as I was unable to clone the entire KIAA1109 gene. However, the ability of the VEGF inducer, GS4012, to rescue the haemorrhagic

phenotype is compelling, suggesting that the phenotype is specific to the actions of the KIAA1109 morpholino, and that haemorrhaging may be caused by a disruption in the VEGF pathway.

I speculate that although the down regulation of KIAA1109 after MI could have multiple explanations, my findings could indicate a potential causative role for KIAA1109 in initiation of myocardial infarction. The presence of neovessels in an atherosclerotic plaque makes it prone to rupture due to their fragile structure, making them susceptible to interplaque haemorrhage. This neovessel haemorrhaging releases red blood cells into the plaque, increasing lipid peroxidation and macrophage activation and eventually leading to a myocardial infarction. Reduced expression of KIAA1109 disrupts vascular integrity of these neovessels, increasing leakage into the plaque and promoting interplaque haemorrhaging. However, since we cannot identify patients who will suffer an ACS prior to presentation, it would be difficult to examine whether reduced KIAA1109 indicates higher risk for plaque rupture at the present time. If advances in imaging allow identification of vulnerable plaques prior to rupture, it would be interesting to examine KIAA1109 expression in these patients' blood.

To better understand the mechanism by which KIAA1109 is disrupting vascular integrity, a custom made microarray was carried out using RNA from whole embryos 36hpf. After analysis of the data, six differentially expressed genes of interest were selected. Of those *LNX1* was up regulated and is known to be part

of the Notch pathway, Protocadherin is down regulated and is part of the cadherin family, which play an important role in vascular integrity as well as being part of the Wnt pathway. *LNX1* has been involved in many pathways as well as biological, cellular and molecular functions, as identified by PANTHER, which are essential for vascular integrity. It has also been previously indicated in a study by Kansaku *et al* implicating its involvement in reorganization of cell junctions (Kansaku et al., 2006).

The mutant, *Cyclops*, is caused by a loss of *Ndr2* signalling causing abnormal patterning and morphogenesis of mesoderm and forebrain (Rebagliati et al., 1998).

These findings can allow speculation of the potential interaction between KIAA1109, VEGF and Notch. The KIAA1109 morphant microarray findings showed no significant difference in the expression of VEGF ligands VEGFaa, VEGFab and VEGFc. However the microarray did not look at the expression of VEGF receptors. Ruch et al showed that if VEGF ligands are stabilised VEGF receptor differential regulation can still have an independent effect (Ruch et al., 2007). An induction of Notch ligand *dll4* has also shown to reduce VEGF, likely via down regulation of VEGFR-2 expression, in cultured endothelial cells (Williams et al., 2006). The morphant microarray results also show that there is an induction of Notch via *LNX1*. As VEGFR2 is associated with vascular integrity and the process by which GS4012 induces VEGF, in order to rescue haemorrhaging in the KIAA1109 morphants is unknown, it could be speculated that it rescues the phenotype via an interaction of VEGFR2 and Notch. As previously suggested if KIAA1109 down regulation in neovessels within the

plaque can lead to an increase in neovessel rupture and therefore interplaque haemorrhage inducing an MI, it could potentially introduce VEGF therapy to reduce the occurrence of plaque rupture.

The identification of these genes and subsequent investigation into their interaction with KIAA1109 will provide a more thorough insight into the mechanism by which KIAA1109 knockdown disrupts vascular integrity.

6.2. Future work

Due to time constraints I was unable to pursue many aspects that would benefit from further investigation.

- During this work, I requested generation of a KIAA1109 mutant zebrafish by the Wellcome Trust Sanger institute, which provides such a service as part of the on going effort to generate mutant zebrafish lines in all protein coding genes (Sanger). Although these were not available for examination during my PhD, four mutant alleles have since been generated three of which, sa3868, sa2675 and sa2712 bear a nonsense mutations and another, sa4495 contains a mutation in an essential splice site.
- These mutants will side step the limitations of morpholino experiments and allow investigation of the effect of KIAA1109 loss of function in adult fish as well.

- Mutant embryos could be used for high throughput drug screens for potential new treatments for vascular stability (seeking to rescue the haemorrhagic phenotype).
- Another microarray could be carried out using a stable line to confirm my data from morphants.
- The natural progression from a zebrafish model is to a higher model such as mice, which are more genetically similar to humans and have been used widely to study cardiovascular disease. Currently a mouse line with a mutation in the KIAA1109 gene is being generated as part of the international knockout mouse consortium. They have generated ES cells for 10 gene trap and 1 targeted mutation knockout mouse models, which have also not yet been phenotyped.
- Myocardial infarction could be induced in KIAA1109 knockdown mice crossed with apoE/LDLR ^{-/-} knock out models and the effect on infarct size and survival assessed.
- It would be important to attempt to reproduce our findings in different patient cohorts, using more time points, as well as recruiting healthy patients as controls.
- A microarray could be carried out on isolated cell types such as leukocytes of ACS patients, to determine the origin of KIAA1109 expression.
- A microarray could be carried out on samples taken from patients before and after an angioplasty. Since this frequently induces small MI, this might inform whether KIAA1109 is down regulated in response to MI.

References

- ABBATE, R., CIONI, G., RICCI, I., MIRANDA, M. & GORI, A. M. 2012. Thrombosis and acute coronary syndrome. *Thromb Res*, 129, 235-40.
- ANTMAN, E. M., TANASIJEVIC, M. J., *et al.* 1996. Cardiac-specific troponin I levels to predict the risk of mortality in patients with acute coronary syndromes. *N Engl J Med*, 335, 1342-9.
- ASAKAWA, K. & KAWAKAMI, K. 2008. Targeted gene expression by the Gal4-UAS system in zebrafish. *Dev Growth Differ*, 50, 391-9.
- BAGINSKY, S., HENNIG, L., ZIMMERMANN, P. & GRUISSEM, W. 2010. Gene expression analysis, proteomics, and network discovery. *Plant Physiol*, 152, 402-10.
- BILL, B. R., PETZOLD, A. M., CLARK, K. J., SCHIMMENTI, L. A. & EKKER, S. C. 2009. A primer for morpholino use in zebrafish. *Zebrafish*, 6, 69-77.
- BIOSYSTEMS, A. Relative Gene Expression Workflow. Available: http://www3.appliedbiosystems.com/cms/groups/portal/documents/generaldocuments/cms_075428.pdf.
- BIOSYSTEMS, A. *TaqMan® Gene Expression Assay Search* [Online]. Available: <http://bioinfo.appliedbiosystems.com/genome-database/gene-expression.html>.
- BLUM, Y., BELTING, H. G., *et al.* 2008. Complex cell rearrangements during intersegmental vessel sprouting and vessel fusion in the zebrafish embryo. *Dev Biol*, 316, 312-22.
- BROWN, M. J. 2007. Renin: friend or foe? *Heart*, 93, 1026-33.
- BUCHNER, D. A., SU, F., *et al.* 2007. pak2a mutations cause cerebral hemorrhage in redhead zebrafish. *Proc Natl Acad Sci U S A*, 104, 13996-4001.
- BURGESS, J. K. 2001. Gene expression studies using microarrays. *Clin Exp Pharmacol Physiol*, 28, 321-8.
- CHENG, C., TEMPEL, D., *et al.* 2006. Atherosclerotic lesion size and vulnerability are determined by patterns of fluid shear stress. *Circulation*, 113, 2744-53.
- COVASSIN, L. D., VILLEFRANC, J. A., KACERGIS, M. C., WEINSTEIN, B. M. & LAWSON, N. D. 2006. Distinct genetic interactions between multiple Vegf receptors are required for development of different blood vessel types in zebrafish. *Proc Natl Acad Sci U S A*, 103, 6554-9.
- COX, J. A., KUCENAS, S. & VOIGT, M. M. 2005. Molecular characterization and embryonic expression of the family of N-methyl-D-aspartate receptor subunit genes in the zebrafish. *Dev Dyn*, 234, 756-66.
- CROCE, K. & LIBBY, P. 2007. Intertwining of thrombosis and inflammation in atherosclerosis. *Curr Opin Hematol*, 14, 55-61.
- DENVIR, M. A., TUCKER, C. S. & MULLINS, J. J. 2008. Systolic and diastolic ventricular function in zebrafish embryos: influence of norepinephrine, MS-222 and temperature. *BMC Biotechnol*, 8, 21.
- EISEN, J. S. & SMITH, J. C. 2008. Controlling morpholino experiments: don't stop making antisense. *Development*, 135, 1735-43.

- ERTER, C. E., SOLNICA-KREZEL, L. & WRIGHT, C. V. 1998. Zebrafish nodal-related 2 encodes an early mesendodermal inducer signaling from the extraembryonic yolk syncytial layer. *Dev Biol*, 204, 361-72.
- FAN, X., HAGOS, E. G., *et al.* 2007. Nodal signals mediate interactions between the extra-embryonic and embryonic tissues in zebrafish. *Dev Biol*, 310, 363-78.
- FEEZOR, R. J., BAKER, H. V., *et al.* 2004. Whole blood and leukocyte RNA isolation for gene expression analyses. *Physiol Genomics*, 19, 247-54.
- FUJITA, M., CHA, Y. R., *et al.* 2011. Assembly and patterning of the vascular network of the vertebrate hindbrain. *Development*, 138, 1705-15.
- GAZES, P. C., MOBLEY, E. M., JR., FARIS, H. M., JR., DUNCAN, R. C. & HUMPHRIES, G. B. 1973. Preinfarctional (unstable) angina--a prospective study--ten year follow-up. Prognostic significance of electrocardiographic changes. *Circulation*, 48, 331-7.
- GLASS, C. K. & WITZTUM, J. L. 2001. Atherosclerosis. the road ahead. *Cell*, 104, 503-16.
- GRIMM, R. H., JR., NEATON, J. D. & LUDWIG, W. 1985. Prognostic importance of the white blood cell count for coronary, cancer, and all-cause mortality. *JAMA*, 254, 1932-7.
- HANSSON, G. K. 2009. Atherosclerosis--an immune disease: The Anitschkov Lecture 2007. *Atherosclerosis*, 202, 2-10.
- HE, Q. Y., LIU, X. H., *et al.* 2006. G8: a novel domain associated with polycystic kidney disease and non-syndromic hearing loss. *Bioinformatics*, 22, 2189-91.
- HERBERT, S. P., HUISKEN, J., *et al.* 2009. Arterial-venous segregation by selective cell sprouting: an alternative mode of blood vessel formation. *Science*, 326, 294-8.
- HUANG DA, W., SHERMAN, B. T. & LEMPICKI, R. A. 2009. Systematic and integrative analysis of large gene lists using DAVID bioinformatics resources. *Nat Protoc*, 4, 44-57.
- IRIZARRY, R. A., BOLSTAD, B. M., *et al.* 2003. Summaries of Affymetrix GeneChip probe level data. *Nucleic Acids Res*, 31, e15.
- ISOGAI, S., HORIGUCHI, M. & WEINSTEIN, B. M. 2001. The vascular anatomy of the developing zebrafish: an atlas of embryonic and early larval development. *Dev Biol*, 230, 278-301.
- ITOH, M., KIM, C. H., *et al.* 2003. Mind bomb is a ubiquitin ligase that is essential for efficient activation of Notch signaling by Delta. *Dev Cell*, 4, 67-82.
- IZANT, J. G. & WEINTRAUB, H. 1984. Inhibition of thymidine kinase gene expression by anti-sense RNA: a molecular approach to genetic analysis. *Cell*, 36, 1007-15.
- JAIN, R. K., FINN, A. V., KOLODGIE, F. D., GOLD, H. K. & VIRMANI, R. 2007. Antiangiogenic therapy for normalization of atherosclerotic plaque vasculature: a potential strategy for plaque stabilization. *Nat Clin Pract Cardiovasc Med*, 4, 491-502.
- JIA, H., KING, I. N., *et al.* 2007. Vertebrate heart growth is regulated by functional antagonism between Gridlock and Gata5. *Proc Natl Acad Sci U S A*, 104, 14008-13.

- JIANG, Y. J., BRAND, M., *et al.* 1996. Mutations affecting neurogenesis and brain morphology in the zebrafish, *Danio rerio*. *Development*, 123, 205-16.
- JIN, S. W., BEIS, D., MITCHELL, T., CHEN, J. N. & STAINIER, D. Y. 2005. Cellular and molecular analyses of vascular tube and lumen formation in zebrafish. *Development*, 132, 5199-209.
- JOHNSON, J. E. 2003. Numb and Numblake control cell number during vertebrate neurogenesis. *Trends Neurosci*, 26, 395-6.
- KANSAKU, A., HIRABAYASHI, S., *et al.* 2006. Ligand-of-Numb protein X is an endocytic scaffold for junctional adhesion molecule 4. *Oncogene*, 25, 5071-84.
- KOLODGIE, F. D., GOLD, H. K., *et al.* 2003. Intraplaque hemorrhage and progression of coronary atheroma. *N Engl J Med*, 349, 2316-25.
- KUO, M. T., WEI, Y., *et al.* 2006. Association of fragile site-associated (FSA) gene expression with epithelial differentiation and tumor development. *Biochem Biophys Res Commun*, 340, 887-93.
- LANDER, E. S. 1999. Array of hope. *Nat Genet*, 21, 3-4.
- LARSON, J. D., WADMAN, S. A., *et al.* 2004. Expression of VE-cadherin in zebrafish embryos: a new tool to evaluate vascular development. *Dev Dyn*, 231, 204-13.
- LAWSON, N. D., SCHEER, N., *et al.* 2001. Notch signaling is required for arterial-venous differentiation during embryonic vascular development. *Development*, 128, 3675-83.
- LAWSON, N. D. & WEINSTEIN, B. M. 2002. In vivo imaging of embryonic vascular development using transgenic zebrafish. *Dev Biol*, 248, 307-18.
- LIANG, P., JONES, C. A., *et al.* 2004. Genomic characterization and expression analysis of the first nonmammalian renin genes from zebrafish and pufferfish. *Physiol Genomics*, 16, 314-22.
- LINDSAY, A. C. & CHOUDHURY, R. P. 2008. Form to function: current and future roles for atherosclerosis imaging in drug development. *Nat Rev Drug Discov*, 7, 517-29.
- LISTER, J. A., ROBERTSON, C. P., LEPAGE, T., JOHNSON, S. L. & RAIBLE, D. W. 1999. nacre encodes a zebrafish microphthalmia-related protein that regulates neural-crest-derived pigment cell fate. *Development*, 126, 3757-67.
- LIU, X., MILO, M., LAWRENCE, N. D. & RATTRAY, M. 2006a. Probe-level measurement error improves accuracy in detecting differential gene expression. *Bioinformatics*, 22, 2107-13.
- LIU, X. J., MILO, M., LAWRENCE, N. D. & RATTRAY, M. 2006b. Probe-level measurement error improves accuracy in detecting differential gene expression. *Bioinformatics*, 22, 2107-2113.
- LONG, Q., MENG, A., *et al.* 1997. GATA-1 expression pattern can be recapitulated in living transgenic zebrafish using GFP reporter gene. *Development*, 124, 4105-11.
- MA, T. K., KAM, K. K., YAN, B. P. & LAM, Y. Y. 2010. Renin-angiotensin-aldosterone system blockade for cardiovascular diseases: current status. *Br J Pharmacol*, 160, 1273-92.

- MATHAVAN, S., LEE, S. G., *et al.* 2005. Transcriptome analysis of zebrafish embryogenesis using microarrays. *PLoS Genet*, 1, 260-76.
- MICHISHITA, E., GARCES, G., BARRETT, J. C. & HORIKAWA, I. 2006. Upregulation of the KIAA1199 gene is associated with cellular mortality. *Cancer Lett*, 239, 71-7.
- MILO, M., FAZELI, A., NIRANJAN, M. & LAWRENCE, N. D. 2003a. A probabilistic model for the extraction of expression levels from oligonucleotide arrays. *Biochem Soc Trans*, 31, 1510-2.
- MILO, M., FAZELI, A., NIRANJAN, M. & LAWRENCE, N. D. 2003b. A probabilistic model for the extraction of expression levels from oligonucleotide arrays. *Biochemical Society Transactions*, 31, 1510-1512.
- MORENO, P. R., PURUSHOTHAMAN, M. & PURUSHOTHAMAN, K. R. 2012. Plaque neovascularization: defense mechanisms, betrayal, or a war in progress. *Ann N Y Acad Sci*, 1254, 7-17.
- MORENO, P. R., SANZ, J. & FUSTER, V. 2009. Promoting mechanisms of vascular health: circulating progenitor cells, angiogenesis, and reverse cholesterol transport. *J Am Coll Cardiol*, 53, 2315-23.
- MOTTERLE, A., XIAO, Q., *et al.* 2012. Influence of matrix metalloproteinase-12 on fibrinogen level. *Atherosclerosis*, 220, 351-4.
- MOULTON, K. S. 2007. Angiogenesis in Cardiovascular Disease. In: LIBBY, R. D. C. A. P. (ed.) *Endothelial Dysfunctions on Vascular Disease*. Oxford, UK: Blackwells.
- MURAKAMI, M., NGUYEN, L. T., *et al.* 2011. FGF-dependent regulation of VEGF receptor 2 expression in mice. *J Clin Invest*, 121, 2668-78.
- MUTCH, D. M., BERGER, A., MANSOURIAN, R., RYTZ, A. & ROBERTS, M. A. 2002. The limit fold change model: A practical approach for selecting differentially expressed genes from microarray data. *Bmc Bioinformatics*, 3.
- NASEVICIUS, A. & EKKER, S. C. 2000. Effective targeted gene 'knockdown' in zebrafish. *Nat Genet*, 26, 216-20.
- NCBI. *EST Profile for KIAA1109* [Online]. Available: <http://www.ncbi.nlm.nih.gov/UniGene/ESTProfileViewer.cgi?uglist=Hs.408142>.
- NERI SERNERI, G. G. & MODESTI, P. A. 1991. [Cellular mechanisms in the pathogenesis of thrombosis]. *Haematologica*, 76 Suppl 3, 261-70.
- NERI SERNERI, G. G., PRISCO, D., *et al.* 1997. Acute T-cell activation is detectable in unstable angina. *Circulation*, 95, 1806-12.
- NEWTON, M. A., KENDZIORSKI, C. M., RICHMOND, C. S., BLATTNER, F. R. & TSUI, K. W. 2001. On differential variability of expression ratios: Improving statistical inference about gene expression changes from microarray data. *Journal of Computational Biology*, 8, 37-52.
- NHS. *NHS - Coronary heart disease* [Online]. Available: <http://www.nhs.uk/Conditions/Coronary-heart-disease/Pages/Introduction.aspx>.
- NIE, J., MCGILL, M. A., *et al.* 2002. LNX functions as a RING type E3 ubiquitin ligase that targets the cell fate determinant Numb for ubiquitin-dependent degradation. *EMBO J*, 21, 93-102.

- NOONAN, J. P., LI, J., *et al.* 2003. Extensive linkage disequilibrium, a common 16.7-kilobase deletion, and evidence of balancing selection in the human protocadherin alpha cluster. *Am J Hum Genet*, 72, 621-35.
- OLSSON, A. K., DIMBERG, A., KREUGER, J. & CLAESSION-WELSH, L. 2006. VEGF receptor signalling - in control of vascular function. *Nat Rev Mol Cell Biol*, 7, 359-71.
- PANTHER. *PANTHER - Classification of Genes and Proteins* [Online]. Available: <http://www.pantherdb.org>.
- PAPAIIOANNOU, T. G., KARATZIS, E. N., VAVURANAKIS, M., LEKAKIS, J. P. & STEFANADIS, C. 2006. Assessment of vascular wall shear stress and implications for atherosclerotic disease. *Int J Cardiol*, 113, 12-8.
- PEARSON, R. D., LIU, X., *et al.* 2009a. puma: a Bioconductor package for propagating uncertainty in microarray analysis. *BMC Bioinformatics*, 10, 211.
- PEARSON, R. D., LIU, X. J., *et al.* 2009b. puma: a Bioconductor package for propagating uncertainty in microarray analysis. *Bmc Bioinformatics*, 10.
- PETERSON, R. T., SHAW, S. Y., *et al.* 2004. Chemical suppression of a genetic mutation in a zebrafish model of aortic coarctation. *Nat Biotechnol*, 22, 595-9.
- PRIMER3PLUS. Available: <http://www.bioinformatics.nl/cgi-bin/primer3plus/primer3plus.cgi>.
- PROJECT, K. O. *Kazusa ORFeome Project* [Online]. Available: <http://www.kazusa.or.jp/kop/>
- QUACKENBUSH, J. 2002. Microarray data normalization and transformation. *Nature genetics*, 32 Suppl, 496-501.
- RAHIMTOOLA, S. H., NUNLEY, D., *et al.* 1983. Ten-year survival after coronary bypass surgery for unstable angina. *N Engl J Med*, 308, 676-81.
- REBAGLIATI, M. R., TOYAMA, R., HAFFTER, P. & DAWID, I. B. 1998. cyclops encodes a nodal-related factor involved in midline signaling. *Proc Natl Acad Sci U S A*, 95, 9932-7.
- REYNIER, F., PACHOT, A., *et al.* 2010. Specific gene expression signature associated with development of autoimmune type-I diabetes using whole-blood microarray analysis. *Genes and immunity*, 11, 269-78.
- RO, H. & DAWID, I. B. 2009. Organizer restriction through modulation of Bozozok stability by the E3 ubiquitin ligase Lnx-like. *Nat Cell Biol*, 11, 1121-7.
- ROTHSCHILD, S. C., LISTER, J. A. & TOMBES, R. M. 2007. Differential expression of CaMK-II genes during early zebrafish embryogenesis. *Dev Dyn*, 236, 295-305.
- RUCH, C., SKINIOTIS, G., STEINMETZ, M. O., WALZ, T. & BALLMER-HOFER, K. 2007. Structure of a VEGF-VEGF receptor complex determined by electron microscopy. *Nature structural & molecular biology*, 14, 249-50.
- SANGER, T. W. T. S. I. *Zebrafish Mutation Project* [Online]. Available: http://www.sanger.ac.uk/Projects/D_rerio/zmp/.
- SANGUINETTI, G., MILO, M., RATTRAY, M. & LAWRENCE, N. D. 2005. Accounting for probe-level noise in principal component analysis of microarray data. *Bioinformatics*, 21, 3748-3754.

- SANTORO, M. M., PESCE, G. & STAINIER, D. Y. 2009. Characterization of vascular mural cells during zebrafish development. *Mech Dev*, 126, 638-49.
- SCHWERTE, T. 2009. Cardio-respiratory control during early development in the model animal zebrafish. *Acta Histochem*, 111, 230-43.
- SHANTSILA, E. & LIP, G. Y. 2009. The role of monocytes in thrombotic disorders. Insights from tissue factor, monocyte-platelet aggregates and novel mechanisms. *Thromb Haemost*, 102, 916-24.
- SHI, L. M., JONES, W. D., *et al.* 2008. The balance of reproducibility, sensitivity, and specificity of lists of differentially expressed genes in microarray studies. *Bmc Bioinformatics*, 9, 19.
- SHIMADA, K. 2009. Immune system and atherosclerotic disease: heterogeneity of leukocyte subsets participating in the pathogenesis of atherosclerosis. *Circ J*, 73, 994-1001.
- SINNAEVE, P. R., DONAHUE, M. P., *et al.* 2009. Gene expression patterns in peripheral blood correlate with the extent of coronary artery disease. *PLoS One*, 4, e7037.
- STAMOVA, B. S., APPERSON, M., *et al.* 2009. Identification and validation of suitable endogenous reference genes for gene expression studies in human peripheral blood. *BMC Med Genomics*, 2, 49.
- STRING. *STRING - Known and Predicted Protein-Protein Interactions* [Online]. Available: <http://string-db.org>.
- SUMMERTON, J. E. 2007. Morpholino, siRNA, and S-DNA compared: impact of structure and mechanism of action on off-target effects and sequence specificity. *Curr Top Med Chem*, 7, 651-60.
- TAKAHASHI, S., IWAMOTO, N., *et al.* 2009. The E3 ubiquitin ligase LNX1p80 promotes the removal of claudins from tight junctions in MDCK cells. *J Cell Sci*, 122, 985-94.
- TAKAYA, N., YUAN, C., *et al.* 2005. Presence of intraplaque hemorrhage stimulates progression of carotid atherosclerotic plaques: a high-resolution magnetic resonance imaging study. *Circulation*, 111, 2768-75.
- TAN, Y. P., LI, S., *et al.* 2010. Regulation of protocadherin gene expression by multiple neuron-restrictive silencer elements scattered in the gene cluster. *Nucleic Acids Res*, 38, 4985-97.
- TAURINO, C., MILLER, W. H., *et al.* 2010. Gene expression profiling in whole blood of patients with coronary artery disease. *Clin Sci (Lond)*, 119, 335-43.
- THATTALIYATH, B., CYKOWSKI, M. & JAGADEESWARAN, P. 2005. Young thrombocytes initiate the formation of arterial thrombi in zebrafish. *Blood*, 106, 118-24.
- THISSE, C. & THISSE, B. 2008. High-resolution in situ hybridization to whole-mount zebrafish embryos. *Nat Protoc*, 3, 59-69.
- TINDALL, E. A., HOANG, H. N., *et al.* 2010. The 4q27 locus and prostate cancer risk. *BMC Cancer*, 10, 69.
- TIWARI, R. L., SINGH, V. & BARTHWAL, M. K. 2008. Macrophages: an elusive yet emerging therapeutic target of atherosclerosis. *Med Res Rev*, 28, 483-544.

- TRIP, M. D., CATS, V. M., VAN CAPELLE, F. J. & VREEKEN, J. 1990. Platelet hyperreactivity and prognosis in survivors of myocardial infarction. *N Engl J Med*, 322, 1549-54.
- TZENG, D. W., LIN, M. H., *et al.* 2007. Molecular and functional studies of tilapia (*Oreochromis mossambicus*) NMDA receptor NR1 subunits. *Comp Biochem Physiol B Biochem Mol Biol*, 146, 402-11.
- VAN HEEL, D. A., FRANKE, L., *et al.* 2007. A genome-wide association study for celiac disease identifies risk variants in the region harboring IL2 and IL21. *Nat Genet*, 39, 827-9.
- VAN ROOIJEN, E., VOEST, E. E., *et al.* 2010. von Hippel-Lindau tumor suppressor mutants faithfully model pathological hypoxia-driven angiogenesis and vascular retinopathies in zebrafish. *Dis Model Mech*, 3, 343-53.
- VARTANIAN, K., SLOTTKE, R., *et al.* 2009. Gene expression profiling of whole blood: comparison of target preparation methods for accurate and reproducible microarray analysis. *BMC Genomics*, 10, 2.
- VERHEUGT, F. W., VAN DER LAARSE, A., *et al.* 1990. Effects of early intervention with low-dose aspirin (100 mg) on infarct size, reinfarction and mortality in anterior wall acute myocardial infarction. *Am J Cardiol*, 66, 267-70.
- VOLPE, M., BATTISTONI, A., CHIN, D., RUBATTU, S. & TOCCI, G. 2012. Renin as a biomarker of cardiovascular disease in clinical practice. *Nutr Metab Cardiovasc Dis*, 22, 312-7.
- WADA, R., ROHATAGI, S., SMALL, D., WINTERS, K. J. & SALAZAR, D. E. 2010. Correlation of inhibition of platelet aggregation with cardiovascular and bleeding outcomes in acute coronary syndromes. *J Clin Pharmacol*, 50, 904-13.
- WILLIAMS, C. K., LI, J. L., MURGA, M., HARRIS, A. L. & TOSATO, G. 2006. Up-regulation of the Notch ligand Delta-like 4 inhibits VEGF-induced endothelial cell function. *Blood*, 107, 931-9.
- WU, Q. 2005. Comparative genomics and diversifying selection of the clustered vertebrate protocadherin genes. *Genetics*, 169, 2179-88.
- ZACHARY, I., MATHUR, A., YLA-HERTTUALA, S. & MARTIN, J. 2000. Vascular protection: A novel nonangiogenic cardiovascular role for vascular endothelial growth factor. *Arterioscler Thromb Vasc Biol*, 20, 1512-20.
- ZFIN. *The Zebrafish Model Organism Database* [Online]. Available: <http://www.zfin.org>.
- ZHAO, C., WANG, X., *et al.* 2011. A novel xenograft model in zebrafish for high-resolution investigating dynamics of neovascularization in tumors. *PLoS One*, 6, e21768.
- ZHERNAKOVA, A., ALIZADEH, B. Z., *et al.* 2007. Novel association in chromosome 4q27 region with rheumatoid arthritis and confirmation of type 1 diabetes point to a general risk locus for autoimmune diseases. *Am J Hum Genet*, 81, 1284-8.

Appendix 1

Patient number	Gender	Ethnicity	Age	Type of event	Troponin Level at Admission	Days before baseline	Hb at Admission	Hb at Visit 1	Cr at Admission	Cr at Visit 1	eGFR visit 1	Angiogram	DIABETES SMOKING	FAMILY HISTORY	HYPER TENSION	IMC. CHOL.	REMAL IMP.	PROIR Hx OF CAD	DAY 1 attendance	DAY 3 attendance	DAY 7 attendance	DAY 30 attendance	DAY 30 Re-admission
CY000003	Male	1. White-British	56.3	NSTEMI	0.1	0	14.2	14.2	100	100	71	71	No	Yes	No	Yes	I	Yes	Yes	Yes	Yes	Yes	No
CY000004	Female	1. White-British	68.3	NSTEMI	153	1	12.7	12.8	54	83	104	63	Yes	Yes	Yes	Yes	I	Yes	Yes	Yes	Yes	Yes	No
CY000005	Male	1. White-British	63.3	NSTEMI	0.08	1	14.8	15.3	93	87	76	82	Impaired	No	Yes	Yes	I	Yes	Yes	Yes	Yes	Yes	No
CY000007	Male	1. White-British	50.3	NSTEMI	0.08	1	14.8	14.8	92	102	71	80	Impaired	Yes	Yes	Yes	I	Yes	Yes	Yes	Yes	Yes	No
CY000009	Female	1. White-British	67.4	STEMI	39.8	1	12.4	12.1	62	69	89	78	No	Yes	No	No	I	Yes	Yes	Yes	Yes	Yes	No
CY000010	Male	1. White-British	55.4	STEMI	>50	1	15.7	15.6	87	95	84	76	Impaired	Yes	No	No	I	No	Yes	Yes	Yes	Yes	No
CY000011	Male	1. White-British	64.3	NSTEMI	>50	1	13.5	13.2	91	90	77	78	No	No	No	No	I	Yes	Yes	Yes	Yes	Yes	No
CY000021	Male	1. White-British	67.3	NSTEMI	<0.05	1	15.5	15.5	114	114	59	59	No	Yes	Yes	Yes	I	Yes	Yes	Yes	Yes	Yes	No
CY000022	Male	1. White-British	64.1	TroponinM	<0.05	0	11.8	11.8	91	91	77	77	NIDDM	No	No	No	I	No	Yes	Yes	Yes	Yes	No
CY000024	Male	1. White-British	55.2	NSTEMI	0.06	1	13.3	12	122	117	57	60	IDDM	Yes	Yes	Yes	III	No	Yes	No	Yes	Yes	No
CY000025	Male	1. White-British	74.1	TroponinM	<0.05	2	12.3	13	95	105	71	64	No	No	No	Yes	I	Yes	Yes	Yes	Yes	Yes	Yes
CY000026	Male	1. White-British	51.3	NSTEMI	0.07	0	14.6	14.6	76	76	104	104	No	No	No	No	I	No	Yes	Yes	Yes	Yes	No
CY000027	Male	1. White-British	66.1	TroponinM	<0.05	1	12.2	12.2	93	85	75	83	IDDM	Yes	No	Yes	I	Yes	Yes	Yes	Yes	Yes	No
CY000028	Female	1. White-British	66.1	TroponinM	<0.05	2	13.6	13.7	49	54	120	108	Diet	Yes	Yes	Yes	I	Yes	Yes	Yes	Yes	Yes	No
CY000030	Female	1. White-British	62.3	NSTEMI	0.16	2	12.4	11.9	92	102	56	51	Impaired	Yes	Yes	No	III	No	Yes	Yes	Yes	Yes	No
CY000054	Male	1. White-British	39.4	STEMI	17	1	14.1	14.3	86	83	91	95	Impaired	No	No	No	I	No	Yes	Yes	Yes	Yes	No
CY000055	Male	1. White-British	43.3	NSTEMI	0.78	1	15.7	15.7	161	172	43	40	Impaired	Yes	Yes	Yes	III	Yes	Yes	Yes	Yes	Yes	No
CY000080	Male	1. White-British	71.1	TroponinM	<0.05	1	14.1	14	82	72	85	89	No	Yes	Yes	Yes		Yes	YES	YES	YES	YES	no
CY000071	Male	1. White-British	69.4	STEMI	>50	1	14.4	12.7	84	90	84	77	No	Current	Yes	No	I	No	YES	YES	YES	YES	No